The role of LEF1 and WNT signaling in growth and differentiation of rhabdomyosarcoma

Dissertation

for the award of the degree

“Doctor rerum naturalium”

of the Georg-August-Universität Göttingen

within the doctoral program Molecular Biology of Cells

of the Georg-August University School of Science (GAUSS)

submitted by

Julia Dräger

from Berlin

Göttingen 2016

Thesis Committee

Prof. Dr. Heidi Hahn

Dept. of Human Genetics; University Medical Center Göttingen

Prof. Dr. Holger Bastians

Dept. of Molecular Oncology; Georg-August-University Göttingen

Prof. Dr. Tobias Pukrop

Dept. of Hematology/Medical Oncology; University Medical Center Göttingen

Clinic for Internal Medicine III, Hematology and Medical Oncology; University Regensburg

Members of the Examination Board

Referee: **Prof. Dr. Heidi Hahn**

Dept. of Human Genetics; University Medical Center Göttingen

2nd Referee: **Prof. Dr. Holger Bastians**

Dept. of Molecular Oncology; Georg-August-University Göttingen

Further members of the Examination Board

Prof. Dr. Matthias Dobbelstein

Dept. of Molecular Oncology; Georg-August-University Göttingen

Prof. Dr. Ralf Dressel

Dept. of Cellular and Molecular Immunology; University Medical Center Göttingen

Prof. Dr. Hubertus Jarry

Dept. of Clinical and Experimental Endocrinology; University Medical Center Göttingen

Prof. Dr. Ralph Kehlenbach

Dept. of Molecular Biology; University Medical Center Göttingen

Date of Disputation: 02.02.2017

Affidavit

I hereby declare that the PhD thesis entitled "The role of LEF1 and WNT signaling in growth and differentiation of rhabdomyosarcoma" has been written independently and with no other sources and aids than quoted.

Julia Dräger

Göttingen, November 2016

Parts of this work have been published:

Nitzki, F., Cuvelier, N., **Dräger, J.**, Schneider, A., Braun, T., Hahn, H. (2016) Hedgehog/Patched-associated rhabdomyosarcoma formation from delta1-expressing mesodermal cells. *Oncogene, 35*(22)

Parts of this work have been submitted for publication:

Dräger, J., Simon-Keller, K., Pukrop, T., Klemm, F., Wilting, J., Sticht, C., Dittmann, K., Schulz, M., Leuschner, I., Marx, A., Hahn, H. (2016) LEF1 reduces tumor progression and induces myodifferentiation in a subset of rhabdomyosarcoma. *Oncotarget*, in revision, November 2016

Contents

List of Figures

List of Tables

1 Summary

Rhabdomyosarcoma (RMS) is the most common type of soft tissue sarcoma in children and shows characteristics of skeletal muscle differentiation. RMS occur in two main histological subtypes in children: alveolar RMS (ARMS) and embryonal RMS (ERMS), which are associated with distinct genetic and molecular alterations. Despite more intensive therapies during the last decades, patients with metastatic RMS have a very poor prognosis. Thus, it is of uttermost importance to increase the knowledge of the basic biology of RMS and to develop new treatment strategies in order to improve the outcome of the disease.

WNT signaling plays an important role in muscle development and differentiation and also contributes to a variety of human diseases including cancer. However, only few data on the role of WNT signaling in RMS have been published and are restricted to β-catenin dependent (canonical) WNT signaling. These data mainly support a tumor suppressive role of canonical WNT signaling in RMS besides promoting myogenic differentiation.

Our findings now demonstrate that the prominent transcription factor of canonical WNT signaling LEF1/*LEF1* can be highly expressed in primary human ARMS and ERMS samples. However, the common absence of nuclear β-catenin and downregulation of *AXIN2* in these RMS samples indicate that canonical WNT signaling is not active and probably inhibited in RMS. Furthermore, our *in vivo* studies reveal that Wnt3a-driven canonical Wnt/β-catenin signaling does not play a prominent role in RMS pathogenesis in mice.

To study the role of LEF1 in RMS in more depth, a stable LEF1 knockdown (LEF1 KD) in the two human ARMS cell lines Rh41 and RMS-13 and in the human ERMS cell line TE671 was established. Our data demonstrate that dependent on the cellular context, LEF1 reduces the aggressiveness of RMS cells. Thus, LEF1 can induce pro-apoptotic signals and can suppress proliferation, migration and invasiveness – especially in the ARMS cell line RMS-13 – both *in vitro* and *in vivo*. This less aggressive phenotype is associated with reduced *c-MYC* and *TCFs* expression. Furthermore, LEF1 can induce myodifferentiation of RMS-13 cells. Importantly, this seems not to involve canonical β-catenin driven WNT signaling activity. Indeed, despite an upregulation of *AXIN2*, Wnt3a stimulation does not induce *SuperTOPFlash* (TOP) reporter activity or nuclear translocation of β-catenin in

ARMS cell lines. Together these data indicate that LEF1 has a tumor suppressive function and can induce myodifferentiation in a subset of RMS. This may also involve TCF factors whereas β-catenin activity plays a subordinate role.

Interestingly, WNT5A a major player of β-catenin independent (non-canonical) WNT signaling is also overexpressed on protein and on transcript level in primary human ARMS and ERMS samples. Moreover, *LEF1* mRNA levels tend to be positively correlated with that of *WNT5A* in primary human ARMS samples. This is similar to the ARMS cell line RMS-13, in which LEF1/*LEF1* expression correlates with that of WNT5A/*WNT5A*. These data indicate that besides LEF1 also WNT5A might be involved in the pathogenesis and aggressiveness of ARMS. Furthermore, in RMS-13 cells, WNT5A expression is accompanied by activation of PI3K/AKT signaling and LEF1 expression is positively regulated by PI3K. We here propose a new model, in which LEF1 and WNT5A establish a positive feedback loop that involves activation of PI3K signaling and counteracts the aggressiveness of a subset of ARMS, which correlates with downregulation of c-MYC.

Recently, activation of β-catenin driven WNT signaling has been proposed as a new treatment option for RMS. However, this may be only of benefit for specific subtypes of RMS, but not for those, in which tumor progression and myogenic differentiation is regulated *via* LEF1/WNT5A interactions in a non-canonical manner. Together, these data show that further investigations are needed to identify the specific RMS subtypes that may respond to activation of either canonical or LEF1/WNT5A-mediated non-canonical WNT signaling.

2 Introduction

2.1 Rhabdomyosarcoma (RMS)

Rhabdomyosarcoma (RMS) accounts for approximately 40 % of all soft tissue sarcoma in children and adolescents under the age of 20 years and therefore is the most common soft tissue sarcoma in children (Dagher *et al.*, 1999; Ognjanovic *et al.*, 2009). Primary RMS in children mainly occur in the head and neck region, the genitourinary tract, and the trunk or limb (reviewed in Sebire *et al.*, 2003). These pediatric tumors are linked to the skeletal muscle lineage, because essentially all of them show nuclear expression of myogenic markers such as MYOGENIN and MYOD1 (Sebire *et al.*, 2003). Based on histopathological features and distinct genetic alterations, RMS can be divided into two major subtypes in children that are alveolar RMS (ARMS) and embryonal RMS (ERMS). ERMS account for approximately two thirds of all RMS cases and frequently show loss of heterozygosity (LOH) at chromosome 11p15 (Dagher *et al.*, 1999; Merlino *et al.*, 1999; Ognjanovic *et al.*, 2009). This subtype is histologically characterized by spindle-shaped cells with a stroma-rich appearance. ARMS exhibit small, round, densely appearing cells lined up along spaces reminiscent of pulmonary alveoli. This subtype can be further divided in fusion gene negative with 25 % and fusion gene positive ARMS with 75 % prevalence. The latter subgroup is characterized by t(2;13) or t(1;13) chromosomal translocations that lead to fusion genes encoding either PAX3-FOXO1 or PAX7-FOXO1 fusion proteins (Dagher *et al.*, 1999). ERMS are always fusion gene negative and are associated with a more favorable prognosis with a 5-year overall survival of approximately 73 % compared to 48 % for ARMS (Dagher *et al.*, 1999; Merlino *et al.*, 1999; Ognjanovic *et al.*, 2009). However, the survival rate for metastatic disease is only 10-30 % for ARMS (De Giovanni *et al.*, 2009) and approximately 40 % for ERMS (Breneman *et al.*, 2003).

2.2 WNT signaling

The WNT pathway is a highly conserved signaling cascade, which controls many developmental processes, tissue regeneration and homeostasis, and also contributes to a variety of human diseases including cancer (reviewed in Clevers *et al.*, 2012). The WNT ligands comprise a large family of secreted glycolipoproteins that can signal through different types of receptors activating a number of intracellular signaling pathways. WNT signaling can be generally divided into the canonical WNT pathway that involves β-catenin-mediated transcriptional activation, and the non-canonical WNT pathways that are β-catenin independent but share several components with the canonical cascade.

2.2.1 β-catenin dependent (canonical) WNT signaling

In the absence of WNT, the β-catenin dependent WNT signaling pathway is inactive (Figure 1A). In the inactive state, β-catenin is phosphorylated by the serine/threonine kinases glycogen synthase kinase 3 (GSK3) and casein kinase 1 (CK1) as a part of the destruction complex. This multiprotein complex furthermore comprises Dishevelled (Dvl), Axin, adenomatosis polyposis coli (APC) gene product and β-transducin repeat containing protein (β-Trcp). Phosphorylated β-catenin is subsequently ubiquitinated by the E3 ubiquitin ligase subunit β-Trcp, and degraded by the proteasome (reviewed in MacDonald *et al.*, 2009).

In the presence of WNT, the pathway is active (Figure 1B). WNT binds to the extracellular region of Frizzled (FZD) and its co-receptor low-density lipoprotein receptor-related protein 6 (LRP6) or LRP5. The formation of a WNT/FZD/LRP complex results in LRP6 phosphorylation and the recruitment of Dvl, and the rest of the destruction complex to the receptors. This inhibits the destruction complex, which is followed by stabilization, accumulation and nuclear translocation of β-catenin where it binds to LEF1/T cell factor (TCF) transcription factors in a complex with other co-activators. This results in the activation of expression of WNT target genes including Cyclin D1, c-Myc and Axin2 (for review see MacDonald *et al.*, 2009; Belyea *et al.*, 2012). Many of WNT/LEF1/TCF/β-catenin target genes are regulated context-dependently and are expressed in a tissue-specific or temporally restricted manner, which may explain how they achieve a wide diversity of transcriptional outputs in different cells, but also the heterogeneous responses of tumor cell lines to WNT ligands (Archbold *et al.*, 2012; Valenta *et al.*, 2012; Pedersen *et al.*, 2015; Seth *et al.*, 2016).

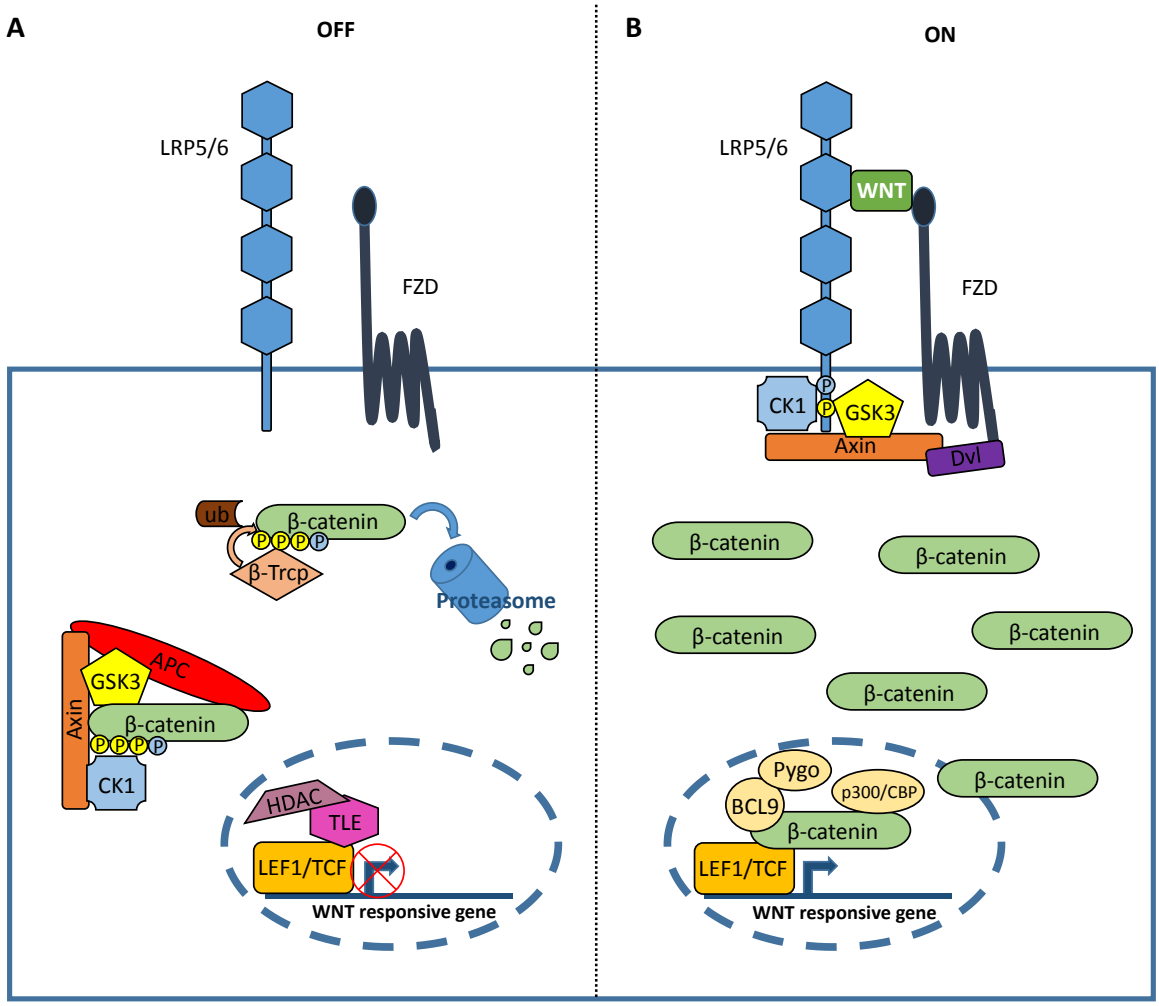

Figure 1: Overview of β-catenin dependent (canonical) WNT signaling. Schematic representation of the canonical WNT pathway in **(A)** off and **(B)** on state. **(A)** In the absence of the WNT ligand, the destruction complex composed of APC, Axin, CK1 and GSK3 presents β-catenin for phosphorylation by CK1 and GSK3. Phosphorylated β-catenin is ubiquitinated and degraded by the proteasome. **(B)** Upon WNT ligand binding, a WNT/FZD/LRP complex forms at the cell membrane, where the kinase activity of CK1 and GSK3 is redirected toward LRP5/6 in complex with Axin and Dvl. Newly synthesized β-catenin is no longer phosphorylated, accumulates and translocates into the nucleus, and induces target gene expression along with LEF1/TCF transcription factors. Modified from McDonald *et al.*, 2009.

2.2.2 Lymphoid enhancer factor 1 (LEF1)

Lymphoid enhancer factor 1 (LEF1) is a central member of the LEF/TCF family of transcription factors that mediate WNT signaling by recruiting the co-activator β-catenin to activate WNT target genes. In mammals, 4 LEF/TCF members exist, which are TCF7 (TCF1), TCF7L1 (TCF3), TCF7L2 (TCF4), and LEF1 (TCF7L3) (reviewed in Arce *et al.*, 2006; Archbold *et al.*, 2012). As the other TCFs, LEF1 contains a β-catenin-binding domain at the *N*-terminus, a high-mobility group (HMG) domain and a nuclear localization signal (NLS). The NLS is recognized directly by importin alpha subunits for nuclear import and the HMG domain recognizes the CCTTTGWW (W represents either T or A) DNA sequence, known as WNT responsive element (WRE). LEF1 also has a context-dependent regulatory domain (CRD). According to the current knowledge, the CRD participates in repression of WNT responsive genes by recruiting pleiotropic co-repressors of the Groucho/Transducin-like enhancer of split (TLE) family (Figure 1A) (Arce *et al.*, 2006). Indeed, in the absence of the WNT signal many targets are strongly repressed by LEF1/TLE complexes (reviewed in Turki-Judeh *et al.*, 2012; Agarwal *et al.*, 2015). Upon WNT-induced β-catenin stabilization and nuclear accumulation, LEF1 interacts with β-catenin. This displaces Groucho/TLE from LEF1 and recruits other co-activators resulting in activation of target genes (Figure 1B). A plethora of co-activators have been identified and include BCL9 and Pygopus (Pygo), Mediator (for transcription initiation), p300/CREB-binding protein (CBP) and TRRAP/TIP60 histone acetyltransferases (HATs), MLL1/2 histone methyltransferases (HMTs), the SWI/SNF family of ATPases for chromatin remodeling, and the PAF1 complex for transcription elongation and histone modifications (MacDonald *et al.*, 2009; Archbold *et al.*, 2012).

However, LEF1 also possesses transcriptional activity that is independent of β-catenin. Grumolato and colleagues uncovered a novel mechanism of LEF1 (and also TCF1) dependent transcription that bypasses β-catenin and increases expression of WNT target genes through interaction of LEF1 with members of the activating transcription factor 2 (ATF2) family of transcriptions factors. Moreover, they revealed that ATF2-induced activation of LEF1 and TCF1 promotes cell growth of hematopoietic tumor cells in the absence of β-catenin stabilization (Grumolato *et al.*, 2013). In addition, the intracellular domain of NOTCH1 (NICD) can function as a co-activator of LEF1 leading to the upregulation of target genes independently of β-catenin (Ross *et al.*, 2001). Moreover, LEF1 can cooperate with SMADs bound to neighboring elements to mediate TGF-β/BMP

regulation of gene targets (reviewed in Arce *et al.*, 2006). Finally, LEF1 together with TCF1 has intrinsic HDAC activity that can repress genes counteracting cellular differentiation in specific contexts (Xing *et al.*, 2016).

Because of these context dependent effects, LEF1 can function either as an oncogene or as a tumor suppressor. For example, transplantation of LEF1-transduced bone marrow leads to acute myeloid leukemia and B-precursor acute lymphoblastic leukemia (ALL) in the mouse (Petropoulos *et al.*, 2008). Conversely, LEF1 can repress the transcription of *MYC* and thus acts as a tumor suppressor in a subset of human T-ALL cases (Gutierrez *et al.*, 2010).

2.2.3 β-catenin independent (non-canonical) WNT signaling

Some WNT ligands also activate the non-canonical WNT signaling pathways that are independent of β-catenin and known as the planar cell polarity (PCP) and the calcium-dependent WNT (WNT/Ca^{2+}) signaling pathways (Figure 2).

The WNT/PCP pathway regulates acquisition of asymmetric cellular morphology, directional cell migration, oriented cell division and cellular orientation in complex tissues (Vladar *et al.*, 2009; Kaucká *et al.*, 2015). This pathway is activated *via* binding of WNT to FZD receptor and its co-receptors such as the tyrosine kinase-like orphan receptor (ROR) 1 and 2, the receptor tyrosine kinase-like (Ryk) or the protein tyrosine kinase 7 (Ptk7) (Figure 2A) (Thiele *et al.*, 2016). The FZD receptor recruits cytoplasmatic Dvl. This results in the activation of the small GTPases Ras homologue (Rho) and Ras-related C3 botulinum toxin substrate (Rac) in parallel pathways. For activation of the Rho branch of signaling, Dvl forms a complex with both Dvl-associated activator of morphogenesis 1 (DAAM1) and Rho, which causes activation of the effector Rho-associated kinase (ROCK). In the second branch of signaling, Dvl forms a complex with Rac, which in turn stimulates MAPK8 (JNK) activity (reviewed in Komiya *et al.*, 2008).

The WNT/Ca^{2+} pathway regulates calcium release from the endoplasmatic reticulum (ER) in order to control intracellular calcium levels (Figure 2B) and functions as a critical modulator of both the canonical and PCP signaling pathways (Komiya *et al.*, 2008). The WNT/Ca^{2+} pathway is activated upon binding of WNT ligands to the FZD receptor leading to the activation of phospholipase C (PLC). If PLC is activated, the plasma membrane component phosphatidylinositol 4,5-bisphosphate is cleaved into 1,2-diacylglycerol and

inositol 1,4,5-trisphosphate (IP_3). IP_3 triggers Ca^{2+} influx from the ER, which activates several Ca^{2+} sensitive effector proteins including protein kinase C (PKC), calcineurin and calcium/calmodulin-dependent kinase II (CaMKII; Komiya *et al.*, 2008). These kinases regulate and activate a multitude of target proteins and can also block β-catenin dependent WNT signaling at several levels (Ishitani *et al.*, 2003; Sato *et al.*, 2010).

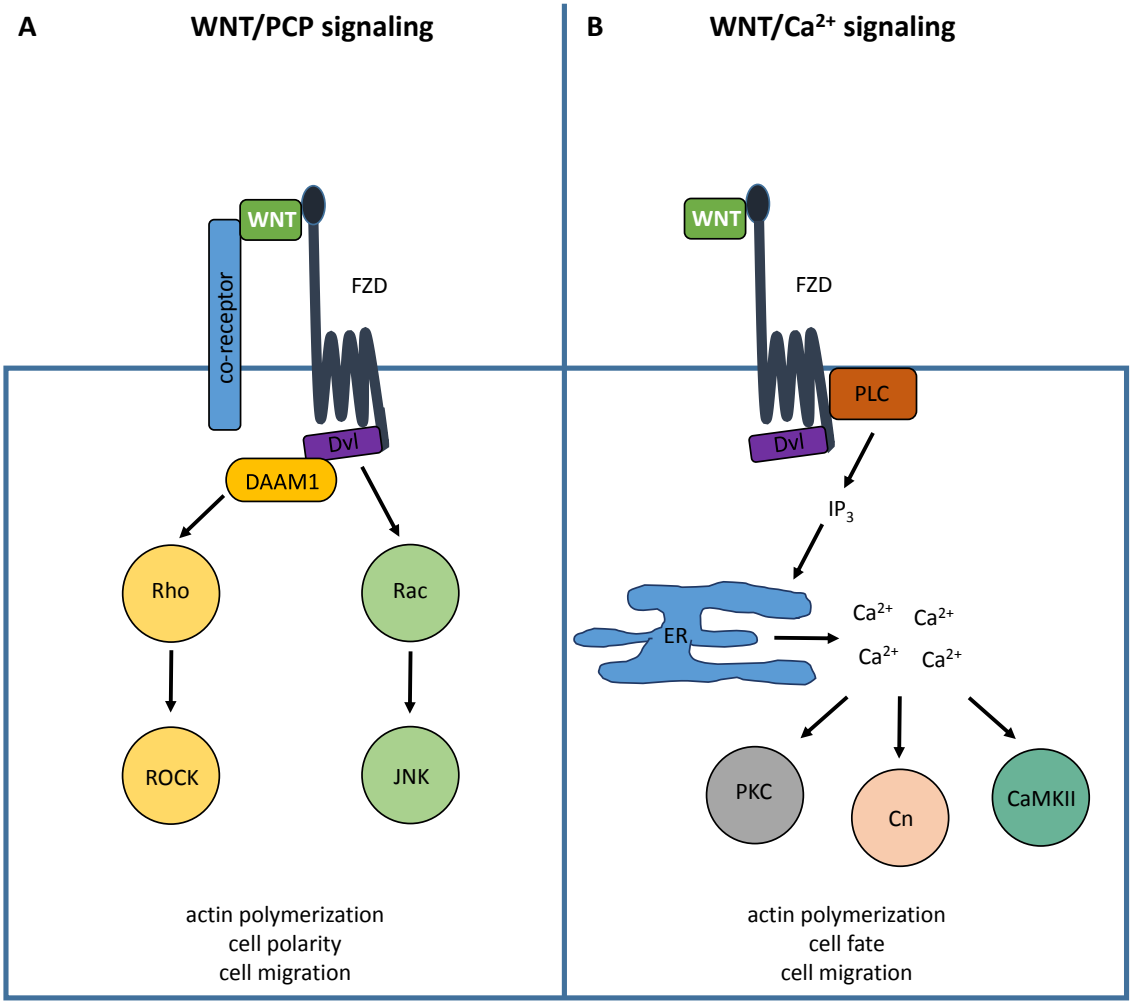

Figure 2: Overview of β-catenin independent (non-canonical) WNT signaling. Schematic representation of the non-canonical **(A)** WNT/PCP and **(B)** WNT/Ca^{2+} pathways. **(A)** WNT/PCP signaling is transduced through FZD and its co-receptors such as ROR1/2, Ryk or Ptk7 leading to the activation of Dvl. Dvl through DAAM1 mediates activation of Rho, which in turn activates ROCK. Dvl also stimulates Rac activity, which leads to the activation of JNK. **(B)** WNT/Ca^{2+} signaling *via* FZD operates through Dvl-dependent activation of PLC, which leads to release of intracellular Ca^{2+}. Elevated cytoplasmatic Ca^{2+} levels induce activation of PKC, calcineurin (Cn) and CaMKII.

2.2.4 WNT5A signaling

One prominent non-canonical WNT ligand is WNT5A that can activate both the WNT/PCP and the WNT/Ca^{2+} pathways (Hogan *et al.*, 2003; Oishi *et al.*, 2003; De, 2011). In the presence of the receptor FZD2, 3, 4, 5 and 6 and their co-receptors ROR1/2, WNT5A activates the WNT/Ca^{2+} signaling pathway (reviewed in De, 2011). This leads to the production of IP_3, the release of Ca^{2+} from the ER and activation of CaMKII (see Chapter 2.2.3). WNT5A/ROR can also stimulate the WNT/PCP pathway by activation of c-Jun and JNK. Oishi and colleagues showed that, beside a physical interaction between WNT5A and ROR molecules, co-expression of WNT5A and ROR2 had an additive effect on phosphorylation of c-Jun and thus on JNK activity (Oishi *et al.*, 2003). Furthermore, dependent on the cellular context and receptor availability, WNT5A can block or activate β-catenin dependent WNT signaling (Mikels *et al.*, 2006; reviewed in Ford *et al.*, 2013).

WNT5A signaling is critical for regulating normal developmental processes, including proliferation, differentiation, migration, adhesion and polarity. However, the aberrant activation or inhibition of WNT5A signaling is emerging as an important event in cancer progression, exerting both oncogenic and tumor suppressive effects (reviewed in Asem *et al.*, 2016). For example, low or loss of WNT5A expression is linked to an increased metastatic and invasive phenotype and poor prognosis in breast and colorectal cancers (reviewed in Kumawat *et al.*, 2016). Likewise, strong expression of WNT5A correlates with cell motility and tumor invasiveness in several tumor entities e.g. of prostate cancer (Yamamoto *et al.*, 2010) and melanoma (Weeraratna *et al.*, 2002). On the other hand, deletion or loss of WNT5A expression is observed in mouse and human B cell lymphomas and myeloid leukemias revealing a tumor suppressive role (Liang *et al.*, 2003; Yuan *et al.*, 2011). Furthermore, WNT5A has been shown to inhibit cell growth, migration and invasiveness of colorectal cancer and to have tumor suppressor activity in thyroid cancer by suppression of c-MYC (Kremenevskaja *et al.*, 2005; reviewed in Kumawat *et al.*, 2016).

2.2.5 WNT signaling in RMS

Currently, the knowledge about the role of WNT in RMS is sparse and restricted to β-catenin dependent WNT signaling. This is due to the fact that RMS do not show mutations in important components of the WNT signaling pathway such as β-catenin (Bouron-Dal Soglio *et al.*, 2009). Moreover, immunohistochemical staining showed that

β-catenin is expressed cytoplasmatically in RMS and does not localize to the nucleus (Bouron-Dal Soglio *et al.*, 2009; reviewed in Belyea *et al.*, 2012). However, a recent paper now shows mutations in β-catenin in 3.3 % of ERMS (Shukla *et al.*, 2012).

In addition, Singh and colleagues showed that the Wnt/β-catenin signaling pathway is inhibited in an ERMS cell line derived from ERMS tumors formed in p53/c-fos double-mutant mouse (Singh, S. *et al.*, 2010). This cell line overexpressed Wnt2, Wnt10a and Wnt8b compared to normal myoblasts. However, the majority of downstream target genes of canonical Wnt/β-catenin signaling, such as c-Myc and cyclins, were not differentially expressed and the Wnt receptors Fzd1, 3 and 5, the signaling mediator Dvl, Lef1 and Pygo were downregulated. In addition, the most highly overexpressed genes were Wnt pathway inhibitors such as Sfrp2, Sfrp4, Dkk1 and Ndk1. TOPflash reporter assay confirmed that canonical Wnt/β-catenin signaling was downregulated in this ERMS cell line when compared with normal myoblasts. Furthermore, activation of the Wnt pathway by LiCl induced MyoD and MyHC expression levels and promoted myoblast fusion. In summary, these results suggest that activation of the Wnt pathway in RMS may mainly promote anti-oncogenic effects and myogenic differentiation (Singh, S. *et al.*, 2010; for review see Roma *et al.*, 2012). With the exception of two ERMS samples, Annavarapu and colleagues confirmed the consistent and cytoplasmatic expression of β-catenin in primary human RMS (Annavarapu *et al.*, 2013). In addition, they showed that the ARMS cell lines Rh4 and Rh30 and the ERMS cell lines RD and RD18 express central regulatory WNT/β-catenin pathway proteins such as GSK3β, DVL3, AXIN1 and LRP6, and that this pathway is functionally active in response to recombinant Wnt3a by means of TOPflash reporter assay and AXIN2 Western blot analysis. Moreover, stimulation with recombinant Wnt3a let to nuclear translocation of β-catenin, which resulted in i) induction of the myogenic differentiation markers MYOGENIN, MYOD and MYF5 in both ARMS and ERMS cell lines and ii) a significant decrease in the proliferation rate of ARMS but not of ERMS. Due to these data, the authors conclude that β-catenin dependent WNT signaling in RMS promotes myogenic differentiation and probably plays a tumor suppressive role in RMS (Annavarapu *et al.*, 2013).

3 Aim of the Study

Canonical WNT/β-catenin signaling is required for normal muscle development and differentiation, and also contributes to a variety of human diseases including cancer. LEF1 – a central regulatory component of WNT signaling – is expressed in 50 % of primary human RMS, which is a tumor that originates from cells that normally develop into skeletal muscles. In this thesis, the role of LEF1 and WNT signaling was studied in more depth in this tumor entity.

First, the role of canonical Wnt signaling activity on RMS growth was studied in a genetic approach. For this purpose, heterogeneous *Ptch*$^{+/-}$ mice (*Ptch*$^{del/+}$) that develop RMS at a high incidence were crossed to mice expressing a hypomorphic Wnt3a allele. Second, we investigated whether the canonical WNT signaling pathway is generally active or can be activated in the human ARMS cell lines Rh41 and RMS-13 and in the ERMS cell line TE671, and if LEF1 is important in this process. For this purpose, stable LEF1 KD cells were used and TOP/FOP reporter assays and immunofluorescence staining were performed. Furthermore, we clarified a potential impact of LEF1 on the regulation of TCF factors in RMS. In addition, the stable LEF1 KD cells were analyzed with respect to proliferation, apoptosis, their migratory and invasive properties, and the expression of the muscle differentiation markers *MYOD*, *MYH1*, *DESMIN* and *CKM*. Finally, the influence of LEF1 on RMS growth, aggressiveness and progression was studied *in vivo* using the chick chorio-allantoic membrane (CAM) model.

Since primary human RMS can also express the major player of non-canonical WNT signaling WNT5A and since *LEF1* gene expression tends to be positively correlated with that of *WNT5A* in some primary human ARMS and in RMS-13 cells, RMS-13 control and RMS-13 LEF1 KD cells were further used to analyze the potential regulation and/or interaction of LEF1 with non-canonical WNT5A signaling.

4 Material

4.1 Technical equipment

Table 1: List of laboratory equipment

Equipment	Supplier
-20 °C Freezer	Liebherr GmbH, Ochshausen
-80 °C Freezer (MDF-U71V)	Sanyo Electric Co., Ltd., Japan
4 °C Fridge	Robert Bosch GmbH, Stuttgart
Agarose gel electrophoresis chamber	Peqlab Biotechnology GmbH, Erlangen
Autoclave (Systec DX-150)	Systec GmbH & Co. KG, Linden
Biophotometer (6131)	Eppendorf AG, Hamburg
Bunsen burner (Gasprofi 2scs)	WLD-TEC GmbH, Göttingen
Centrifuges (Biofuge fresco, primo)	Kendro Laboratory Products GmbH, Hanau
Cold Plate (EG 1150 C)	Leica Microsystems GmbH, Wetzlar
Digital monochrome printer (P91D)	Mitsubishi, Ratingen
Digital photo camera (PowerShot G2)	Canon Deutschland GmbH, Krefeld
Dissecting set	Karl Hammacher GmbH, Solingen
Electronic pipettor (Accu-jet)	Brand GmbH & Co. KG, Wertheim
Electrophoresis System (XCell4 SureLock™ Midi-Cell)	Invitrogen GmbH, Karlsruhe
FACS Calibur	BD Biosciences GmbH, Heidelberg
Freezing Container (Mr. Frosty™)	Thermo Fisher Scientific GmbH, Schwerte
Heating block (Thermomixer)	Eppendorf AG, Hamburg
Heating stirrer (MR 3000/3001)	Heidolph Instruments GmbH & Co. KG, Schwabach
High-precision scales (Sartorius Basic plus)	Sartorius AG, Göttingen
Hybridization oven (HB-1000 Hybridizer)	UVP, Inc., Upland, USA
Imaging system Fluorchem Q	Fisher Scientific GmbH, Schwerte

Equipment	Supplier
Incubator (6000, BBD 6220)	Kendro Laboratory Products GmbH, Hanau
Inverted tissue culture fluorescence microscope (Axiovert 25)	Carl Zeiss Jena GmbH, Jena
Laboratory animal computed tomography system (QuantumFX)	PerkinElmer Health Sciences, Hopkinton USA
Liquid nitrogen tank	L'air liquid S.A., Paris, France
Mastercycler (EP gradient S)	Eppendorf AG, Hamburg
Microplate reader (Synergy Mx)	BioTek Instruments, Inc., Bad Friedrichshall
Microscope (Olympus BX 60)	Olympus Deutschland GmbH, Hamburg
Microtom (HN 40)	Leica Microsystems GmbH, Wetzlar
Microwave (Dimension 4)	Panasonic, Hamburg
Mini centrifuge	Carl Roth GmbH & Co. KG, Karlsruhe
Multifuge (Heraeus 3LR)	Thermo Scientific, Wilmington, USA
NEON Transfection System	Thermo Scientific, Wilmington, USA
Orbital shaker (Unimax 1010)	Heidolph Instruments GmbH & Co. KG, Schwabach
Paraffin dispenser (Dispenser PAG 12)	Medite GmbH, Burgdorf
Paraffin tissue floating bath	Medax GmbH & Co. KG, Rendburg
PCR machine	Eppendorf, Hamburg
pH-meter (inoLab pH Level 1)	WTW GmbH, Vienna, Austria
Pipettes (Multipette, One-channel)	Eppendorf AG, Hamburg
Power supply for electrophoresis	Peqlab Biotechnology GmbH, Erlangen
Real-Time PCR System (ABI Prism 7900HT)	Life Technologies GmbH, Darmstadt
Spectrophotometer (NanoDrop 8000)	Thermo Scientific, Wilmington, USA
Sterile bench (Euroflow Class IIA)	Clean Air Techniek bv, Woerden, Netherlands

Equipment	Supplier
Tissue embedding and rehydrating machine (TP 1020)	Leica Microsystems GmbH, Wetzlar
Tank electroblotting system (Owl™ VEP-2 Mini)	Thermo Scientific, Wilmington, USA
UV transilluminator	Intas Science Imaging GmbH, Göttingen
Vacuum pump	Schütt Labortechnik, Göttingen
Vortexer-Genie 2	Scientific Industries, Woburn, USA
Water purification system (Arium® 611 VF)	Sartorius, Göttingen

4.2 Consumables

Table 2: List of consumable materials

Consumer good	Supplier
1.5 ml reaction tubes	Ochs GmbH, Bovenden/Lenglern
1.5 ml safeseal microtubes	Sarstedt AG & Co., Nürnberg
2.0 ml reaction tubes	Sarstedt AG & Co., Nürnberg
15 ml centrifuge tubes	Greiner Bio-One GmbH, Frickenhausen
50 ml centrifuge tubes	Greiner Bio-One GmbH, Frickenhausen
96-well assay plate	Nunc GmbH & Co. KG, Wiesbaden
96-well reaction plate (black)	Costar Corning Incorporated, Corning, USA
96-well PCR plate (non-skirted)	4titude Ltd., Berlin
384-well PCR plate (Framestar)	4titude Ltd., Berlin
4-chamber culture slides	Thermo Fisher Scientific GmbH, Schwerte
BD Discardit™ II (2, 10, 20 ml)	BD Biosciences GmbH, Heidelberg
BD Microfine + Demi	BD Biosciences GmbH, Heidelberg
BD Plastipak	BD Biosciences GmbH, Heidelberg
Blotting paper (GB 33 B003)	Heinemann Labortechnik GmbH, Duderstadt

Consumer good	Supplier
Cell culture dishes (Nunclon Surface)	Nunc GmbH & Co.KG, Wiesbaden
Cell culture inserts (24-well, 8 µm)	BD Biosciences GmbH, Heidelberg
Cell scraper	Sarstedt AG & Co., Nürnberg
Combitips (0.2, 0.5, 2.5, 5, 10, 25, 50 ml)	Eppendorf AG, Hamburg
Coverslips	Menzel GmbH & Co.KG, Braunschweig
CryoPure tubes	Sarstedt AG & Co., Nürnberg
Cuvette (UVette)	Carl Roth GmbH & Co. KG, Karlsruhe
Disposable needles (Sterican Ø 0,45 x 12 mm)	B. Braun Medical AG, Emmenbrücke
Feeding tubes (1.0 x 60 mm)	Unimed SA, Lausanne, Schweiz
Filter tips (10 µl)	Sarstedt AG & Co., Nürnberg
Filter tips (100 µl, 200 µl, 1000 µl)	Kisker Biotech GmbH & Co. KG, Steinfurt
Flow cytometry tube	Sarstedt AG & Co., Nürnberg
Fluted filters	Sartorius AG, Göttingen
Glassware	Schott AG, Mainz
Milliporefilter (Nuclepore Track-Etch Membran)	Whatman GmbH, Dassel
Microscope slides (SuperFrost Plus)	Menzel GmbH & Co.KG, Braunschweig
Neubauer counting chamber	Brand GmbH & Co KG, Wertheim
Nitrocellulose membrane (Hybond ECL)	GE Healthcare Europe GmbH, Freiburg
NuPAGE Novex 4-12 % Bis-Tris Midi Gel	Invitrogen GmbH, Karlsruhe
Pasteur pipettes	Brand GmbH & Co.KG, Wertheim
Petri dishes	Ochs GmbH, Bovenden/Lenglern
Pipette tips (10 µl, 200 µl)	Ochs GmbH, Bovenden/Lenglern
Pipette tips (20 µl, 1000 µl)	Sarstedt AG & Co., Nürnberg
QPCR adhesive clear seal	4titude Ltd., Berlin
Scalpel blade (10, 24)	Aesculap AG & Co.KG, Tuttlingen

Consumer good	Supplier
Serological pipettes (2 ml, 5 ml, 10 ml, 25 ml)	Sarstedt AG & Co., Nürnberg
Sterile filter	Omnilab-Krannich, Göttingen
SOC Medium	Invitrogen GmbH, Karlsruhe
Syringe (30, 50 ml)	Terumo Medical Corp., Elkton, MD, USA
Tissue culture plates (6-, 12-, 24-well)	Sarstedt AG & Co., Nürnberg

4.3 Reagents and chemicals

Chemicals which are not listed below were purchased from Sigma-Aldrich Chemie GmbH, Steinheim.

Table 3: Utilized reagents and chemicals

Reagents and chemicals	Supplier
50 bp, 100 bp plus, 1 kb DNA Ladder	Fermentas GmbH, St. Leon-Rot
7-Amino-Actinomycin D (7-AAD)	BD Biosciences GmbH, Heidelberg
Agarose	Bio-Budget Technologies GmbH, Krefeld
Ampuwa	Fresenius Kabi Deutschland GmbH, Bad Homburg
APC AnnexinV	BD Biosciences GmbH, Heidelberg
Boric acid	Carl Roth GmbH & Co. KG, Karlsruhe
Bovine serum albumin (BSA)	Carl Roth GmbH & Co. KG, Karlsruhe
Chloroform	Carl Roth GmbH & Co. KG, Karlsruhe
Citric acid	Carl Roth GmbH & Co. KG, Karlsruhe
Deoxyribonucleotide triphosphate (dNTP)	Roche Diagnostics GmbH, Mannheim
Dithiothreitol, 100 mM (DTT)	Invitrogen GmbH, Karlsruhe
DNase/RNase-free distilled water	GIBCO Invitrogen GmbH, Karlsruhe
Eosin Y	Merck KGaA, Darmstadt
Ethanol (EtOH) 99 %	J.T. Baker B.V., Deventer, Netherlands

Reagents and chemicals	Supplier
Ethidium bromide (0.07 %)	inna-TRAIN-Diagnostics, Kronberg
Ethylenediaminetetraacetic acid (EDTA)	ICN Biochemicals Inc., AuRORa, USA
EtOH 99 % denatured	CVH Chemie-Vertrieb GmbH & Co. Hannover KG, Hannover
Haematoxylin, Mayer's	Merck KGaA, Darmstadt
Isopropyl alcohol	Carl Roth GmbH & Co. KG, Karlsruhe
Laemmli loading buffer, non-reducing, 4 x	bioPlus, Mol, Belgium
Matrigel	Costar Corning Incorporated, Corning, USA
Methanol	Carl Roth GmbH & Co. KG, Karlsruhe
NovocastraTM Epitope Retrieval Solution, pH 6.0; pH 9.0	Leica Microsystems GmbH, Wetzlar
NuPAGE MES SDS Running Buffer, 20 x	Invitrogen GmbH, Karlsruhe
Paraformaldehyde	Carl Roth GmbH & Co. KG, Karlsruhe
Peroxidase-Blocking solution	DAKO GmbH, Hamburg
Pertex mounting medium	Medite Medizintechnik GmbH, Burgdorf
Phosphatase inhibitor cocktail tablets (PhosSTOP)	Roche Diagnostics GmbH, Mannheim
Phosphate buffered saline (PBS)-Tablets	GIBCO Invitrogen GmbH, Karlsruhe
Potassium aluminum sulfate	Merck KGaA, Darmstadt
Powdered milk	Carl Roth GmbH & Co. KG, Karlsruhe
ProLong Gold antifade mountant with DAPI	Thermo Fisher Scientific GmbH, Schwerte
Propidium Iodide (PI)	Miltenyi Biotec, Bergisch Gladbach
Protease inhibitor cocktail tablets (Complete, mini)	Roche Diagnostics GmbH, Mannheim
Proteinase K	Carl Roth GmbH & Co. KG, Karlsruhe
Random Hexamer-Oligonucleotides	Invitrogen GmbH, Karlsruhe
SeeBlue® Plus2 Pre-Stained Standard	Invitrogen GmbH, Karlsruhe
Sodiumdodecylsulfate (SDS)	Carl Roth GmbH & Co. KG, Karlsruhe

Reagents and chemicals	Supplier
Trichloro acetaldehyde hydrate	Merck KGaA, Darmstadt
TRIzol Reagent	Invitrogen GmbH, Karlsruhe
Xylene	J.T. Baker B.V., Deventer, Netherlands

4.4 Signaling pathway inhibitors

Drugs, their appropriate solvents and final concentrations for *in vitro* analyses are listed in Table 4.

Table 4: List of applied inhibitors

Inhibitor	Solvent	Concentration	Supplier
GDC-0941	DMSO	10 μM	Genentech, San Francisco, USA
MK-2206	DMSO	1 μM	Selleckchem, Munich
PI103	DMSO	3 μM	Axxora Deutschland GmbH, Lörrach

4.5 Kits and ready-to-use reaction systems

Unless indicated otherwise, all kits and ready-to-use reaction systems were used according to the manufacturer's instructions.

Table 5: Kits and ready-to-use reaction systems

Reaction system	Supplier
Amersham ECL Plus™ Western Blotting Detection Reagents	GE Healthcare Europe GmbH, Freiburg
10 x AnnexinV binding buffer	BD Biosciences GmbH, Heidelberg
Cell Proliferation ELISA, BrdU (chemiluminescent)	Roche Diagnostics GmbH, Mannheim
Dual-Luciferase®Reporter Assay System	Promega GmbH, Mannheim
NEON Transfection Kit	Thermo Scientific, Wilmington, USA
Pierce BCA Protein Assay Kit	Thermo Fisher Scientific GmbH, Schwerte
Platinum SYBR Green qPCR SuperMix	Invitrogen GmbH, Karlsruhe

Reaction system	Supplier
PureLink®HiPure Plasmid Filter Midiprep Kit	Invitrogen GmbH, Karlsruhe
PureLink®HiPure Plasmid Midiprep Kit	Invitrogen GmbH, Karlsruhe
Reverse Transcriptase (SuperScriptII®)	Invitrogen GmbH, Karlsruhe
RevertAid™ H Minus First Strand cDNA Synthesis	Thermo Fisher Scientific GmbH, Schwerte
Taq-Polymerase (MolTaq)	Molzym GmbH & Co. KG, Bremen

4.6 Buffers and solutions

Unless mentioned otherwise, all solutions were prepared with double distilled water (ddH_2O).

Table 6: Buffers and solutions and their respective composition

Buffer	Composition
6 x SDS loading buffer	35 % (v/v) Glycerol 9 % (w/v) SDS 8.5 % (w/v) DTT 0.1 % (w/v) Bromphenolblue dissolved in Upper gel buffer
10 x PBS, pH 7.4	1.4 M NaCl 65 mM Na_2HPO4 27 mM KCl 15 mM KH_2PO_4
10 x Tris-boric acid-EDTA (TBE), pH 8.0	890 mM Tris/HCl 730 mM Boric acid 12.5 mM EDTA
10 x Tris-buffered saline (TBS), pH 7.4	150 mM NaCl 10 mM Tris/HCl, pH 8.0
Blotting buffer	200 mM Glycine 25 mM Tris 20 % (v/v) Methanol

Buffer	**Composition**
BSA-azide	0.02 % Sodium azide 2 % BSA dissolved in TBST
Cresol	0.1 % (w/v) Cresol saturated sucrose solution
dNTP-Mix	10 mM dATP 10 mM dCTP 10 mM dGTP 10 mM dTTP
Eosin solution	80 % (v/v) EtOH 1 % (w/v) Eosin y (water soluble)
Haematoxylin solution, Mayer's	5 % (w/v) Potassium aluminum sulfate 5 % (w/v) Trichloro acetaldehyde hydrate 1 % (w/v) Citric acid 0.1 % (w/v) Haematoxylin 0.015 % (w/v) Sodium iodate
LB-agar	1.5 % (w/v) Agar in LB-medium
Lysis buffer, pH 8.8	120 mM NaCl 30 mM Tris/HCl, pH 7.5 10 % (v/v) Glycerol 1 % (v/v) Triton X-100 Protease and phosphatase inhibitors (1 tablet/50 ml) added directly before use: 2 mM DTT 500 µM Phenylmethanesulfonylfluoride (PMSF)
Lysogeny broth medium (LB medium)	1 % (w/v) Bacto-tryptone 1% (w/v) NaCl (pH 7.0) 0.5 % (w/v) Yeast extract
Paraformaldehyde (PFA)	4 % (w/v) Paraformaldehyde dissolved in PBS
PBS (cell culture)	1 PBS tablet ad 500 ml ddH_2O

Buffer	Composition
Proteinase K, pH 8.0	50 mM Tris/HCl 5 mM EDTA 10 mg/ml Proteinase K
STE-Buffer, pH 8.0	100 mM NaCl 50 mM Tris/HCl 1 mM EDTA 1 % (w/v) SDS
TBS-Triton X-100	0.1 % Triton X-100 dissolved in TBS
TBS-Tween (TBST)	0.05 % Tween-20 dissolved in TBS
Trypan blue	0.4 % (w/v) Trypan blue dissolved in PBS
Upper gel buffer, pH 6.8	6 % (w/v) Tris 0.4 % (v/v) SDS

4.7 Media

4.7.1 Media and agar plates for culture of prokaryotic cells

LB medium and LB agar plates were prepared as described in Table 7. After autoclaving and cooling to 55 °C either 50 µg/ml ampicillin or 25 µg/ml kanamycin (Carl Roth GmbH, Karlsruhe) were added. Both, media and plates, were stored at 4 °C.

4.7.2 Media and reagents for culture of eukaryotic cells

Cell culture media and supplements for culture of eukaryotic cell lines are listed in Table 7.

Table 7: Media and reagents used for cell culture of eukaryotic cells

Media and reagents	Supplier
Accutase	PAA Laboratories GmbH, Pasching
Dulbecco's Modified Eagle Medium (DMEM)	Gibco, Invitrogen GmbH, Karlsruhe
Fetal calf serum (FCS)	Gibco, Invitrogen GmbH, Karlsruhe
G 418 disulfate salt solution (50 mg/ml)	Sigma-Aldrich Chemistry GmbH, Steinheim
Penicillin (10.000 U/ml)/Streptomycin (10 mg/ml) (P/S)	PAN Biotech GmbH, Aidenbach

Media and reagents	Supplier
Puromycin dihydrochloride (10 mg/ml)	Sigma-Aldrich Chemistry GmbH, Steinheim
RPMI 1640 (RPMI)	Gibco, Invitrogen GmbH, Karlsruhe
TrypLE Express	Gibco, Invitrogen GmbH, Karlsruhe
Taq-Polymerase (MolTaq)	Molzym GmbH & Co. KG, Bremen

4.8 Biological material

4.8.1 Bacterial strains

For transformation and amplification of plasmid DNA the chemical competent *Escherichia coli* (*E. coli*) strain DH5α (Invitrogen GmbH, Karlsruhe) was used.

4.8.2 Eukaryotic cell lines

The eukaryotic cell lines used in this thesis and their appropriate culture conditions are listed in Table 8.

Table 8: List of eukaryotic cell lines and culture conditions

RMS cell line	Subtype	Medium and supplements	Supplier
Rh41	human ARMS	RPMI, 20 % FCS, 1 % P/S	ATCC
RMS-13	human ARMS	RPMI, 10 % FCS, 1 % P/S	ATCC
TE671	human ERMS	RPMI, 10 % FCS, 1 % P/S	ATCC
Other cell line	**Origin**	**Medium and supplements**	**Supplier**
HEK293	human embryonic kidney	DMEM, 10 % FCS, 1 % P/S	ATCC
Lcells	murine fibroblasts	DMEM, 10 % FCS, 1 % P/S	ATCC
Wnt-3A Lcells	murine fibroblasts stably overexpressing Wnt3a	DMEM, 10 % FCS, 1 % P/S, 0.4 µg/ml G 418	ATCC

4.8.3 Mouse lines

For *in vivo* studies and to inhibit canonical Wnt signaling in RMS, heterozygous *Ptch*$^{+/-}$ mice (*Ptch*$^{del/+}$) mice were bred to *Wnt3a*$^{vt/vt}$ (*Wnt*$^{vt/vt}$) mice, which were obtained from the Department of Developmental Genetics, Max-Planck-Institute for Molecular Genetics, Berlin. The *vt* (*vestigial tail*) mutation is a hypomorphic Wnt3a allele that in the homozygous state results in loss of caudal vertebrae and thus loss of the tail (Greco *et al.*, 1996). The resulting *Ptch*$^{del/+}$*Wnt*$^{vt/vt}$ were on a 50 % Balb/c and a remaining undefined mixed genetic background (C57BL/6N x 129/SvEv x C3H). For this purpose, the respective *Ptch*$^{del/+}$*Wnt*$^{+/vt}$ littermates served as control group. The *Wnt*$^{vt/vt}$ genotype was determined by lack of tail (Greco *et al.*, 1996). Primers and respective PCR conditions for genotyping of *Ptch*$^{del/+}$ mice are shown in Table 9 and Table 18.

The heterozygous *Ptch*$^{del/+}$ mice were generated and bred in-house. In *Ptch*$^{del/+}$ mice exons 8 and 9 of the *Ptch* gene are deleted resulting in an aberrant *Ptch* transcript (Zibat *et al.*, 2009; Nitzki *et al.*, 2012).

All experiments using animals were performed in agreement with all relevant legal and ethical requirements.

4.8.4 Biopsies

A tissue microarray (TMA) with 125 RMS biopsies from the Paediatric Tumor Register, Kiel, Germany and 20 fresh-frozen RNA samples from the CWS ("Cooperative Weichteilsarkom Studiengruppe") tissue bank, Stuttgart, Germany (S1 - S20) were studied. Histopathology of all cases was centrally reviewed by Prof. I. Leuschner (Paediatric Tumor Registry, Kiel, Germany). All patients were treated according to CWS protocols. All studies were approved by the appropriate ethics and review committees. Written informed consent according to the Declaration of Helsinki was obtained from all patients or their legal guardians, depending on the patients' age.

4.9 Synthetic DNA-oligonucleotides

Synthetic DNA-oligonucleotides (primers) were obtained from Eurofins MWG Operon, Ebersberg. For long-term storage (at -80 °C) 100 µM stock solutions in ddH_2O were prepared and 10 µM working solutions were used for polymerase chain reaction (PCR) methods.

PCR for genotyping of mice was performed using the primers presented in Table 9.

Table 9: Oligonucleotides for genotyping of mice

Allele	Primer name	Primer sequence (5'-3' orientation)	Reference
Ptch del	Exon 7-F	AGGAAGTATATGCATTGGCAGGAG	(Uhmann *et al.*, 2007)
	Neo-R	GCATCAGAGCAGCCGATTGTCTG	
Ptch wt	mPTCNx_f	TGGTAATTCTGGGCTCCCGT	(Uhmann *et al.*, 2007)
	mPTCwt_r.2	ACACAACAGGGTGGAGACCACT	

del: deletion, wt: wildtype

Oligonucleotides used for analysis of gene expression levels *via* quantitative real-time PCR (qRT-PCR) are listed in Table 10. All primer pairs were intron-flanking, except of the primers for *18S* and *hMYOD* that were located within a single exon.

Table 10: Oligonucleotides for qRT-PCR

Transcript	Primer name	Primer sequence (5'-3' orientation)	Location in exon
18S	18S-fwd	CGCAAATTACCCACTCCCG	1
	18S-rev2	TTCCAATTACAGGGCCTCGAA	1
hAXIN2	hAxin2-F	GCCAACGACAGTGAGATATCC	2
	hAxin2-R	CTCGAGATCAGCTCAGCTGCA	4
hCKM	CKM_RT_F2	TGGTGTGGGTGAACGAGGAGGAT	3
	CKM_RT_R2	AACTTGGGGTGCTTGCTCAGGTG	3,4
*hCTNNB1**	CTNNB1_RT_For	GAAACGGCTTTCAGTTGAGC	12
	CTNNB1_RT_Rev	CTGGCCATATCCACCAGAGT	14
hDESMIN	Desmin_RT_F1	CATCGCGGCTAAGAACATTT	4
	Desmin_RT_R1	GCCTCATCAGGGAATCGTTA	5,6
*hGAPDH**	GAPDH_For	TGCACCACCAACTGCTTAGC	5
	GAPDH_Rev	GGCATGGACTGTGGTCATGAG	5/6
hLEF1	FL-hLEF1-F	TAGCTGACATCAAGTCTTCCT	1
	FL-hLEF1-R	AGATCCATTTGACATGTATGGG	3
*hLEF1**	Lef1_RT_F	CGGGTACATAATGATGCCAA	3
	Lef1_RT_R	CGTCACTGTAAGTGATGAGGG	4
hMYH1	hsMYH1F.1	TGTGCAGCAGGTGTACAATGC	13,14
	hsMYH1R.1	TGCACAGCTGCTCCAGGCT	15
hMYOD	hMYOD F	CGAACCCCCAACCCGATA	3
	hMYOD R	GAAAAAACCGCGCTGTGT	3
hTCF1	TCF-1_RT_F	GCAACCTGAAGACACAAGCA	4/5
	TCF-1_RT_R	GCAATGACCTTGGCTCTCAT	5
hTCF3	TCF-3_RT_F	GAGTCGGAGAACCAGAGCAG	1
	TCF-3_RT_R	CTGTCCTGAGGCCTTCTCAC	2/3

hTCF4	TCF-4_RT_F	ATGCTTCCATGTCCAGGTTC	8/9
	TCF-4_RT_R	CACTCTGGGACGATTCCTGT	9
hWNT5A	hsWNT-5aF.1	GCTCCTACGAGAGTGCTCGCAT	4
	hsWNT-5aR.1	ACTTGCCCCGGCTGTTGA	5
*hWNT5A**	WNT5A_RT_F	TGGCTTTGGCCATATTTTTC	1
	WNT5A_RT_R	CCGATGTACTGCATGTGGTC	2

***** oligonucleotides used for qRT-PCR analyses of primary human ARMS and ERMS samples

4.10 Synthetic RNA-oligonucleotides

The following RNA-oligonucleotides were used for knockdown experiments in human RMS cell lines.

Table 11: Oligonucleotides for transfection

Application	RNA	Information/ Sequence	Supplier
β-catenin knockdown	siRNA	ON-TARGETplus siRNA pool J-003482-09, J-003482-12	Dharmacon
LEF1 knockdown	shRNA	TGGAGTTGACATCTGATGG (mature sequence)	Thermo Scientific
scrambled siRNA	siRNA	AllStars negative	Qiagen

4.11 Plasmids

The following plasmids were used for transfection and viral transduction of human RMS cell lines.

Table 12: Plasmids used for human RMS cell lines

Plasmid name	Application	Supplier/ Reference
pCl-neo-β-cateninS33Y	Dual-Luciferase	(Morin *et al.*, 1997)
pCR3.1	Dual-Luciferase	Invitrogen GmbH, Karlsruhe
pGIPZ	Lentiviral transduction	GIPZ Lentiviral shRNAmir Library, Thermo Scientific Open Biosystems
pRL-CMV	Dual-Luciferase	Promega GmbH, Mannheim
SuperTOPFlash	Dual-Luciferase	(Korinek *et al.*, 1997)
SuperFOPFlash	Dual-Luciferase	(Korinek *et al.*, 1997)

4.12 Antibodies

The following antibodies in Table 13 were used for Western blot of human RMS cell lines. Antibodies used for immunohistochemistry of primary RMS samples and for immunofluorescence staining of human RMS cell lines are shown in Table 14.

Table 13: Antibodies for Western blot

Antibody	Dilution	Source	Supplier
Primary antibody			
Anti-AKT; (610861)	1:1000	Mouse, mAB	BD Biosciences
Anti-β-Actin; (13E5)	1:1000	Rabbit, mAB	Cell Signaling
Anti-β-catenin; (610153)	1:10000	Mouse, pAB	Beckton Dickinson GmbH
Anti-HSC-70; (sc-7298)	1:10000	Mouse, mAB	Santa Cruz
Anti-LEF1; (C18A7)	1:1000	Rabbit, mAB	Cell Signaling
Anti-pAKT (Ser473); (193H12)	1:1000	Rabbit, mAB	Cell Signaling
Anti-WNT5A; (MAB645)	1:2000	Rat, mAB	R&D Systems
Secondary antibody			
Anti-Mouse/HRP; (NA931)	1:5000	Sheep, pAB	GE Healthcare
Anti-Rabbit/HRP; (A0545)	1:5000	Goat, pAB	Sigma-Aldrich
Anti-Rat/HRP; (3030-05)	1:10000	Goat, pAB	Southern Biotech

mAB: monoclonal antibody, pAB: polyclonal antibody

Table 14: Antibodies for immunohistochemistry/immunofluorescence

Antibody	Dilution	Source	Supplier
Primary antibody			
Anti-β-catenin; (610153)	1:250	Mouse, pAB	Beckton Dickinson GmbH
Anti-β-catenin; (CAT-5H10)*	1:200	Mouse, mAB	Zymed
Anti-WNT5A; (MA5-15511, clone 3D10)*	1:100	Mouse, mAB	ThermoFisher
Anti-HLA-A,B,C; (311402)	1:100	Mouse, mAB	BioLegend
Anti-LEF1; (EPR2029Y)*	1:250	Rabbit, mAB	Abgent

Antibody	Dilution	Source	Supplier
Secondary antibody			
Anti-Mouse Alexa Fluor 594 IgG2a (γ2a); (A-21135)	1:200	Goat, pAB	ThermoFisher
Anti-Mouse Rhodamine (TRITC) (H+L); (715-025-150)	1:200	Donkey, pAB	Jackson ImmunoResearch
EnVision Detection Systems Peroxidase/DAB/Rabbit/Mouse; (K4065)*	Manufacturer instructions	pAB	DAKO

*antibodies used for immunohistochemistry; mAB: monoclonal antibody, pAB: polyclonal antibody

4.13 Software

Table 15: List of used software

Software	Developer
Adobe Photoshop CS5	Adobe Systems Incorporated, San Jose, USA
AlphaView Q SA 3.2.2	Cell Bioscience, California, USA
CellSens Dimension	Olympus GmbH, Hamburg
Endnote X5	Thomson ISI ResearchSoft, California, USA
FlowJo	Tree Star Inc., Oregon, USA
GraphPad Prism 6	GraphPad Software, Inc., La Jolla, CA, USA
Intas GDS	Intas Science Imaging Instruments GmbH, Göttingen
Gen5 1.11	BioTek Instruments, Inc., Bad Friedrichshall
Microsoft Office	Microsoft Co., Redmont, USA
SDS 2.2	Applied Biosystems, Darmstadt
Statistica 10	StatSoft GmbH, Hamburg

4.14 Databases

Table 16: List of uses databases

Database	Homepage
BasicLocalAlignmentSearchTool (BLAST)	http://blast.ncbi.nlm.nih.gov/Blast.cg
Ensembl	http://www.ensembl.org/index.html
MGI 3.43-mouse genome informatics	http://www.informatics.jax.org/
National Center for Biotechnology Information (NCBI)	http://www.ncbi.nlm.nih.gov/

5 Methods

5.1 Molecular biology methods

5.1.1 Nucleic acid isolation

5.1.1.1 Isolation of genomic DNA

For isolation of genomic DNA (gDNA) from mouse tissue, tail or ear biopsies were incubated overnight at 55 °C in 500 µl of STE buffer containing 0.5 mg/ml Proteinase K. Afterwards undigested tissue debris was removed by centrifugation for 10 min at 13000 rpm. The supernatant was transferred into a fresh reaction tube containing 1 ml cold 99 % EtOH and was shaken thoroughly to precipitate the nucleic acid. The gDNA was pelleted by centrifugation (25 min, 13000 rpm), washed with 500 µl 70 % ethanol and centrifuged again (10 min, 13000 rpm). Finally, the gDNA was dried for 10 min at 55 °C, solved in 125 µl ddH_2O for 10 min at 42 °C and 1400 rpm and stored at -20 °C for further analyses.

5.1.1.2 Isolation of total RNA

Extraction of total RNA from cell culture and RMS biopsies was performed by using TRIzol reagent according to the manufacturer's instructions. All steps were carried out on ice if not otherwise stated to avoid RNA degradation. Briefly, the cells were washed with cold PBS and detached by adding 1 ml TRIzol. Samples were transferred into 2 ml reaction tubes, vortexed for 2 min and incubated for 5 min at room temperature (RT). Subsequently, 200 µl of chloroform were added followed by vortexing for 15 sec and incubation for another 3 min at RT. After phase separation by centrifugation (10 min, 13000 rpm, 4 °C) the upper aqueous phase (containing the RNA) was transferred into 1 ml isopropyl alcohol and precipitated overnight at -20 °C. Afterwards the samples were centrifuged (30 min, 13000 rpm, 4 °C), the supernatant was removed and the pellet was washed two times with 500 µl 70 % DNase/RNase-free EtOH (-20 °C) by centrifugation (10 min, 13000 rpm, 4 °C). The pellet was dried for 10 min at RT and dissolved in DNase/RNase-free H_2O for 5-10 min at 56 °C. The RNA was stored at -80 °C before use.

5.1.1.3 Medium-scale plasmid purification

Medium-scale plasmid purification was performed using the PureLink®HiPure Plasmid Midiprep or PureLink®HiPure Plasmid Filter Midiprep kit according to the manufacturer's instructions. The plasmid DNA was solved in DNase/RNase-free H_2O. To increase

plasmid purity, the plasmid DNA was precipitated by isopropyl alcohol. In brief, an equal volume of isopropyl alcohol was added to the plasmid DNA solution, mixed thoroughly and precipitated overnight at -20 °C. The DNA was pelleted by centrifugation (30 min, 13000 rpm, 4 °C), washed with 500 µl 70 % DNase/RNase-free EtOH (-20 °C) by centrifugation (10 min, 13000 rpm, 4 °C) and dried at RT for 10 min. Finally, the plasmid DNA was resuspended in DNase/RNase-free H_2O for 10 min at 42 °C and 1400 rpm and stored at -20 °C.

5.1.2 Photometric quantification of nucleic acids

DNA and RNA concentration was quantified using a spectrophotometer (NanoDrop 8000) by determination of the optical density at 260 nm (OD_{260}). Since an OD_{260} of 1.0 corresponds to 50 µg/ml pure DNA or 40 µg/ml pure RNA, concentrations were calculated according to the following formula:

$$\text{concentration c } \left(\frac{\text{ng}}{\mu\text{l}}\right) = OD_{260} \text{ x 50 (DNA) or 40 (RNA)}$$

Because the OD at 280 nm (OD_{280}) provides the protein concentration of the sample, the ratio OD_{260}/OD_{280} was used to determine nucleic acid purity. A ratio of 1.8 and 2.0 is generally considered for pure DNA and RNA preparation, respectively.

5.1.3 Reverse transcription of RNA (cDNA synthesis)

For synthesis of complementary DNA (cDNA) from cultured cells, 2 µg of RNA were reversely transcribed using the SuperScriptII Reverse Transcriptase System in a final reaction volume of 20 µl. The RNA was incubated with 250 ng hexamers for 10 min at 70 °C. Afterwards 10 mM DTT and 0.5 mM dNTPs in 1st strand buffer were added and incubated at RT for 10 min. Following pre-warming of the samples to 42 °C for 2 min, 1 µl of SuperScriptII (200 U/µl) was added and the mixture was incubated for 1 h at 42 °C. The synthesis reaction was stopped at 70 °C for 10 min. Assuming that the reverse transcription reaction is 50 % efficient, the final concentration of cDNA was 50 ng/µl.

Furthermore, cDNA of 20 fresh-frozen RNA samples from the CWS (“Cooperative Weichteilsarkom Studiengruppe”) tissue bank, Stuttgart, Germany was synthesized by Dr. Katja Simon-Keller using the RevertAid H Minus First Strand cDNA Synthesis Kit and provided for further analysis.

5.1.4 Polymerase chain reaction (PCR)

5.1.4.1 PCR-based genotyping of mouse tail or ear gDNA

PCR-based amplification of gDNA was carried out in reaction volumes of 10 or 20 µl per assay and performed with the reagents and final concentrations shown in Table 17.

Table 17: Reaction mixture for genotyping of mouse tail or ear gDNA

Concentration	Component
10-100 ng	gDNA template
0.5 µM	forward primer
0.5 µM	reverse primer
0.2 mM	dNTP-Mix
10 % (v/v)	Cresol
1x	Polymerase buffer
0.1 U	Taq-Polymerase

The primer sequences used for genotyping are given in Table 9 and respective PCR conditions are shown in Table 18.

Table 18: PCR conditions for genotyping of mice

	Step	*Ptch del*	*Ptch wt*
1	Initiation	5 min	2 min
2	Denaturation	1 min	20 sec
3	Annealing	1 min	20 sec
4	Elongation	3 min	45 sec

del: deletion, wt: wildtype

The steps 2 to 4 were repeated for 35 cycles. The reaction was terminated by a final elongation step for 5 min at 72 °C. The samples were subsequently analyzed by agarose gel electrophoresis.

5.1.4.2 Quantitative Real-Time PCR (qRT-PCR)

Gene expression was analyzed using SYBR Green based assays. Primers for amplification of the target transcripts are listed in Table 10. The assays were performed in a total reaction mixture of 10 µl using the reagents listed in Table 19. Amount of ddH_20 and SYBR Green depended on the analyzed gene.

Table 19: Reaction mixture for qRT-PCR

Amount/ Concentration	Component
2 µl	cDNA template
0.4 µM	forward primer
0.4 µM	reverse primer
2.2 or 3.2 µl	ddH_20
4 or 5 µl	SYBR Green

Gene expression levels were calculated using the standard curve method. For quantification of the RNA levels a standard curve for each respective gene was prepared by 5-fold serial dilutions of 20 ng cDNA (80 pg cDNA for *18S* rRNA) of a standard sample. Standard samples were derived from tissue or cells known to express the target gene. The logarithm of each known cDNA concentration in the dilution series was plotted against the respective measured cycle threshold. The derived linear trend line with the corresponding equation ($y = mx + b$) served to interpolate the amount of cDNA in each sample. Finally, the transcript levels of each sample were normalized to the expressed housekeeper gene *18S* rRNA. The samples were measured in triplicates. Analysis was done using the SDS 2.2, Microsoft Excel and GraphPad Prism 6 software.

Gene expression analyses of primary human ARMS and ERMS from fresh-frozen RNA samples were performed by Dr. Katja Simon-Keller on the Step one plus system. Amplification of *GAPDH* mRNA served to normalize the amount of sample DNA. The primers are shown in Table 10.

5.1.5 Agarose gel electrophoresis

Gel electrophoresis was performed to separate DNA fragments by their size. Agarose gels were prepared by boiling 1 % to 2 % (w/v) agarose in 1 x TBE buffer for 2-3 min at 1000 W in a microwave. After cooling down, liquid gels were supplemented with 5-10 drops of 0.07 % ethidium bromide and polymerized at RT. Afterwards gels were placed in 1 x TBE buffer in an electrophoresis chamber, and an appropriate DNA ladder and the DNA samples were loaded onto the gels. The gels were run constantly at 100 to 150 V. For documentation an UV transilluminator was used.

5.1.6 Cloning techniques

5.1.6.1 Transformation of bacteria

50 µl competent *E. coli* DH5α were thawed on ice, mixed with 50-100 ng of plasmid DNA and incubated on ice for 20 min. Following a 45 sec heat shock at 42 °C, the samples were returned to ice for 2 min before adding 500 µl of SOC medium (super optimal broth with catabolite repression medium). The bacterial solution was gently shaken at 900 rpm and 37 °C for 1 h. 25-100 µl of the solution was plated out onto LB agar plates containing the adequate antibiotics and incubated ON at 37 °C. The next day, Midi DNA preparations (see Chapter 5.1.1.3) were started by picking single bacterial colonies that were inoculated into 100 ml LB medium containing the adequate antibiotic and incubated at 37 °C and 225 rpm ON.

5.1.6.2 Restriction hydrolysis

For test restriction of plasmids for TOP/FOP reporter assays (see Table 12, see Chapter 5.2.6) the total reaction mixture of 10 µl was prepared as shown in Table 20 with the appropriate enzymes and buffers according to the manufacturer's instructions.

Table 20: Reaction mixture for restriction hydrolysis

Amount/ Concentration	Component
100-200 ng	plasmid DNA
0.1 U	restriction enzyme
1 x	restriction buffer
ad 10 µl	ddH_20

If necessary and possible a double restriction digest was performed and each reaction was carried out for 1 h at the optimal temperature for each enzyme. Restriction hydrolysis was stopped by heat-inactivation if required. Finally, the sample DNA was separated by agarose gel electrophoresis. All used enzymes were purchased from NEB (Ipswich, USA) or Invitrogen (Karlsruhe).

5.2 Cell biology methods

5.2.1 Culture of eukaryotic cells

All eukaryotic cell lines were cultured in an incubator at constant 37 °C, 5 % CO_2 and 95 % humidity. Every second to forth day the media were refreshed and cells were split when reaching 80 % to 90 % confluence. Splitting of the cells was performed by detaching the cells with 1-3 ml of TrypLE Express. After the cells started to detach the reaction was stopped by adding FCS-containing medium. Cells were separated by gentle pipetting and an adequate amount of the cell suspension was transferred to a new culture ware containing fresh medium. An overview about the used cell lines and the respective culture conditions is given in Table 8. The number of seeded cells and culture conditions used for *in vitro* assays are listed in Table 21. Depending on the experimental settings, human RMS cells were incubated with drugs (Western blot, Table 4), transfected and treated with Wnt3a conditioned medium (Wnt3a CM) as indicated in the respective experiments.

Table 21: Cell culture conditions for *in vitro* assays

Assay	Format	cells/well
qRT-PCR	6-well plate	30×10^4
Western blot	10 cm-culture dishes	15×10^5
TOP/FOP reporter	96-well plate	5000
Proliferation	96-well plate	6000
Apoptosis	6-well plate	22×10^4
Migration	24-well plate	10^5
Invasion	Modified Boyden chamber (24-well format)	10^5
Immunofluorescence staining	4-chamber culture slides	4×10^4

5.2.2 Cryopreservation of eukaryotic cells

For long-term storage eukaryotic cell lines were stored in liquid nitrogen. Cells were rinsed with PBS and detached as described above. Afterwards the cell suspensions were transferred into a 15 ml reaction tube, pelleted by centrifugation (5 min, 750 rpm, 4 °C) and resuspended in FCS supplemented with 5 % DMSO. Subsequently, 1 ml aliquots in cryo tubes were frozen in a Mr. Frosty freezing container at -80 °C. After 16 h the cells were transferred to liquid nitrogen.

For thawing, the cells were rapidly warmed and transferred to 10 ml medium, pelleted (5 min, 750 rpm, 4 °C) and resuspended in fresh culture medium. Cells were transferred to the required cell culture plates or flasks and grown ON in an incubator. The next day, medium was refreshed to ensure a complete elimination of DMSO.

5.2.3 Retroviral transduction of eukaryotic cells

For generation of stable LEF1 knockdown (LEF1 KD) cell lines, RMS cells were either transduced with lentiviral *pGIPZ* vector containing the LEF1 silencing sequence or with the empty vector using the packaging cell line HEK293T (ATCC, Rockville, USA). For this purpose, HEK293T cells were transiently co-transfected with plasmids expressing the viral envelope and other viral proteins necessary for proper packaging and generation of functional virus particles. The stable transduction of the RMS cell lines was performed in collaboration with Prof. Dr. Tobias Pukrop and Dr. Florian Klemm at the Department of Hematology and Oncology, University Medical Center Göttingen.

Stable cell lines were selected in medium with puromycin. The concentration of puromycin used for selection was 0.5 µg/ml for RMS-13 and 2 µg/ml for Rh41 and TE671. Since the *pGIPZ* vector expresses GFP, shRNA expressing cells could also be visualized and monitored directly by fluorescence.

5.2.4 Transfection of eukaryotic cells

RMS cells were transfected using the NEON Transfection System according to the manufacturer's protocol. In brief, RMS cells were grown to 70-90 % confluence, harvested and counted. After washing, the cell pellet was resuspended in Resuspension Buffer R (included in the NEON Kit) with a final density of 4×10^6 cells/ml. For transfection 4×10^5 cells were mixed with 5 µg siRNA or 6.3 µg plasmid DNA in a final volume of 100 µl Buffer R and subjected to electroporation under the following conditions: 1000 V,

2 pulses, pulse time 30 msec. After 48 h the cells were collected by centrifugation (5 min, 750 rpm, 4 °C) and used for subsequent experiments (i.e. for transient β-catenin knockdown and TOP/FOP reporter assay).

5.2.5 Transient β-catenin knockdown (β-catenin KD)

Knockdown of *β-catenin* (*CTNNB1*) in RMS cell lines was achieved by using a β-catenin-specific siRNA pool (see Table 11) as described in Chapter 5.2.4. Scrambled siRNA was used as control siRNA (Table 11). Knockdown experiments were performed twice followed by qRT-PCR and Western blot analysis. For qRT-PCR analysis, 30 x 10^4 siRNA-transfected RMS cells were seeded, incubated in 6-well plates for 24 h and RNA was isolated afterwards.

5.2.6 TOP/FOP reporter assay

Canonical β-catenin-driven WNT signaling activity in RMS cell lines was measured after transfection with 3 µg *SuperTOPFlash* (TOP) containing multiple TCF/LEF-binding sites or its negative control vector *SuperFOPFlash* (FOP) as described above. *Renilla* reporter plasmid *pRL-CMV* was used for normalization. Co-transfection with 3 µg *pCl-neo-β-cateninS33Y* served as positive control. Consequently, 5000 transfected cells/well were seeded in 96-well plates. After 24 h, the cells were incubated for additional 48 h with Wnt3a CM. Luciferase activity was measured in triplicates for each condition using the Dual-Luciferase reporter assay system (see below).

5.2.7 Dual-Luciferase assay

Dual-luciferase assays of RMS cells were performed in 96-well plates using the Dual-Luciferase reporter assay system according to the manufacturer's instruction. In brief, the cells were washed and lysed in 20 µl 1 x passive lysis buffer (PLB) per well. The plates were incubated on an orbital shaker for 15 min at 250 to 300 rpm and RT. Afterwards the plates were frozen and stored at -80 °C until use. LAR II and Stop'n'Glo solutions were prepared and stored as described in the manufacturer's instruction. Prior to the measurement the LAR II and Stop'n'Glo solutions were allowed to equilibrate to RT for at least 15 min. The measurement was conducted on a Synergy MX luminometer. The firefly luciferase values were normalized to the respective renilla luciferase values.

5.2.8 Generation of Wnt3a conditioned medium

Wnt3a CM or respective control CM were obtained from murine L-cells stably transfected with Wnt3a expression plasmid or from non-transfected L-cells, respectively. Culture conditions are given in Table 8. Wnt3a CM and control CM were prepared as described by a protocol provided by ATCC (Willert *et al.*, 2003). Briefly, the cells (for Wnt3a CM and control CM) were split 1:10 and cultured in 10 ml fresh medium without G 418 for four days. The medium was removed, clarified with a 0.2 µm sterile filter and placed to 4 °C. Fresh medium (10 ml) was added for another three days and processed as described. The first and second batches of conditioned media were pooled and stored at 4 °C.

5.2.9 Proliferation assay

Cellular proliferation was analyzed using the 5-Bromo-2-Deoxyuridine (BrdU) cell proliferation kit according to the manufacturer's instructions. Measurement of BrdU incorporation was determined by luminescence in a microplate reader. In brief, 6000 cells/well were seeded in 96-well plates. After 12 h, the cells were incubated for 22 h with medium supplemented with 10 µM BrdU. After fixation of the cells and denaturation of the DNA for 30 min, peroxidase coupled BrdU antibody (anti-BrdU-POD) was added for 1 h. After thorough washing, peroxidase substrate was added to the plates. All samples were measured in triplicates. The data was analyzed and plotted using Microsoft Excel and GraphPad Prism 6 software.

5.2.10 Apoptosis assay

Cellular apoptosis was analyzed by flow cytometry after staining of the cells with allophycocyanin (APC) AnnexinV and 7-Amino-Actinomycin D (7-AAD). 22 x 10^4 cells/well were seeded in 6-well plates. After 12 h, cells were washed with PBS, detached with 1 ml accutase/well, transferred into a 15 ml reaction tube and pelleted by centrifugation (5 min, 1000 rpm, 4 °C). After washing with PBS the cells were incubated with 100 µl AnnexinV binding buffer supplemented with 2 µl APC AnnexinV for 10 min, followed by incubation with 7-AAD for 5 min at RT and under light exclusion. Finally, 300 µl AnnexinV binding buffer was added to the cell suspension and measurement of fluorescence was performed on a LSRII flow cytometer. All samples were measured in duplicates and analyzed using the software FlowJo, Microsoft Excel and GraphPad Prism 6.

5.2.11 Migration assay

For cell migration assay 10^5 cells were seeded onto membrane-inserts (translucent track-etched polyethylene terephthalate [PET] membranes) with 8 µm pores and incubated for 18 h in a 24-well-plate in 500 µl medium. Afterwards the membrane-inserts were transferred into a new 24-well-plate containing 5 µM calcein in 500 µl fresh medium and the cells were stained for 1 h at 37 °C. After washing with PBS and removing of cells on top of the membrane (cells which had not migrated), the cells at the bottom of the membrane were analyzed. For this purpose, 6-7 consecutive pictures at 10-fold magnification were taken of each well and cells were counted manually using AlphaView Q Imaging software.

To exclude that cellular proliferation influenced the results, 10^5 cells/well were seeded simultaneously in 24-well-plates and cultured for 18 h. Afterwards, cells were washed with PBS, detached with 0.5 ml TrypLE Express/well, transferred into a 15 ml reaction tube and pelleted by centrifugation (5 min, 750 rpm, 4 °C). After removal of the supernatant, the pellet was resuspended in 1 ml culture medium. To determine cell viability, the cell suspension was diluted 1:10 with trypan blue solution and cells were counted using a Neubauer counting chamber.

All measurements were performed in duplicates and analyzed and displayed by Microsoft Excel and GraphPad Prism 6.

5.2.12 Invasion assay

Invasion was measured together with Matthias Schulz (Department of Hematology/Medical Oncology, University Medical Center Göttingen) by assessment of the RMS cell migration rate using an artificial basement membrane in a modified Boyden chamber as described (Hagemann *et al.*, 2004).

The membrane consisted of polycarbonate (10 µm pore diameter) and was coated on ice with Matrigel (ECM gel) diluted 1:4 in serum-free RPMI. 10^5 RMS cells in 500 µl medium were seeded into the upper well of the chamber, while the lower well was filled up to the top with RPMI. 10 % FCS served as a chemoattractant. After 96 h, the floating cells in the lower well were collected, pelleted by centrifugation, resolved in 1 ml PBS and counted using a Neubauer counting chamber.

Simultaneously, 10^5 cells/well were seeded in 24-well-plates in medium and cultured for 96 h to analyze cell proliferation as described above in Chapter 5.2.11.

All samples were measured in duplicates. Data analysis was performed with Microsoft Excel and GraphPad Prism 6.

5.3 Protein chemistry and immunohistochemistry

5.3.1 Protein isolation from cell culture

For protein isolation from cultured cells, the cells were washed and scraped in 2 ml cold PBS using a cell scraper and centrifuged (5 min, 1000 rpm, 4 °C). After removal of the supernatant, the pellet was resuspended in 200 to 500 µl PBS and transferred into a 1.5 ml reaction tube followed by a second washing step. Subsequently, the pellet was shock frozen in liquid nitrogen, thawed on ice for 20 min and incubated with 40-200 µl lysis buffer supplemented with 500 µM PMSF and 2 mM DTT for additional 30 min on ice. Finally, the lysates were centrifuged (30 min, 13000 rpm, 4 °C) and the supernatant containing the soluble proteins was transferred to a new 1.5 ml reaction tube and stored at -80 °C until use. The protein concentration was measured using the Pierce BCA Protein Assay Kit according to manufacturer's instructions.

5.3.2 Western blot

For Western blot analysis protein lysates were denatured in SDS loading buffer for 5 min at 96 °C and 450 rpm in a shaker. The exception was the analysis of WNTA protein that was carried out under non-denaturing conditions with β-mercaptoethanol-free loading buffer. Afterwards protein samples were loaded on 4-12 % Bis-Tris Gels (NuPAGE Novex) and electrophoresed in running buffer (NuPAGE MES SDS) at 160 mA, 160 V and 100 W for 1.5-3 h. A protein marker (SeeBlue Plus2 Pre-Stained) was loaded to allow an accurate estimation of the molecular weight of the proteins. Next, the proteins were transferred from the gel onto a nitrocellulose membrane by wet blotting in blotting buffer at 100 V, 500 mA and 100 W for 80 min in a cold room. For visualization of proteins, the membrane was blocked with 5 % (w/v) milk powder/TBST for 1-1.5 h at RT. After washing three times in TBST for 10 min, the membrane was incubated with primary antibodies (see Table 13) at 4 °C ON. The next day, the membrane was washed again three times for 10 min in TBST and subsequently incubated with adequate HRP conjugated secondary antibodies for 1 h at RT (see Table 13). After an additional washing

step in TBST, the membrane was incubated with the detection reagent ECL for 1 min at RT. Then the ECL was removed and detection was accomplished with a Fluorchem Q Imaging system. All primary antibodies were dissolved in BSA-azide/TBST and all secondary antibodies were dissolved in 5 % milk powder/TBST.

5.3.3 Haematoxylin eosin (HE) staining

For HE staining, mouse tissue fixed in 4 % PFA was embedded in paraffin, cut into 4-5 µm sections and mounted onto glass slides. The sections were deparaffinized two times in xylene for 10 min and subsequently rehydrated by descending ethanol solutions (99 % to 70 %). After short washing with ddH_2O, slides were stained in haematoxylin solution for 15 min and washed with lukewarm tap water for at least 2 min. Slides were then placed in 1 % eosin solution for a maximum of 20 sec and washed again with ddH_2O. Then the sections were dehydrated using ascending ethanol solutions (70 % to 99 %) and placed again in xylene. Afterwards the sections were mounted in Pertex and dried at 55 °C for 20 min.

5.3.4 Immunohistochemical staining of tissues

Staining of a TMA consisting of 25 ARMS and 100 ERMS samples (biopsies from the Paediatric Tumor Register, Kiel, Germany) was performed in collaboration with Dr. Katja Simon-Keller at the Institute of Pathology, University Medical Center Mannheim. The RMS biopsies were embedded in paraffin and sectioned at 5 µm. After quality control, 41 ERMS and 7 fusion-positive ARMS samples were evaluable. Immunohistochemistry was performed as described in detail elsewhere (Zeitler *et al.*, 2004) using the following chemicals and reagents: antigen retrieval in antigen retrieval solution pH 6.0 or pH 9.0; blocking of endogenous peroxidase and detection of bound antibodies by the immunoperoxidase/DAB-based detection system (Table 5). Used primary antibodies are shown in Table 14.

5.3.5 Immunofluorescence staining

5.3.5.1 Immunofluorescence staining of cryosections

Immunofluorescence staining of RMS cryosections derived from the CAM assay was performed in collaboration with Prof. Dr. Jörg Wilting at the Institute of Anatomy and Cell Biology, University Medical Center Göttingen. After incubation for 1 h with blocking reagent (PBS, 1 % BSA), sections were incubated ON with the primary anti-HLA-A,B,C antibody followed by staining for 1 h with secondary TRITC-conjugated antibody diluted

in antibody solution mixed with DAPI (1:10000). After every step specimens were rinsed twice with PBS. Samples were mounted with Fluoromount-G and dried ON at RT. Stained specimens were studied with Zeiss Axio Imager.Z1 (Carl Zeiss Göttingen) and filter sets 38HE, 43 and 49. Used primary antibodies and corresponding secondary antibodies are shown in Table 14.

5.3.5.2 Immunofluorescence staining of cells

For immunofluorescence staining of cells, 4 x 10^4 cells/chamber were seeded in 4-chamber culture slides and after 24 h incubated with Wnt3a CM or control CM for additional 3 h. Cells grown on 4-chamber culture slides were fixed with 2 % PFA at RT for 10 min and with methanol at -20 °C for additional 5 min. Fixed cells were washed twice in PBS. After permeabilization with 0.5 % Triton X-100 (in PBS) for 5 min at RT, unspecific antigens were blocked with 4 % BSA (in PBS) for 1 h in a moist chamber and slides were rinsed twice with PBS. Subsequently, the cells were stained with anti-β-catenin antibody ON at 4 °C followed by staining with TRITC-conjugated anti-mouse antibody as secondary antibody for 1 h at RT. Finally, cells were mounted with ProLong Gold antifade reagent with DAPI and analyzed by fluorescence microscopy (Olympus BX 60, equipped with U-RLF-T). Serial pictures at 60-fold magnification were taken for each chamber of the slides and fluorescence images were acquired by using a Color View camera operated by CellSens software. Two independent experiments were performed. Used primary antibodies and corresponding secondary antibodies are shown in Table 14.

5.4 *In vivo* tumor model and animal experiments

5.4.1 Chorio-allantoic membrane (CAM) assay

The CAM assay was performed in collaboration with Prof. Dr. Jörg Wilting at the Institute of Anatomy and Cell Biology, University Medical Center Göttingen. All experiments were performed according to the guidelines of the European Parliament (2010/63/EU) and the council for the protection of animals in science (§14 TierSchVersV).

Fertilized White Leghorn chick eggs were incubated at 80 % relative humidity and 37.8 °C. The eggs were windowed at day 3 of chick development and the window was sealed with cellotape. At day 10 of chick development, 2 x 10^6 RMS-13 cells were resuspended in 50 % RPMI-medium and 50 % Matrigel, incubated for 30 min at 37 °C, 5 % CO_2 and applied on the CAM. The tumors and surrounding CAM were dissected after

seven days (day 17 of chick development), fixed in 4 % PFA for 20 min, washed twice in PBS and transferred into 10 % sucrose for 3 h at 4 °C and afterwards into 30 % sucrose ON at 4 °C. The next day, the tumors were embedded in tissue freezing medium and cut with a cryotome into 14 µm thick sections.

Tumors and tumor cells were visualized by intravital GFP imaging at day 3 and 7 post inoculation. Cryosections of CAM-bearing tumors were analyzed by immunofluorescence staining (see Chapter 5.3.5.1).

5.4.2 Breeding of mice

Mice were bred and housed in the animal facility of the Institute of Human Genetics, University of Göttingen, Germany. Animals were kept in Makrolon cages type II and III. The animals were supplied with rodent pellets and tap water *ad libitum* and maintained at a 12 h light-dark cycle (light period: 6 a.m.–6 p.m.), a temperature of 20±2 °C and a relative humidity of 50±10 %.

5.4.3 Tissue biopsies and genotyping of mice

To identify the genotype and to mark the mice, tail clipping (from the tip of the tail) and ear marking of weaned 4 weeks old mice was done by the staff of the animal facility. Genotyping was performed by isolation of gDNA from tail tissue or ear punches followed by PCR using the primers and conditions shown in Table 9 and Table 18.

5.4.4 Monitoring of RMS bearing mice

In order to record the occurrence of RMS, mice were monitored once a week by manual palpation and careful viewing. If possible the animals were kept for at least 250 days after birth. Then all mice were sacrificed and autopsied. Animals that had lost 20 % of their body weight or were at poor general conditions or carried tumors exceeding a size of 1 cm were sacrificed immediately and autopsied.

5.4.5 Preparation and isolation of RMS

Tumors, skeletal muscle, cysts and irregular or suspicious tissues were excised and carefully washed with PBS. Part of the tumor and reference tissues was formalin fixed and embedded in paraffin for HE staining. Remaining tumor tissue and skeletal muscle were frozen on dry ice and stored at -80 °C for further experiments.

5.5 Statistics

Unless indicated otherwise, statistical and graphical analyses were conducted using the programs GraphPad Prism 6, MS Office Excel or Statistica 10. Data were considered significant if *P* values were <0.05. When comparing two samples, statistical differences were analyzed using Student's t-test or unpaired, non-parametric t-test (Mann-Whitney) as indicated in the respective experiments. Correlation of mRNA expression levels in primary human RMS samples was tested by a parametric Pearson test and a non-parametric Spearman test. For the *in vivo* data, statistical significance of the RMS-free survival was tested by log-rank (Mantel-Cox) test and the multiplicity by Chi-square test.

6 Results

The results of this thesis are divided into two parts. The first part focuses on the function of LEF1 and β-catenin dependent WNT signaling in RMS pathogenesis. The second part is dedicated to the role of LEF1 in context with non-canonical WNT5A signaling in RMS.

6.1 LEF1 and β-catenin expression in primary human RMS

To examine the role of LEF1 and β-catenin in primary human RMS, a TMA and qRT-PCR analysis on fresh frozen samples were performed in collaboration with Dr. Katja Simon-Keller and Prof. Dr. Alexander Marx from the Institute of Pathology, University Medical Center Mannheim. Finally, 41 ERMS from the TMA and 10 fresh-frozen ERMS samples could be analyzed, whereas only 7 ARMS from the TMA, but also 10 fresh-frozen ARMS samples were available for analysis. All ARMS samples were fusion-positive. The results of the TMA revealed that LEF1 can be highly expressed in fusion-positive ARMS and ERMS. 44 % of the RMS samples were positive for LEF1, however to a variable extend with some individual tumors showing a very heterogeneous LEF1 distribution (Figure 3A). Consequently, the studied samples were subdivided into low, intermediate or high expressers according to the scoring range of <50, 50-150 or >150, respectively. The score was calculated by multiplying the percentage of positive cells by the intensity of the staining (weak staining: 1, moderate staining: 2, or strong staining: 3) (reviewed in Fedchenko *et al.*, 2014). No ARMS with a high LEF1 score was detected and in general the LEF1 score was higher in ERMS compared to ARMS, however without reaching significance. LEF1 protein was exclusively found in the nucleus. Likewise, heterogeneous overexpression of *LEF1* was also seen on mRNA level in 10 human fusion-positive ARMS and 10 human ERMS compared to normal skeletal muscle (n=4; Figure 4A). Similar to the results from the TMA, the ERMS samples showed generally higher *LEF1* mRNA levels than ARMS samples, however without reaching significance.

When β-catenin expression was analyzed, 48 % of the RMS samples were stained positive (Figure 3B). Signals were detected in the cytoplasm but absent in the nuclei with the exception of one ERMS case that additionally showed nuclear β-catenin expression. On mRNA level all RMS expressed unequivocal high levels of *CTNNB1* when compared to normal muscle (Figure 4B), but no correlation with LEF1/*LEF1* expression was observed (data not shown).

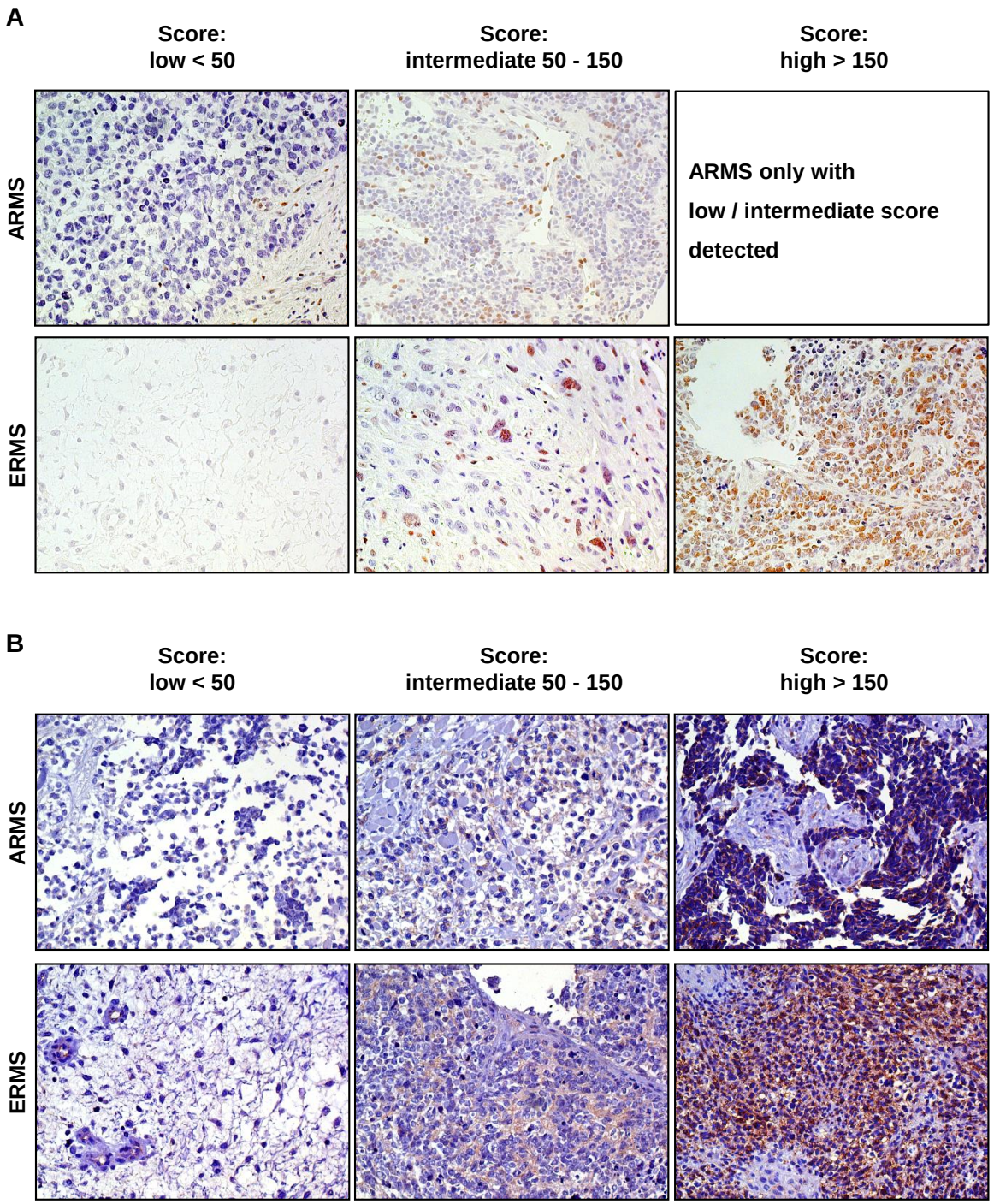

Figure 3: Immunohistochemical analyses of LEF1 and β-catenin in human RMS biopsies. Representative immunohistochemistry staining of **(A)** LEF1 and **(B)** β-catenin in primary human fusion-positive ARMS (n=7) and human ERMS (n=41). Results were scored by multiplying the percentage of positive cells by the intensity of the staining to subdivide studied samples into low, intermediate and high expressers. The proportion of LEF1-and β-catenin-positive cells as well as the intensity of the staining was estimated by a pathologist. Magnification 200-fold.

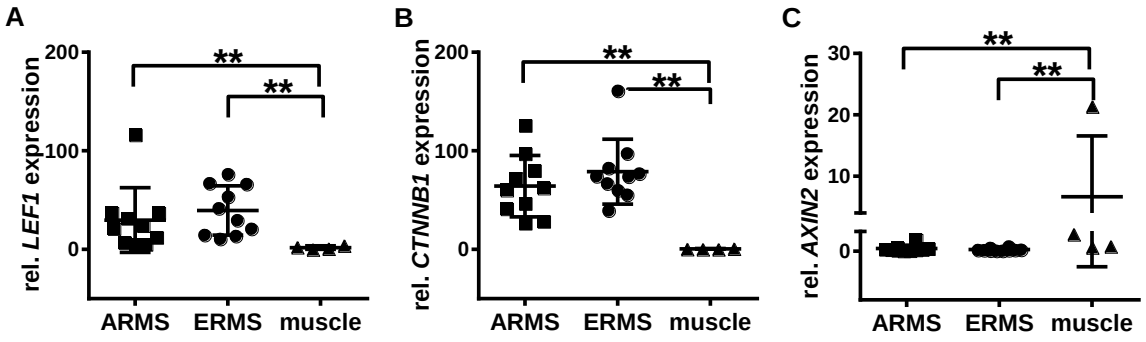

Figure 4: qRT-PCR analyses of *LEF1*, *CTNNB1* and *AXIN2* in human RMS biopsies. (A) *LEF1*, **(B)** *CTNNB1* and **(C)** *AXIN2* expression levels analyzed by qRT-PCR in fresh-frozen biopsies of human fusion-positive ARMS (n=10) and human ERMS (n=10) compared to normal muscle (n=4). Gene expression levels were normalized to *GAPDH* expression levels. Bars, 95 % confidence intervals and mean values; ***P*<0.01 by Mann-Whitney t-test.

Furthermore, mRNA expression of *AXIN2* – the major downstream target of β-catenin dependent WNT signaling – was significantly downregulated in both ARMS and ERMS compared to normal skeletal muscle (Figure 4C).

In summary, approximately half of fusion-positive ARMS and ERMS samples express nuclear LEF1 and cytoplasmatic β-catenin with however variable intensity and lack of any correlation. The common absence of nuclear β-catenin and of *AXIN2* expression suggests that canonical WNT signaling in general is not active in RMS.

6.2 *In vivo* effect of Wnt3a on RMS development

To get an impression whether canonical Wnt signaling may actually not influence RMS growth and progression *in vivo*, a genetic approach was conducted using $Ptch^{del/+}$ mice that develop RMS with high incidence. For this purpose, $Ptch^{del/+}$ mice were crossed with $Wnt^{vt/vt}$ (*vestigial tail*) mice. $Wnt^{vt/vt}$ mice carry a hypomorphic Wnt3a allele and therefore generally express Wnt3a to a lesser extent. The resulting $Ptch^{del/+}Wnt^{vt/vt}$ mice and the respective control littermates $Ptch^{del/+}Wnt^{+/vt}$ were monitored weekly for a minimum of 250 days to record RMS formation. Afterwards mice were sacrificed and autopsied. All tumors were removed and histologically evaluated using HE-stained paraffin sections. As shown in Table 22 and Figure 5A, the overall RMS incidence (38 % versus 31 %) and the latency time until occurrence of RMS (206 days versus 220 days) in $Ptch^{del/+}Wnt^{vt/vt}$ and $Ptch^{del/+}Wnt^{+/vt}$ control mice was very similar in both groups.

Table 22: Effect of Wnt3a on RMS development. Absolute numbers, percentages and latency time of RMS of *Ptch*$^{del/+}$*Wnt*$^{+/vt}$ and *Ptch*$^{del/+}$*Wnt*$^{vt/vt}$ mice.

Genotype	n	Mice with palpable RMS	Median latency time of RMS (days)	Mice with multiple RMS
***Ptch*$^{del/+}$*Wnt*$^{+/vt}$**	36	11 (31 %)	220	5 (14 %)
***Ptch*$^{del/+}$*Wnt*$^{vt/vt}$**	40	15 (38 %)	206	2 (5 %)

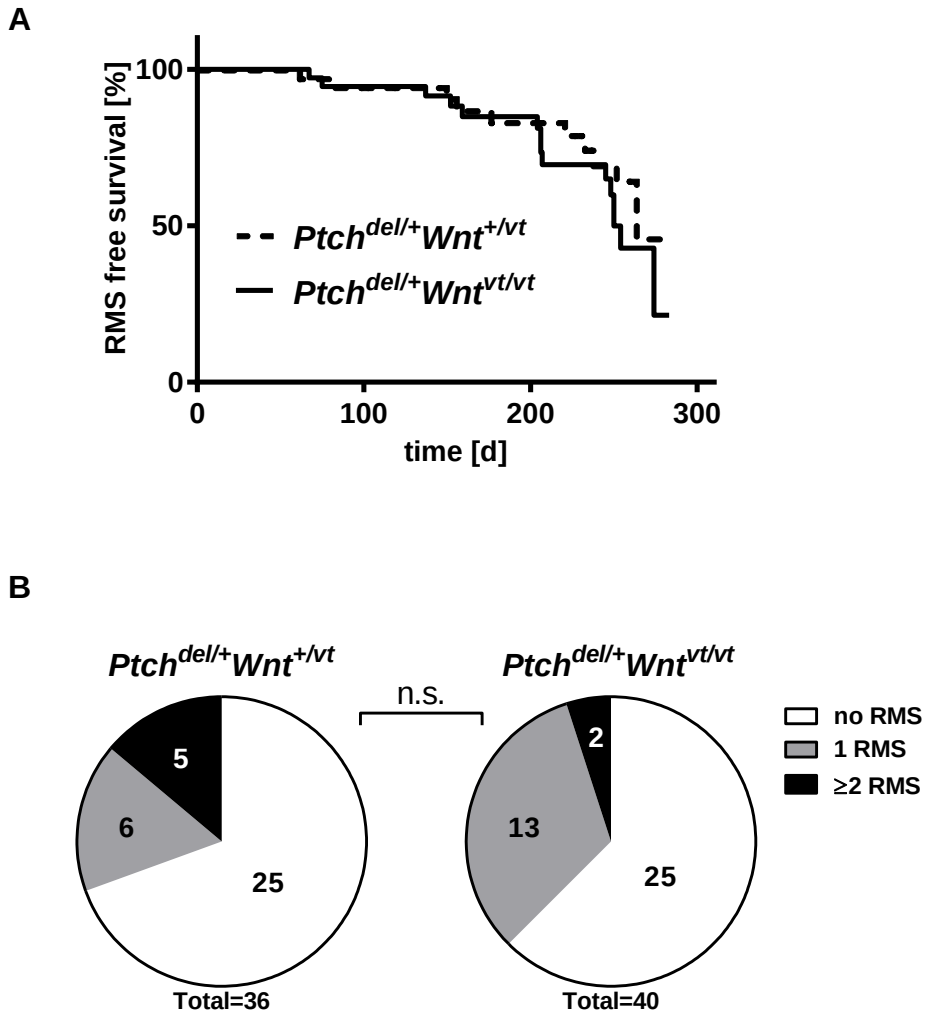

Figure 5: Effect of Wnt3a on RMS development. (A) Kaplan Meyer curve showing the RMS free survival of *Ptch*$^{del/+}$*Wnt*$^{+/vt}$ mice (dashed line) and *Ptch*$^{del/+}$*Wnt*$^{vt/vt}$ mice (solid line). All mice were monitored for a minimum of 250 days, if possible. Each event represents the detection of the first RMS in a mouse. According to the log-rank test that was used to analyze differences in the survival curves the *P*-value was *P*=0.6493 versus control littermates. **(B)** Graphs show tumor multiplicity as RMS/animal of *Ptch*$^{del/+}$*Wnt*$^{+/vt}$ mice and *Ptch*$^{del/+}$*Wnt*$^{vt/vt}$ mice. Statistical significance was analyzed by Chi-square (χ^2) test (*P*=0.626). Published in *Nitzki et al.* 2016.

Although the tumor multiplicity was lower in *Ptch*$^{del/+}$*Wnt*$^{vt/vt}$ mice (5 %=2/40 versus 14 %=5/36 in control mice; Table 22) this difference was not significant according to Chi-square testing (Figure 5B).

This indicates that Wnt3a-driven canonical Wnt/β-catenin signaling does not play a prominent role in RMS pathogenesis in mice. The data have been published in Nitzki *et al.*, 2016.

6.3 Generation of stable LEF1 KD RMS cell lines

Since WNT/β-catenin driven signaling activity apparently did not play a prominent role in RMS pathogenesis, we next analyzed the function of LEF1 in RMS in more detail. For this purpose, the human ARMS cell lines Rh41 and RMS-13 and the ERMS cell line TE671 were used. All of these RMS cell lines express full-length LEF1 isoform of 44 kDa, whereas the truncated isoforms lacking the β-catenin binding site 31 kDa and 23 kDa (see Van de Wetering *et al.*, 1996; Hovanes *et al.*, 2001) were merely detected (Figure 6A). Western blot was also performed with the human breast cancer cell line SKBR3, which overexpresses LEF1, and with the LEF1-negative human Jurkat T cells.

Subsequently, LEF1 was stably deleted in the RMS cell lines by retroviral shRNA transfer in collaboration with Prof. Dr. Tobias Pukrop and Dr. Florian Klemm, Department of Haematology/Medical Oncology, University Medical Center Göttingen. As verified on protein level, LEF1 was efficiently deleted in all RMS LEF1 KD cell lines when compared to the respective control transduced (control) cells (Figure 6A).

The stable LEF1 KD in the cell lines resulted in a significant downregulation of the LEF1 target *AXIN2* in RMS-13 cells when compared to control cells that were set to 1 (Figure 6B). Interestingly, the LEF1 target *c-MYC* was significantly increased in RMS-13 LEF1 KD and Rh41 LEF1 KD cells (Figure 6B) in comparison to the respective control cells. No significant effects of the LEF1 KD on the expression of the two mentioned genes were seen in TE671 cells.

In brief, LEF1 has different effects in the three used cell lines. Thus, it blocks the expression of *c-MYC* in both ARMS cell lines but not in TE671 cells, and activates *AXIN2* expression in RMS-13 cells.

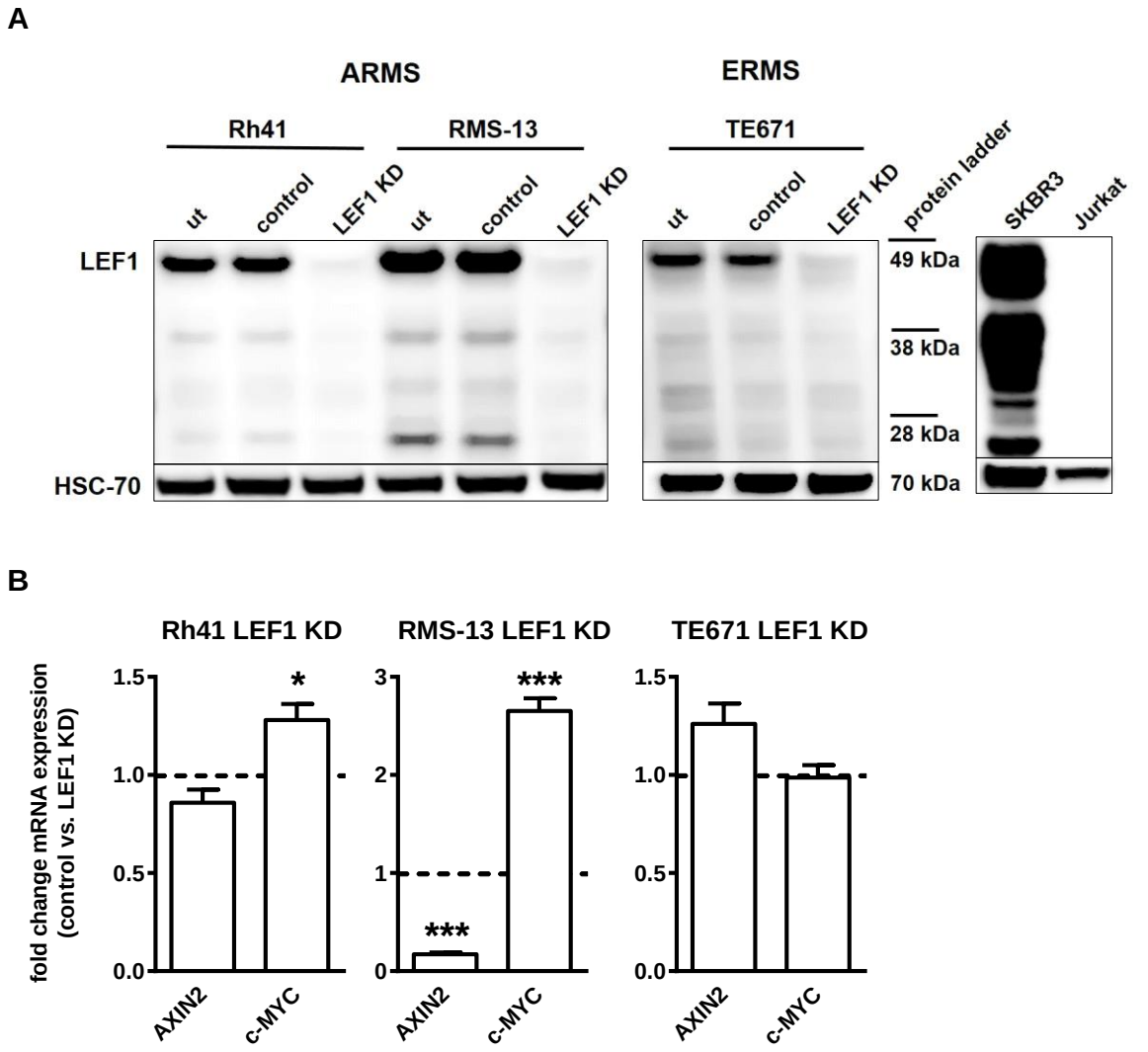

Figure 6: Generation of stable LEF1 knockdown (LEF1 KD) RMS cell lines and expression analyses of WNT target genes. (A) Representative LEF1 Western blot of the human ARMS cell lines Rh41 and RMS-13 and the human ERMS cell line TE671. The cell lines were either untransduced (ut) or stably transduced with empty vector control (control) or LEF1 shRNA (LEF1 KD). HSC-70 expression levels served as loading control and protein ladder is shown for estimation of protein size. SKBR3 and Jurkat T cells were used as positive and negative controls. **(B)** mRNA levels of *AXIN2* and *c-MYC* in Rh41 LEF1 KD, RMS-13 LEF1 KD and TE671 LEF1 KD cells are shown as fold change to the respective control cells that were set to 1 (dashed line). Gene expression levels were normalized to *18S* rRNA expression levels. Data represent mean+SEM of three independent experiments performed in duplicates and measured in triplicates; **P*<0.05, ****P*<0.001 by Students t-test.

6.4 Analysis of canonical WNT signaling activity in human RMS cell lines

We next investigated whether β-catenin driven WNT signaling activity can be activated in RMS cell lines and if LEF1 is important for its maintenance. For this purpose, the stable RMS LEF1 KD cells and their respective control cells were transfected with the *SuperTOPFlash* (TOP) plasmid containing multiple TCF/LEF-binding sites or its negative control vector *SuperFOPFlash* (FOP) along with *Renilla* reporter plasmid for normalization. WNT signaling was activated by incubation with Wnt3a CM for 48 h. As a positive control, the *pCl-neo-β-cateninS33Y* (β-catS33Y) plasmid was co-transfected. Moreover, analyses of *AXIN2* transcription levels served as approved readout for active canonical WNT signaling.

As shown in Figure 7, *AXIN2* mRNA expression was significantly increased after treatment with Wnt3a CM for 48 h in all cell lines when compared to control CM. However, the TOP reporter was not significantly activated by Wnt3a in the ARMS cell lines Rh41 and RMS-13. Thus, and as shown in Figure 8, TOP reporter activity was only marginally induced in Rh41 control (1.7-fold) and Rh41 LEF1 KD cells (2.7-fold) by Wnt3a CM in comparison to control CM incubation (that was set to 1). This was similar in RMS-13 LEF1 KD cells (3-fold induction in response to Wnt3a CM), whereas RMS-13 control cells did not show any luciferase induction in response to Wnt3a when compared to control CM treated cells. In contrast, TE671 control and LEF1 KD cells showed a more than 10-fold induction of TOP activity after Wnt3a CM treatment. Co-transfection with activated β-catenin (β-catS33Y) revealed strong luciferase induction in all settings, except in RMS-13 LEF1 KD cells.

Incubation with Wnt3a CM after FOP-transfection did not induce luciferase activity in any of the cell lines (Figure 9). Surprisingly, co-transfection of FOP-transfected TE671 control cells with β-catS33Y induced luciferase activity (1.4-fold; P=0.041) when compared to solvent. The reason for this induction is not clear. However, since the luminescence activity following β-catS33Y/TOP-transfection was 43 times higher than the activity of β-catS33Y/FOP-transfected cells, the experiment was considered as valid.

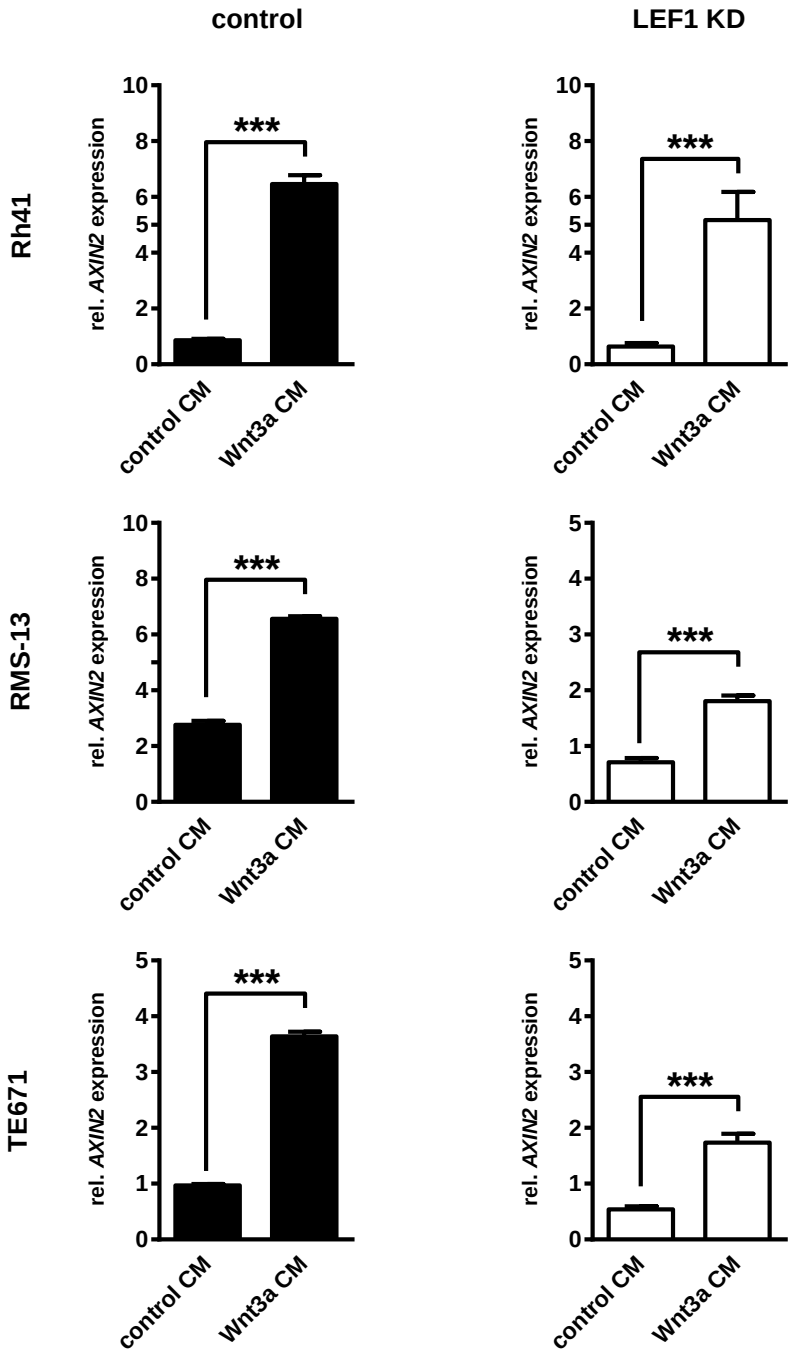

Figure 7: Activation of β-catenin dependent WNT signaling in human RMS cell lines. qRT-PCR analysis of *AXIN2* in Rh41, RMS-13 and TE671 control and the respective LEF1 KD cells after incubation with Wnt3a CM for 48 h in comparison to the control CM treated cells. *AXIN2* expression was normalized to *18S* rRNA expression levels. Data represent two independent experiments performed in duplicates and measured in triplicates. All data are displayed as mean+SEM; ****P*< 0.001 by Students t-test.

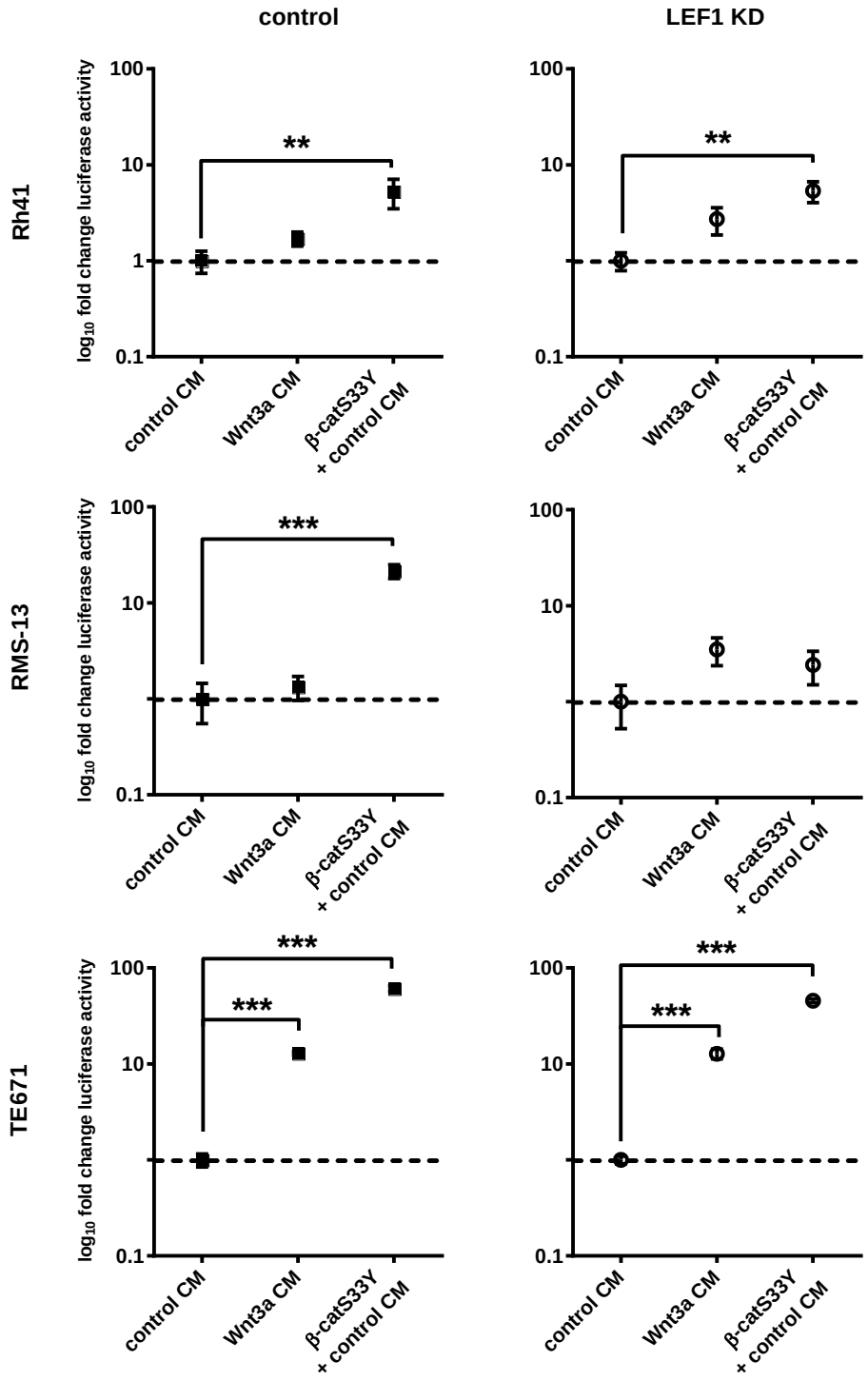

Figure 8: β-catenin driven WNT signaling activity in RMS cell lines. To analyze β-catenin dependent WNT signaling activity Rh41, RMS-13 and TE671 control and LEF1 KD cells were transfected with TOP plasmid containing multiple TCF/LEF-binding sites. Luciferase activity was measured five days after transfection in response to Wnt3a CM or control CM. Data show the 95 % confidence intervals of two independent experiments performed in triplicates and are depicted as fold change luciferase activity to the respective control CM treated cells that was set to 1 (dashed line). Statistical significance was tested using Students t-test with $^{**}P < 0.01$, $^{***}P < 0.001$.

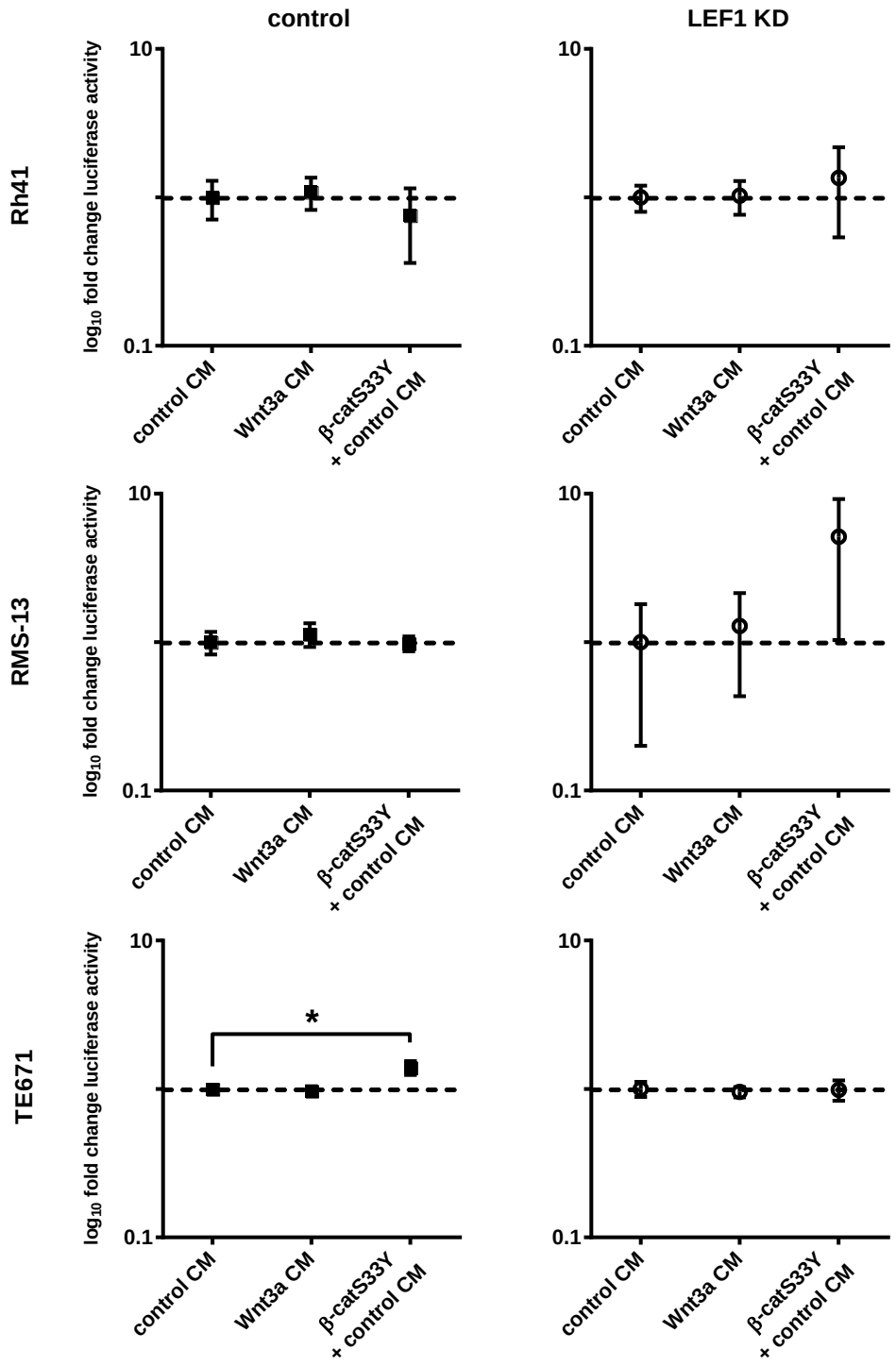

Figure 9: Control experiments of data shown in Figure 8. Rh41, RMS-13 and TE671 control and LEF1 KD cells were transfected with FOP plasmid containing mutated and thereby inoperable TCF/LEF-binding sites as negative control for data shown in Figure 8. Luciferase activity was measured five days after transfection in response to Wnt3a CM or control CM. Data show the 95 % confidence intervals of two independent experiments performed in triplicates and are depicted as fold change luciferase activity to the respective control CM treated cells that was set to 1 (dashed line). Statistical significance was tested using Students t-test with $*P < 0.05$.

In order to evaluate to which extend the LEF1 KD influences Wnt3a-mediated TOP induction, the values from the TOP luciferase activity of the LEF1 KD cells were normalized to that of the respective control cells (that were set to 1, Figure 10A). Importantly, the LEF1 KD in all TOP-transfected RMS cell lines did not significantly influence reporter activity when compared to respective control cells after incubation with Wnt3a, i.e. no significant alterations in luciferase activity was obtained that could be ascribed to LEF1 KD (Figure 10A). Furthermore, none of the settings had any effect on the luciferase activity in FOP-transfected RMS LEF1 KD cells compared to FOP-transfected control cells (Figure 10B).

The TOP/FOP reporter assay was also performed in the presence of the GSK3β inhibitor LiCl that – similarly to Wnt3a – activates canonical WNT signaling. Notably, the results using LiCl were conform to those after incubation with Wnt3a CM in RMS-13 and TE671 control and LEF1 KD cells. However, the data obtained from Rh41 control and LEF1 KD cells were rather inconsistent, making it impossible to analyze them. Therefore, the results regarding LiCl incubation are not shown in this thesis.

To sum up, the data show that despite an upregulation of *AXIN2* – as readout for active canonical WNT signaling – Wnt3a stimulation does not change TOP reporter activity in Rh41 and RMS-13 control cells but induces it in TE671 control cells. Thus, canonical WNT signaling appears to be functionally active in the mentioned ERMS cell line but not in both ARMS cell lines. Furthermore, the data indicate that LEF1 is not necessary for activation of the TOP reporter, i.e. it is dispensable for β-catenin driven WNT signaling activity in all three RMS cell lines. Due to the fact that β-catS33Y did not induce signaling activity in RMS-13 LEF1 KD cells, it can be further speculated that LEF1 depletion prevents β-catS33Y from binding to the TCF-binding sites of the reporter plasmid.

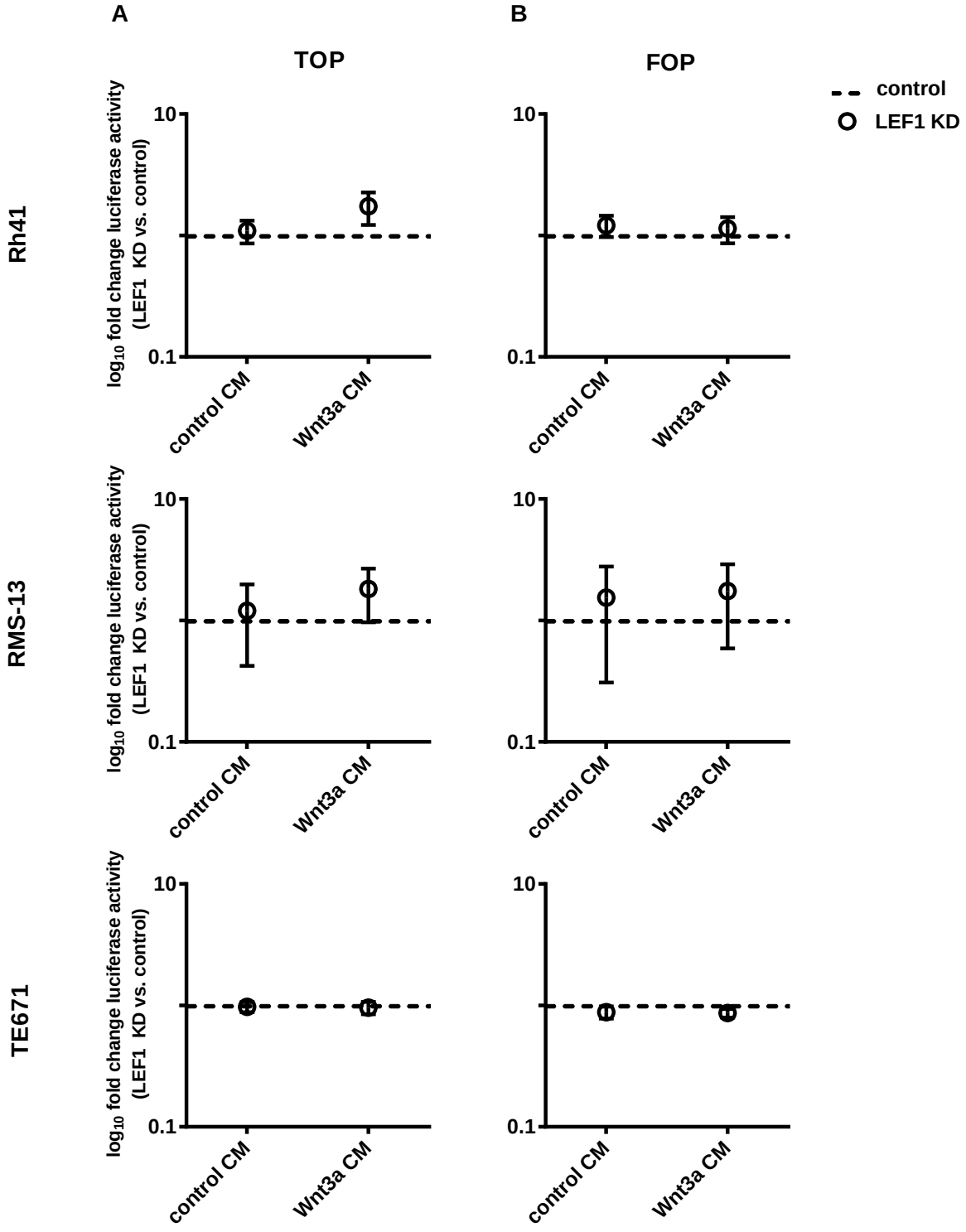

Figure 10: LEF1-dependent modulation of β-catenin driven WNT signaling activity in RMS cell lines. Data of **(A)** TOP-transfected and **(B)** FOP-transfected Rh41 LEF1 KD, RMS-13 LEF1 KD and TE671 LEF1 KD cells after incubation with control CM and Wnt3a CM for 48 h are calculated as fold change luciferase activity in comparison to the respective TOP-or FOP-transfected control cells that were set to 1 (dashed line). Data show the 95 % confidence intervals of the same two independent experiments shown in Figures 8 and 9.

6.5 Analysis of β-catenin functionality and LEF1-dependent expression of TCF factors in RMS cell lines

In the ARMS cell lines Rh41 and RMS-13, *AXIN2* expression was induced by Wnt3a CM despite lack of TOP reporter activity (see Figure 7 and Figure 8). Thus, the expression of *AXIN2* seems to be independent of β-catenin and regulated by other factors. Since β-catenin in the analyzed cell lines was not mutated (as analyzed by our collaborator Dr. Katja Simon-Keller; data not shown), the lack of TOP reporter activity in ARMS cells also suggested that the parental RMS-13 and Rh41 cells may possess a mechanism that prevents endogenous β-catenin from binding to the reporter plasmid. For instance, it is possible that β-catenin is retained in the plasma membrane or cytoplasm (for review see Kimelman *et al.*, 2006). Finally, the fact that activated β-catS33Y did not induce signaling activity in RMS-13 LEF1 KD cells (see Figure 8) additionally argued for a factor that prevents β-catS33Y from binding to the TCF-binding sites of the reporter plasmid after LEF1 depletion.

To answer these issues, we analyzed whether β-catenin was able to translocate to the nucleus after stimulation with Wnt3a (see Chapter 6.5.1). Moreover, the expression of the other TCF factors that also interact with β-catenin and generally can activate (TCF1 and TCF4) or inhibit (TCF3 and TCF4) canonical WNT signaling (Cadigan *et al.*, 2012; Shah *et al.*, 2015) was examined in dependency of LEF1 (see Chapter 6.5.2).

6.5.1 Effect of Wnt3a on subcellular localization of β-catenin in RMS cell lines

We first analyzed whether activation of canonical WNT signaling resulted in translocation of β-catenin to the nucleus. For this purpose, the cells were stimulated with Wnt3a CM for 3 h and after that stained for β-catenin immunofluorescence (red) and counterstained with DAPI (blue) to determine β-catenin subcellular localization. Merged images of β-catenin immunofluorescence and DAPI staining are shown in Figure 11. Compared to the control CM, immunofluorescence staining of the ERMS cell line TE671 demonstrated predominant nuclear accumulation of β-catenin upon Wnt3a treatment. In contrast, nuclear β-catenin was never detectable in RMS-13 cells, whereas a very weak but distinct nuclear β-catenin staining was detected in approximately 10 % of Rh41 cells after incubation with Wnt3a CM (Figure 11). This is similar to the results of the TOP/FOP reporter assay that showed a 1.3-fold and 1.7-fold induction of TOP activity in RMS-13 and Rh41 control cells after Wnt3a treatment, respectively, when compared to control CM (see Figure 8).

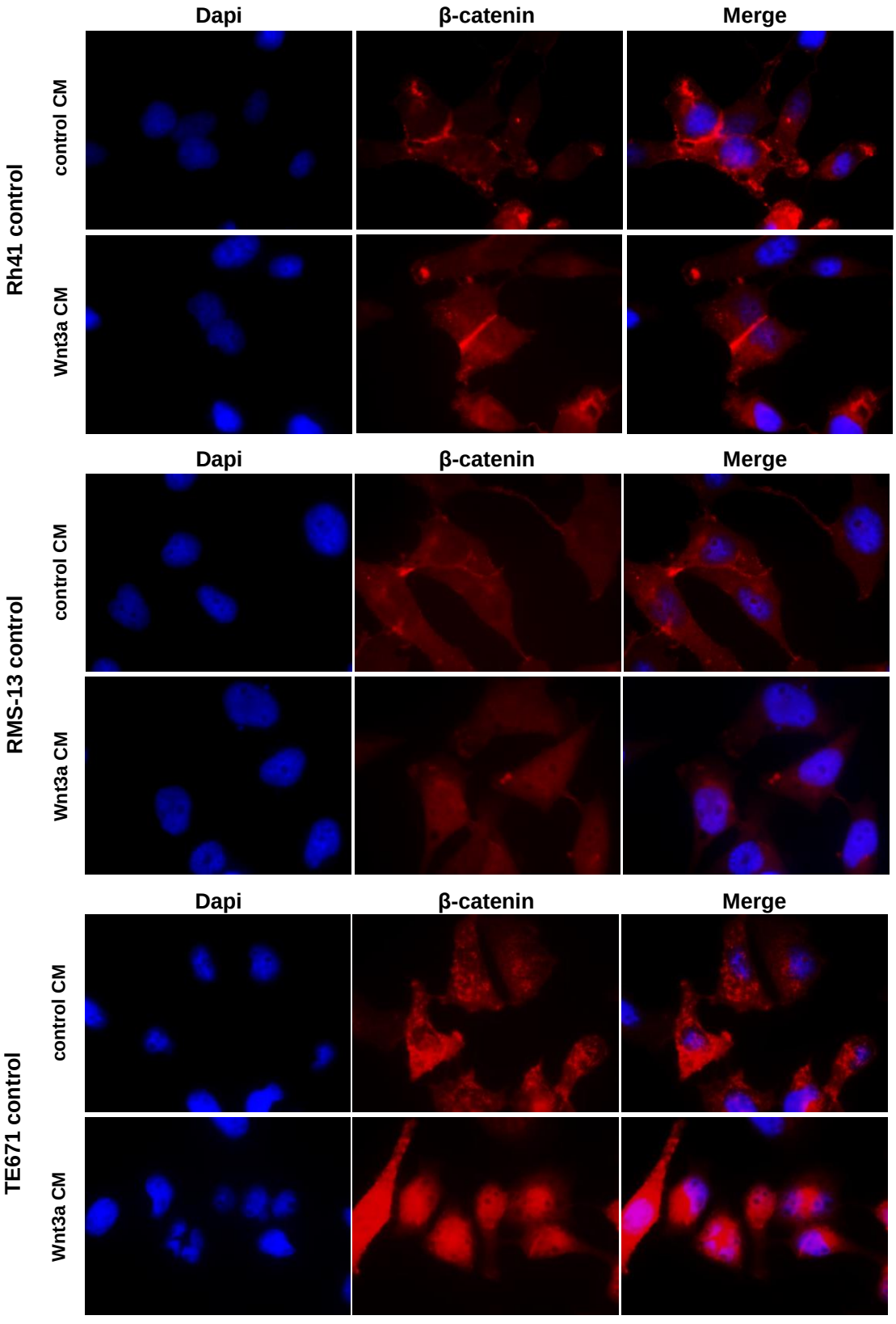

Figure 11: Localization of β-catenin after Wnt3a stimulation in RMS cell lines. Representative images of β-catenin immunofluorescence staining (red) in Rh41, RMS-13 and TE671 control transduced (control) cell lines cultured in Wnt3a CM or control CM for 3 h. DAPI was used to stain cell nuclei (blue). Images (60-fold magnification) are representative of two independent experiments.

To sum up, the immunofluorescence staining support the hypothesis that endogenous β-catenin in Rh41 and RMS-13 is hold back at the plasma membrane or in the cytoplasm (Figure 11). This is in contrast to the ERMS cell line TE671, in which canonical WNT signaling is functionally active (see Figure 8 and Figure 11).

6.5.2 Effect of LEF1 KD on the expression of *TCF* factors in RMS cell lines

Next, the influence of LEF1 on the expression of *TCF*s was examined by qRT-PCR in collaboration with Dr. Katja Simon-Keller at the Institute of Pathology, University Medical Center Mannheim. Our data reveal that all *TCF* factors were significantly upregulated in Rh41 LEF1 KD cells, whereas all of them were significantly downregulated in RMS-13 LEF1 KD cells (Figure 12) when compared to the respective control cells (that were set to 1). In TE671 LEF1 KD cells, we did not find any significant changes in comparison to control cells.

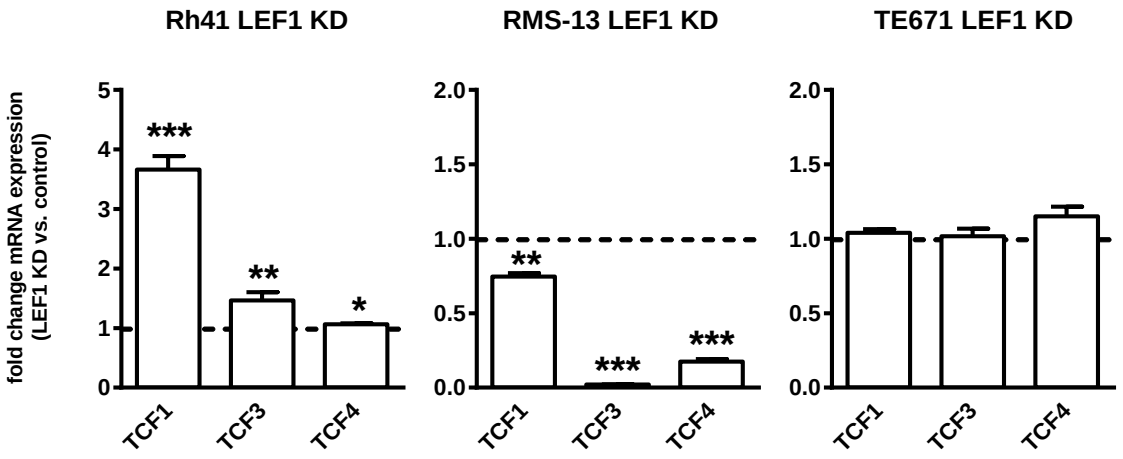

Figure 12: LEF1-dependent expression of *TCF* factors in RMS cell lines. Expression of *TCF1*, *TCF3* and *TCF4* in Rh41 LEF1 KD, RMS-13 LEF1 KD and TE671 LEF1 KD are shown as fold expression to the respective control cells that were set to 1 (dashed line). Gene expression levels were normalized to *GAPDH* expression levels. Data represent mean+SEM of four independent experiments measured in triplicates; **P*<0.05, ***P*<0.01, ****P*<0.001 by Students t-test.

Together, LEF1 rather suppresses the expression of *TCFs* in Rh41 cells, whereas it induces *TCF* factors in RMS-13 cells. The extreme downregulation of all *TCF*s upon LEF1 depletion in RMS-13 cells may be the reason for the lack of TOP activation in β-catS33Y-transfected RMS-13 LEF1 KD cells (see Figure 8).

6.6 Effects of LEF1 KD on cellular processes in RMS cell lines

The stably transduced RMS LEF1 KD cell lines were also analyzed with respect to proliferation, apoptosis and their migratory and invasive properties.

6.6.1 Effect on proliferation

The LEF1 KD increased the proliferative capacity of all three RMS cell lines (Figure 13A). In Rh41 and RMS-13 LEF1 KD cells, the proliferation rate was significantly elevated by approximately 10 % and 50 %, respectively, when compared to control transduced cells. In the ERMS cell line TE671, LEF1 KD also resulted in a 10 % increase in BrdU incorporation when compared to the control, however without reaching significance.

6.6.2 Effect on apoptosis

LEF1 KD did not provoke any significant differences in the number of apoptotic cells in Rh41 and TE671 cells when compared to the respective control cells (Figure 13B). In contrast, the LEF1 KD in RMS-13 significantly decreased the number of AnnexinV positive i.e. apoptotic cells by more than 60 % in comparison to control cells.

6.6.3 Effect on migration and invasion

In RMS-13, the stable LEF1 KD resulted in a significant increase of the number of cells that migrated trough the membrane inserts or invaded the Matrigel in the Boyden chamber invasion assay (Figure 13C, D). Thus, the LEF1 KD in RMS-13 increased the migratory and invasive capacity approximately 8 times and 1.5 times, respectively, in comparison to RMS-13 control cells. In contrast, LEF1 KD had no impact on the migration rate of Rh41 and TE671 cells, but led to a significant decrease or increase of cell invasiveness in Rh41 LEF1 KD and TE671 LEF1 KD cells, respectively, when compared to control cells (Figure 13C, D).

In summary, the results reveal that the effect of LEF1 KD on cellular processes is heterogeneous depending on the individual cell line. Nevertheless, and despite the fact that LEF1 KD decreases the invasive capacity of Rh41 cells, the data show that depletion of LEF1 in general results in increased RMS proliferation, and further can enhance migratory/invasive properties and also inhibit apoptosis. In other words, the presence of LEF1 can attenuate the aggressiveness of RMS cell lines.

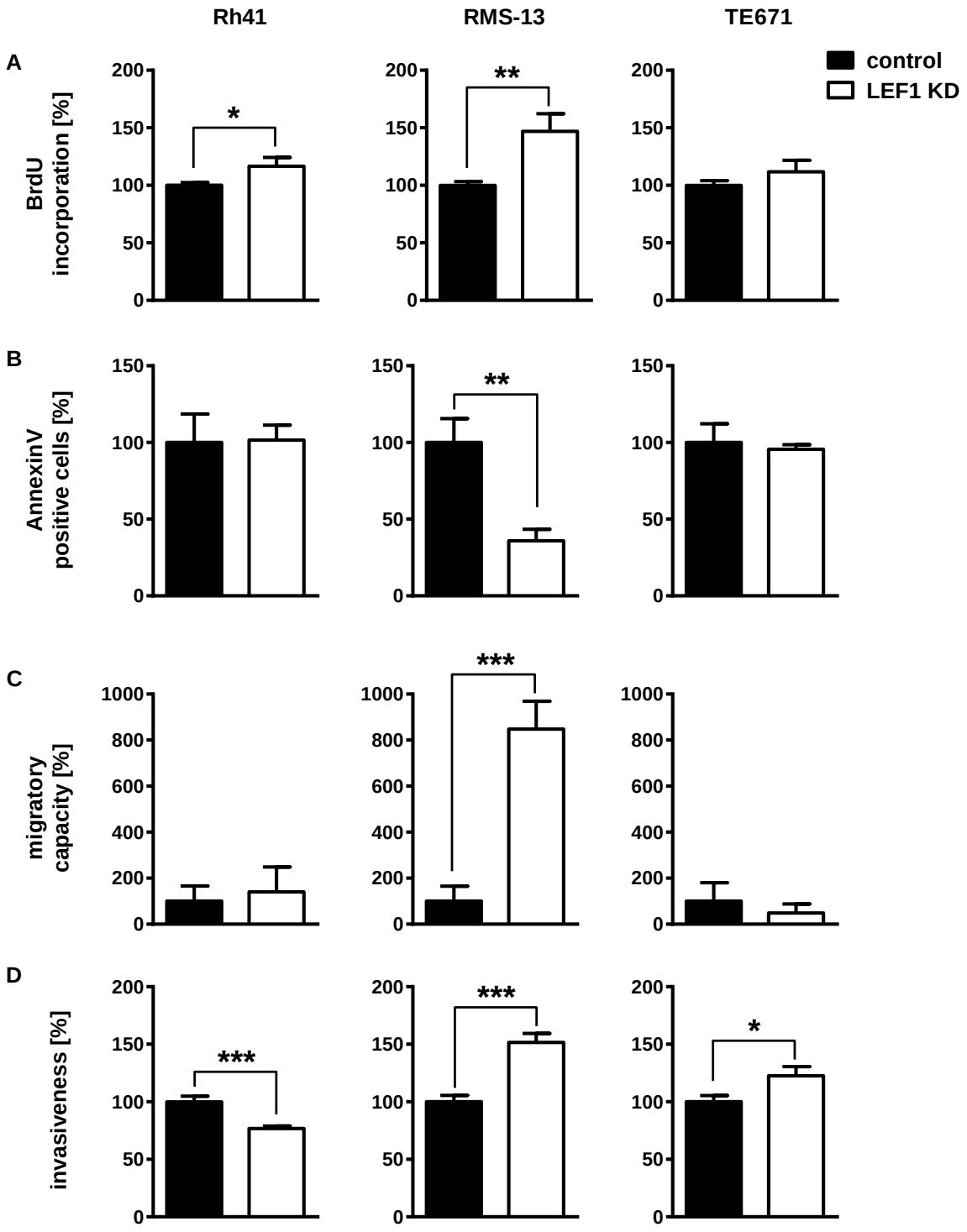

Figure 13: LEF1-dependent regulation of proliferation, apoptosis, migration and invasiveness of RMS cell lines. (A) Proliferation, **(B)** apoptosis, **(C)** migratory capacity and **(D)** invasiveness of the Rh41, RMS-13 and TE671 control and LEF1 KD cells were analyzed by BrdU incorporation assay, FACS, trans-well migration and Boyden chamber assay. The values of the respective control cells were set to 100 % (black bar). Data represent mean+SEM of two independent experiments performed in triplicates (BrdU incorporation assay, migration assay for RMS-13) or duplicates (apoptosis, invasion and migration assay). Comparisons were made with Students t-test; **P*<0.05, ***P*< 0.01, ****P*< 0.001.

6.6.4 Effect of LEF1 KD on RMS growth and aggressiveness *in vivo*

To confirm that LEF1 is associated with a less aggressive phenotype, a CAM assay was performed, which is an established *in vivo* model for tumor growth and invasiveness. To this end, RMS-13 LEF1 KD and RMS-13 control cells were seeded on the CAM of chicken embryos and were allowed to form tumors for seven days. Due to stable transduction with the lentiviral *pGIPZ* vector that expresses GFP the growth and invasive potential of the cells could be visualized by fluorescence.

Three days after inoculation, the RMS-13 LEF1 KD cells have formed larger tumors in comparison to the control cells (Figure 14A). Seven days after inoculation, LEF1 KD tumors showed massive infiltration of tumor cell clusters into the surrounding stroma. This was accompanied by destruction of vessels and hemorrhage, which was not observed in the control tumors (Figure 14B, C). Moreover, whole-mount GFP imaging revealed that RMS-13 LEF1 KD cells migrated long distances from the primary tumor (Figure 14C). Indeed, HLA immunofluorescence staining detected human MHC-positive RMS-13 LEF1 KD cells in the stroma of the CAM several millimeters apart from the primary tumor (Figure 14D).

To sum up, the results from the *in vivo* CAM assay demonstrate that LEF1 inhibits growth as well as the migratory and invasive properties of RMS-13 cells. This is in agreement with the *in vitro* experiments and indicates that LEF1 has a tumor suppressive function in RMS-13.

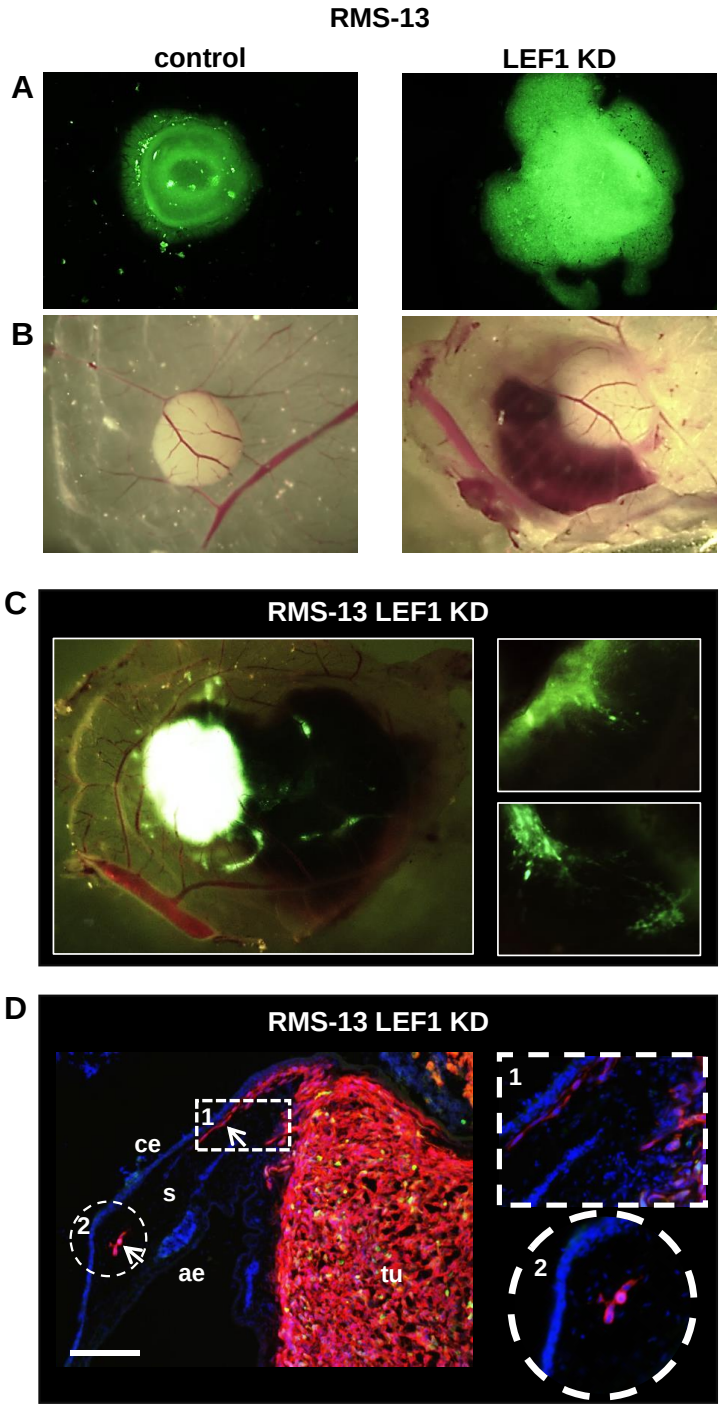

Figure 14: LEF1-dependent regulation of proliferation and invasion of RMS-13 cell line in the CAM assay. Shown are representative whole-mount images of **(A)** RMS-13 control tumors (n=7) and RMS-13 LEF1 KD tumors (n=7) at day 3 post inoculation visualized by GFP-fluorescence (20-fold magnification), **(B)** RMS-13 control tumors (n=7) and RMS-13 LEF1 KD tumors (n=6) at day 7 post inoculation (10-fold magnification) and **(C)** RMS-13 LEF1 KD tumors and invading cells visualized by GFP-fluorescence (10-fold magnification; insets: 125-fold magnification). **(D)** Immunofluorescence staining of cryosections of RMS-13 LEF1 KD tumors with anti-HLA-A,B,C antibody (red) and DAPI (blue). White arrows mark tumor cells invading the stroma (s) and are enlarged in the insets (125-fold magnification). Depicted are the chorion epithelium (ce), the allantoic epithelium (ae) and the tumor (tu). Scale bar 70 µm.

6.7 Effect of LEF1 KD on the expression of muscle differentiation markers in RMS cell lines

To investigate whether LEF1 affects myogenic differentiation of RMS cell lines, expression of the early muscle differentiation marker *MYOD* (Berkes *et al.*, 2005) and the late muscle differentiation markers myosin heavy chain 1 (*MYH1*), *DESMIN* and muscle creatine kinase (*CKM*) (Owens, 1995; Novitch *et al.*, 1996; Li *et al.*, 1997; Iezzi *et al.*, 2002; Schiaffino *et al.*, 2015) were analyzed by qRT-PCR.

Since recent papers proposed an important role of β-catenin in myogenic differentiation of RMS cells (Singh, S. *et al.*, 2010; Annavarapu *et al.*, 2013), we also investigated if β-catenin is essential in this process. For this purpose, RMS control and LEF1 KD cell lines were transiently transfected with *CTNNB1* specific siRNA and the successful β-catenin KD was verified for all cell lines by qRT-PCR (Figure 15, upper panel) and for RMS-13 and TE671 additionally by Western blot (Figure 15, lower panel). Hereby, β-catenin expression was reduced by more than 90 % on mRNA level and merely detected on protein level when compared to the respective control or LEF1 KD cells, which have been transfected with scrambled (scr) siRNA.

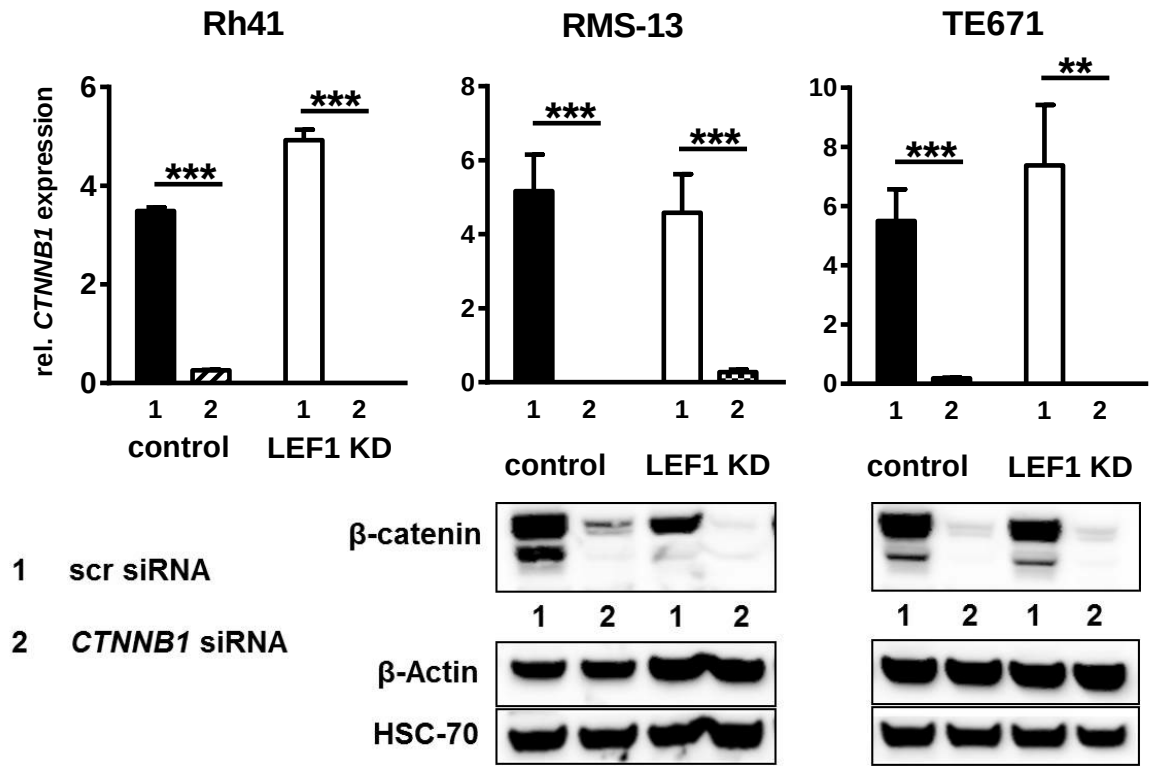

Figure 15: β-catenin KD in human RMS cell lines. Upper panel qRT-PCR analysis of *CTNNB1* in Rh41, RMS-13 and TE671 control and the respective LEF1 KD cells after transfection with scrambled (scr) siRNA (1) or *CTNNB1* siRNA (2). Data represent two independent experiments performed in duplicates and measured in triplicates. Gene expression levels were normalized to *18S* rRNA expression levels and data are displayed as mean+SEM; ***P*< 0.01, ****P*< 0.001 by Students t-test. **Lower panel** Western blot analysis of β-catenin in RMS-13 and TE671 control and the respective LEF1 KD cells performed 96 h after transfection with scr siRNA (1) or *CTNNB1* siRNA (2). β-Actin and HSC-70 served as loading control.

As shown in Figure 16A, the LEF1 KD in Rh41 cells significantly increased *MYH1* mRNA level but did not alter the expression of *MYOD*, *DESMIN* and *CKM* when compared to the values of control transduced cells that were set to 1. In contrast, RMS-13 LEF1 KD cells revealed an almost complete transcriptional suppression of all analyzed muscle differentiation markers compared to the respective control cells. In the ERMS cell line TE671, the LEF1 KD did not result in any significant changes regarding differentiation.

The β-catenin KD significantly downregulated or upregulated the expression of *MYH1* and *DESMIN*, respectively, in Rh41 LEF1 KD cells when compared to the scramble transfected LEF1 KD cells (Figure 16B). However, in all other settings the regulation of muscle differentiation markers was completely independent of the β-catenin KD.

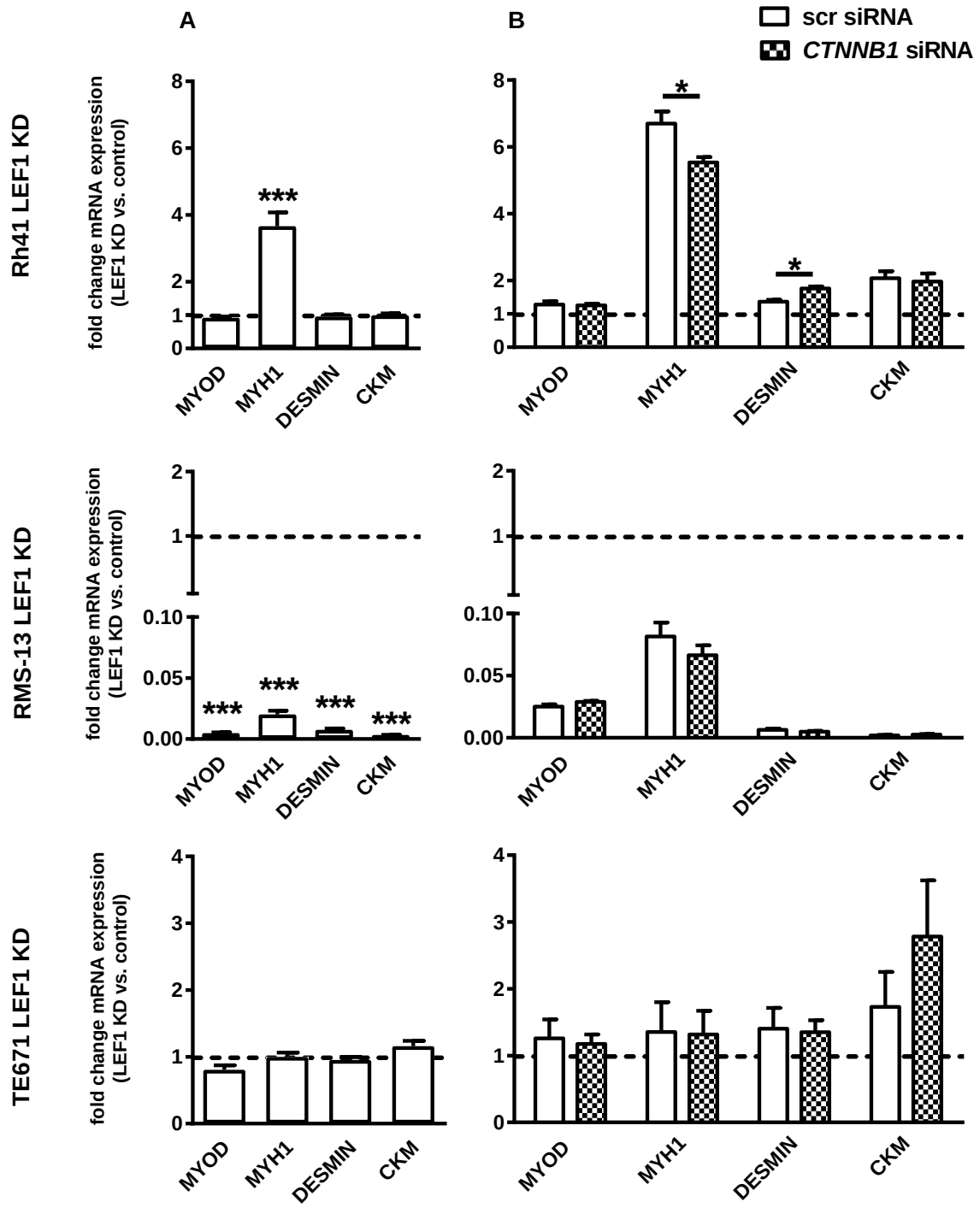

Figure 16: LEF1-dependent expression of muscle differentiation markers in RMS cell lines.(A) Expression of *MYOD*, *MYH1*, *DESMIN* and *CKM* in Rh41 LEF1 KD, RMS-13 LEF1 KD and TE671 LEF1 KD cells are shown as fold change to the respective control cells that were set to 1 (dashed line). **(B)** Expression of the same markers in the same cells after transfection with scr or *CTNNB1* siRNA. Indicated significances are shown for values after transfection with scr siRNA versus *CTNNB1* siRNA. **(A)** and **(B)** Gene expression levels were normalized to *18S* rRNA expression levels. Data represent mean+SEM of at least two independent experiments performed in duplicates and measured in triplicates; **P*<0.05, ****P*< 0.001 by Students t-test.

To summarize, the LEF1 again provokes heterogeneous effects in the used RMS cell lines. Thus, LEF1 apparently is involved in a more differentiated phenotype of RMS-13 cells, whereas it promotes a less differentiated one in Rh41 cells (Figure 16A). In contrast, except a significant change in *DESMIN* and *MYH1* mRNA levels in Rh41 LEF1 KD cells, β-catenin does not change the expression of muscle differentiation markers (Figure 16B).

Together these data suggest that LEF1 is one of the major regulators of myodifferentiation in RMS and that β-catenin plays an inferior role in this process.

6.8 WNT5A expression in primary human RMS

After examining the interplay of LEF1 with WNT/β-catenin signaling, we next started to analyze whether LEF1 might interact with the β-catenin independent (non-canonical) WNT signaling in RMS. Thus, staining of the TMA of human RMS biopsies (see Chapter 6.1) with anti-WNT5A antibody revealed that WNT5A was highly expressed in all fusion-positive ARMS and ERMS samples (Figure 17A). The studied samples could not be scored because the protein expression levels were very intense throughout the samples. This hampered the exact definition of cells that were negative, intermediately or intensely positive cells. Furthermore, the mRNA levels of *WNT5A* in the set of 10 human fusion-positive ARMS and 10 human ERMS samples were analyzed. As shown in Figure 17B, *WNT5A* was also overexpressed on transcript level when compared to normal skeletal muscle (n=4). Moreover, the data showed that *LEF1* mRNA levels positively correlate with that of *WNT5A* in ARMS, which just missed significance as estimated by Spearman correlation (Figure 17C). In contrast, the ERMS samples did not show any correlation (data not shown).

To sum up, the data indicate that besides LEF1, also WNT5A might be involved in the pathogenesis of ARMS and ERMS. In addition, *LEF1* and *WNT5A* expression might even correlate with each other in at least subtypes of ARMS. However, since WNT5A staining of the TMA was very strong, whereas WNT5A mRNA levels were only moderately elevated, the antigen retrieval conditions for WNT5A immunohistochemistry should be further optimized. Furthermore, *LEF1* and *WNT5A* correlation has to be verified and strengthened in a larger set of samples.

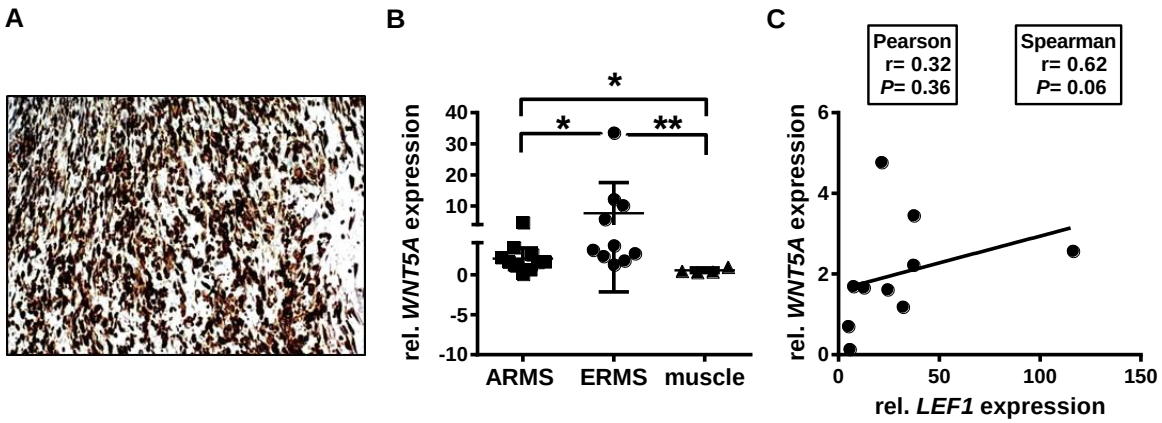

Figure 17: Immunohistochemical and qRT-PCR analyses of WNT5A in human RMS biopsies. (A) Representative immunohistochemical staining of WNT5A of primary human RMS. Magnification 200-fold. **(B)** *WNT5A* expression levels were analyzed by qRT-PCR in fresh-frozen biopsies of human fusion-positive ARMS (n=10) and human ERMS (n=10) compared to normal muscle (n=4). Gene expression levels were normalized to *GAPDH* expression levels. Bars, 95 % confidence intervals and mean values; **P*<0.05, ***P*<0.01 by Mann-Whitney t-test. **(C)** Parametric Pearson and non-parametric Spearman correlation analyses of *LEF1* with *WNT5A* expression levels in human fusion-positive ARMS biopsies. Regression line, 95 % confidence interval and correlation coefficient r for Pearson and Spearman test are given.

6.9 Effect of LEF1 KD on *WNT5A* expression in RMS cell lines

In parallel, we analyzed the effect of LEF1 KD on the expression of *WNT5A* in RMS cell lines. As shown in Figure 18, in RMS-13 LEF1 KD cells *WNT5A* mRNA levels were significantly downregulated when compared to control cells (that were set to 1). In contrast, LEF1 deletion in Rh41 and TE671 cells did not change the expression of *WNT5A* when compared to the respective control cells.

This indicates that – similarly to some primary ARMS samples – *LEF1* expression positively correlates with *WNT5A* expression in the cell line RMS-13.

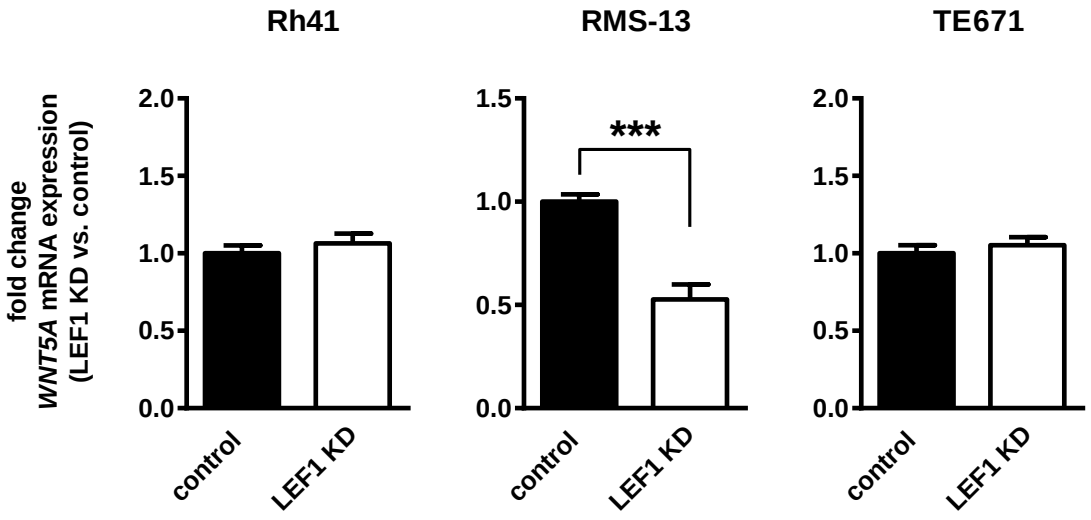

Figure 18: LEF1-dependent modulation of *WNT5A* expression in RMS cell lines. qRT-PCR analysis of *WNT5A* in Rh41 LEF1 KD, RMS-13 LEF1 KD and TE671 LEF1 KD cells are shown as fold change to the respective control cells that were set to 1 (black bar). *WNT5A* expression levels were normalized to *18S* rRNA expression levels. Data represent mean+SEM of three independent experiments performed in duplicates and measured in triplicates. ****P*< 0.001 by Students t-test.

6.10 Effect of LEF1 on WNT5A expression in RMS cell lines

Since *LEF1* expression also tends to positively correlate with *WNT5A* expression in primary human ARMS samples, we assumed that RMS-13 cells are an appropriate model to study the molecular basis of the observed LEF1/WNT5A interaction.

First, the positive correlation of LEF1 and WNT5A was confirmed by Western blot analysis. As shown in Figure 19, the LEF1 KD in RMS-13 cells correlated with a remarkable decrease in WNT5A protein level when compared to control cells, which was in line with the mRNA data shown in Figure 18. In contrast, and similar to what was seen on mRNA level, WNT5A protein level upon LEF1 KD was slightly increased in Rh41 LEF1 KD cells when compared to control transduced cells.

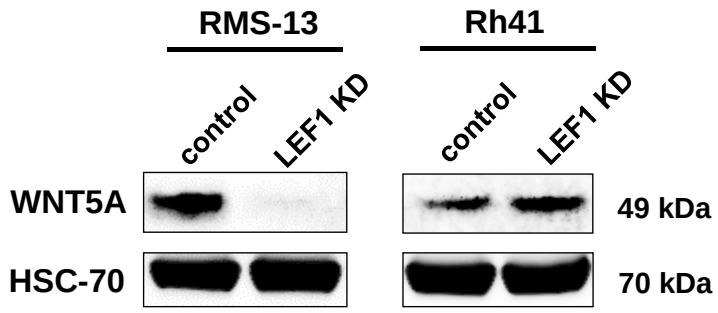

Figure 19: LEF1-dependent modulation of WNT5A protein level in ARMS cell lines. Western blot analysis of WNT5A in the ARMS cell lines RMS-13 and Rh41 stably transduced with empty vector control (control) or LEF1 shRNA (LEF1 KD). HSC-70 expression levels served as loading control. The data are representative of three independent experiments.

Since WNT5A/*WNT5A* is significantly downregulated in RMS-13 LEF1 KD cells, we hypothesized that LEF1 is necessary for WNT5A expression. We also hypothesized that WNT5A signals back to the RMS cell lines in a para- or autocrine manner and fosters LEF1 expression in a positive feedback. This hypothesis is based on data from the literature. Thus, WNT5A signaling can activate PI3K-mediated AKT-phosphorylation (Zhang, S. *et al.*, 2012; Zhao *et al.*, 2015). Due to the fact that RMS frequently show phosphorylation of AKT (Cen et al., 2007) and since LEF1 can be upregulated by PI3K/AKT signaling (Huang *et al.*, 2012), we so far have investigated whether i) LEF1 expression was dependent on activation of this pathway and ii) the decrease of WNT5A levels upon deletion of LEF1 in RMS-13 cells was associated with inhibition of PI3K/AKT signaling.

Indeed, phosphorylation of AKT was decreased in RMS-13 LEF1 KD cells when compared to the respective control transduced cells (Figure 20). This effect was not seen in Rh41 LEF1 KD cells, in which WNT5A/*WNT5A* expression is rather not modulated by LEF1.

Consequently, WNT5A expression positively correlates with pAKT protein level in RMS-13 cells.

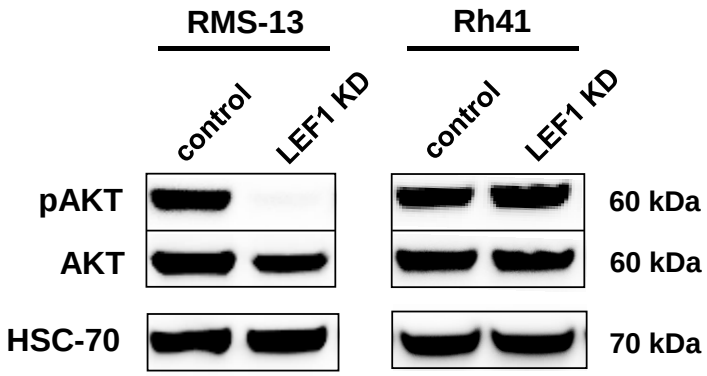

Figure 20: LEF1-dependent modulation of pAKT/AKT protein level in ARMS cell lines. Western blot analysis of pAKT/AKT in the ARMS cell lines RMS-13 and Rh41 stably transduced with empty vector control (control) or LEF1 shRNA (LEF1 KD). HSC-70 expression levels served as loading control. The data are representative of three independent experiments.

In order to analyze whether LEF1 expression was dependent on activation of PI3K/AKT signaling, RMS-13 control cells were incubated with the dual PI3K/mTOR inhibitor PI103, the pure PI3K inhibitor GDC-0941 or the pure AKT inhibitor MK-2206 and LEF1 protein levels were analyzed by Western blot (Figure 21). Analysis of the phosphorylation status of AKT served as readout for PI3K/AKT activity.

As shown in Figure 21, all inhibitors potently inhibited the phosphorylation of AKT when compared to the solvent. Moreover, the incubation of RMS-13 control cells with PI103 and GDC-0941 markedly decreased LEF1 protein levels when compared to the solvent treated cells. In contrast, LEF1 protein levels almost remained unaffected after incubation with MK-2206 compared to solvent.

Together, these data indicate that in RMS-13 cells, PI3K signaling results in upregulation of LEF1 expression in an AKT-independent manner.

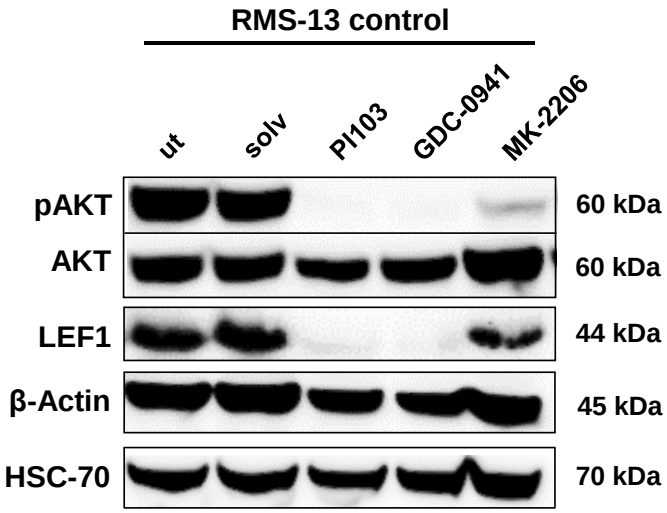

Figure 21: Effect of PI3K/pAKT/mTOR inhibitors on LEF1 protein levels in RMS-13. Western blot analysis of RMS-13 control cells incubated for 48 h with 3 µM PI103, 10 µM GDC-0941 or 1 µM MK-2206 in comparison to untreated (ut) or solvent (solv) treated cells. β-Actin and HSC-70 expression levels served as loading control. The data are representative of two independent experiments.

7 Discussion

Until now only few data on the role of WNT signaling in RMS have been published and are restricted to β-catenin dependent (canonical) WNT signaling. These data suggest that canonical WNT signaling is functionally active in RMS cell lines and that activation of this pathway is associated with a more differentiated phenotype in ARMS as well as in ERMS and inhibited proliferation in ARMS (Singh, S. *et al.*, 2010; Annavarapu *et al.*, 2013). Thus, these findings support a potential tumor suppressive role of canonical WNT signaling in RMS that additionally promotes myogenic differentiation. The authors also propose that canonical WNT signaling might be a potential therapeutic target in the combat against RMS, in particular for patients with ARMS who currently have a poor outcome with limited therapeutic options (Annavarapu *et al.*, 2013). Indeed, several studies suggest that canonical WNT pathway activity can inhibit cancer progression and predicts a better prognosis for a broad variety of solid tumor entities. Thus, elevated levels of nuclear β-catenin correlate with improved patient outcome in medulloblastoma, malignant melanoma, ovarian cancer and prostate cancer (Gamallo *et al.*, 1999; Ellison *et al.*, 2005; Horvath *et al.*, 2005; Chien *et al.*, 2009; Anastas *et al.*, 2013). On the other hand, nuclear β-catenin accumulation and therefore activity of canonical WNT signaling is frequently involved in the development of tumors including colorectal, prostate and lung cancer (reviewed in Heuberger *et al.*, 2010; Anastas *et al.*, 2013). This reveals that in dependency on the cellular context canonical WNT signaling activity can either have a tumor suppressive or an oncogenic function.

Likewise, the interaction partner of β-catenin, LEF1 can function as either an oncogene or a tumor suppressor in different cellular contexts. Consequently its activity can be both, positively and negatively correlated with patient outcomes in different types of cancer. For instance, the fact that transplantation of bone marrow cells overexpressing LEF1 leads to acute myeloid leukemia and B-precursor ALL in mice argues for a role as an oncogene (Petropoulos *et al.*, 2008). However, LEF1 can also act as a tumor suppressor due to transcriptional repression of *c-MYC*. This has been found in a subset of T-ALL cases, in which *LEF1* inactivation showed increased levels of *c-MYC* expression, which might be an important step in the molecular pathogenesis of T-ALL (Gutierrez *et al.*, 2010).

The aim of this thesis was to elucidate the role of LEF1 in RMS in more depth and to shed some light into its potential interactions with the canonical and non-canonical WNT signaling pathways.

7.1 Wnt3a-driven β-catenin dependent (canonical) WNT signaling seems to play a subordinate role in RMS

The TMA analysis revealed that 21 out of 48 primary human RMS samples express LEF1, which was exclusively found in the nucleus (Figure 3A). Thereby the number of LEF1 positive cells and the intensity of LEF1 signals were higher in the less aggressive ERMS subtype compared to ARMS. Consistent with the results of the TMA, qRT-PCR analysis in fresh-frozen human fusion-positive ARMS and ERMS samples revealed heterogeneous *LEF1* overexpression when compared to normal skeletal muscle (Figure 4A). Likewise, 21 out of 48 primary human RMS samples of the TMA were positive for β-catenin but no correlation between LEF1 and β-catenin protein levels was observed (Figure 3B). However, nuclear β-catenin expression was only detected in one ERMS. This is in line with previously published data, in which approximately 24 out of 44 human ARMS and ERMS biopsies showed membranous/cytoplasmatic β-catenin expression, whereas nuclear expression was only seen in two cases of ERMS (Annavarapu *et al.*, 2013). Similarly, the study by Shukla *et al.* revealed β-catenin mutations in two out of 60 ERMS samples that could be responsible for nuclear β-catenin accumulation (Shukla *et al.*, 2012). The very low number of RMS showing nuclear β-catenin is also in agreement with studies by Bouron-Dal Soglio and colleagues, who did not find activating β-catenin mutations in their patient cohort (Bouron-Dal Soglio *et al.*, 2009). Moreover, in our collection of human ARMS and ERMS samples, the expression of the major downstream target of canonical WNT signaling *AXIN2* was rather downregulated compared to normal muscle (Figure 4C). Together, these data suggest that canonical WNT signaling is not active in most RMS, despite of sometimes high levels of LEF1/*LEF1*.

The lack of canonical WNT signaling activity in primary human ARMS samples and activity in only few ERMS samples is also in line with our cell culture experiments using Wnt3a. The cell culture experiments suggest that activation of WNT/β-catenin signaling is only possible in subsets of RMS, such as specific ERMS subtypes. Hence, TOP/FOP reporter assay and immunofluorescence staining in RMS cell lines revealed that activation of canonical WNT signaling by Wnt3a (as shown by *AXIN2* upregulation; Figure 7) induced neither TOP activity nor nuclear translocation of β-catenin in the ARMS cell lines Rh41 and RMS-13 (Figure 8 and Figure 11). In contrast, the ERMS cell line TE671 showed strong luciferase induction and predominant nuclear accumulation of β-catenin in response to Wnt3a (Figure 8 and Figure 11). Annavarapu and colleagues also demonstrated

functional activation of the canonical WNT signaling in the human ERMS cell line RD18 (Annavarapu *et al.*, 2013). On the other hand, they also showed that this pathway is functionally active in the ARMS cell line Rh30. This is in contrast to our data, because the ARMS cell line RMS-13 (which was used in our study) is sometimes thought to be related to Rh30 and perhaps derived from the same patient tumor as Rh30. However, the origin of RMS-13 and Rh30 is not completely clear (reviewed in Hinson *et al.*, 2013). Therefore, the differences between the studies may reflect heterogeneity of different RMS cell clones. Likewise, the observed differences between the cell lines might also depend on the histology of the individual tumor part that has been used for establishment of the individual cell line.

Moreover, the lack of TOP reporter activity and common absence of nuclear β-catenin after Wnt3a treatment in ARMS cells also suggest that Rh41 and RMS-13 cells may i) have a mutation in the endogenous β-catenin that prevents induction of Wnt3a-mediated signaling activity or ii) possess a mechanism, which retains endogenous β-catenin in the cytoplasm or at the plasma membrane and thus impedes its nuclear translocation (Kimelman *et al.*, 2006). Importantly, we found no β-catenin mutations in any of the RMS cell lines examined (data not shown). Thus, these results indicate that β-catenin is functional and suggest the existence of mechanism(s) specific for ARMS, in which endogenous β-catenin is rather hold back at the plasma membrane/cytoplasm. In fact, several studies indicate that cadherins and other catenins i.e. α-catenin or p120 catenin can sequester β-catenin at the cell membrane in order to mediate cell-cell adhesion. This can largely affect the signaling capacity of β-catenin (reviewed in McEwen *et al.*, 2012; McCrea *et al.*, 2015). Indeed, our immunofluorescence staining are in favor of a much stronger β-catenin staining at the cell membrane between adjacent ARMS cells, especially in Rh41, than in the ERMS cells (see Figure 11). The same observation has been made in a study, in which the expression and localization of cadherins and catenins in five ERMS and four ARMS cell lines was examined. Thus, ARMS cell lines showed generally stronger expression of N-cadherin and M-cadherin when compared to ERMS cell lines. In addition, immunofluorescence staining revealed that cadherins and catenins including β-catenin were barely detectable at intercellular contacts of ERMS cells, whereas in ARMS cells specific persistent localization was observed at the sites of cell-to-cell contact (Charrasse *et al.*, 2004). Hence, it is tempting to speculate that the increased interaction of cadherins/catenins at the cell membrane of ARMS cells results in β-catenin sequestration,

reduction of the cytosolic β-catenin pool and thus could prevent nuclear translocation of β-catenin in Rh41 and RMS-13. This is different in ERMS cells i.e. in TE671 cells, in which low cadherin expression and missing localization of cadherin/catenin at the sites of cell-to-cell contact results in nuclear translocation of cytoplasmatic β-catenin, where it can activate canonical WNT signaling in response to Wnt3a. However, this hypothesis remains to be elucidated in the future.

Although canonical WNT signaling is not functionally active in the ARMS cell lines, *AXIN2* was significantly upregulated in response to Wnt3a (Figure 7). Thus, expression of *AXIN2* must be regulated by other factors independently of β-catenin. Indeed, studies reported that E2F1, a transcription factor involved in cell cycle regulation and synthesis of DNA, can induce *AXIN2* expression (Hughes *et al.*, 2005; reviewed in Poppy Roworth *et al.*, 2015). Likewise, the caudal-related homeobox transcription factor 2 (CDX2) has been shown to stimulate *AXIN2* expression in colon cancer cell lines (Olsen *et al.*, 2013). Moreover, expression of both transcription factors can be induced in response to Wnt3a (Khan *et al.*, 2007; Sherwood *et al.*, 2012).

However, the fact that *AXIN2* activation was not expressed in primary RMS samples (but in all cell lines upon Wnt3a treatment) argues for a minor role of WNT3A in the pathogenesis of RMS.

This assumption was confirmed by an *in vivo* approach when heterozygous $Ptch^{del/+}$ mutants were crossed with $Wnt^{vt/vt}$ mice. The *vt* mutation is a naturally occurring hypomorphic mutation of Wnt3a, which decreases the level of Wnt3a expression and abrogates tail formation in homozygous mice (Greco *et al.*, 1996). Wnt3a is a major activator of WNT/β-catenin dependent signaling. Since Wnt3a is expressed during the period of initial somite development and is essential for mesoderm and myotome formation (Ikeya *et al.*, 1998; reviewed in von Maltzahn *et al.*, 2012), we reasoned that $Wnt^{vt/vt}$ mice represent a valuable model for attenuation of Wnt3a-driven canonical Wnt signaling during RMS formation. Our data show that RMS incidence, multiplicity and latency time in $Ptch^{del/+}Wnt^{vt/vt}$ mice was similar to that of the control mice (Table 22 and Figure 5) (Nitzki *et al.*, 2016). Furthermore, growth characteristics of RMS *in vivo* were also not affected by a heterozygous inactivating *β-catenin* mutation (Nitzki *et al.*, 2016). Altogether, this indicates that Wnt3a/β-catenin-driven Wnt signaling plays a subordinate role in RMS pathogenesis. However, this speculation remains to be further investigated. Thus, it is also

possible that other upregulated Wnt ligands such as Wnt4, that can activate canonical Wnt signaling and regulate the myogenic fate of somites (Bernardi *et al.*, 2011), might compensate for the decreased canonical Wnt pathway activity in *Ptch*$^{del/+}$*Wnt*$^{vt/vt}$ mice. However, the lack of *AXIN2* expression in primary RMS samples rather argues against such a scenario.

The minor role of canonical WNT signaling in RMS is further fostered by the results of the TOP/FOP reporter assay. This assay revealed that the tumor suppressive function of LEF1 does not require activation of β-catenin driven WNT signaling (Figure 10). Since LEF1 is expressed in primary human RMS samples, it can be speculated that LEF1 exerts functions in RMS that are independent of β-catenin activity. Indeed, β-catenin independent LEF1 functions are well known and examples encompass interaction with ATF2 factors (Grumolato *et al.*, 2013) and with the intracellular domain of Notch (Ross *et al.*, 2001). This is also in line with our data, showing that the LEF1-induced effects on myogenic differentiation are mostly independent of β-catenin in all RMS cell lines. Thus, except a β-catenin-mediated up- or downregulation of *DESMIN* and *MYH1*, respectively, in Rh41 LEF1 KD cells, the β-catenin KD itself did not change the expression of muscle differentiation markers in RMS LEF1 KD cells (Figure 16B). Likewise, experiments in presomitic mesoderm explants revealed that MyoD and Myf5 expression can be activated by Pax3 despite the absence of functional β-catenin (Brunelli *et al.*, 2007).

In summary, β-catenin mediated WNT signaling seems to play a subordinate role in RMS and thus the LEF1-mediated effects are independent of this pathway, at least in a subset of RMS.

However, in contrast to canonical WNT signaling, we have strong evidence that non-canonical WNT signaling might play a role in RMS. The first hint came from a genetic approach, in which *Ptch*$^{del/+}$ mutants were bred to *Wif1*$^{-/-}$ mice. The latter do not express the Wnt inhibitory factor 1, which encodes an endogenous secreted Wnt pathway antagonist. In these mice RMS multiplicity was significantly decreased upon *Wif1* deletion. Thus, whereas 41 % of *Ptch*$^{del/+}$*Wif1*$^{+/-}$ animals have developed multiple RMS, the percentage of *Ptch*$^{del/+}$*Wif1*$^{-/-}$ mice with multiple RMS significantly decreased to 11 % (Nitzki *et al.*, 2016). Together with the fact that canonical Wnt signaling activity does not play a prominent role in RMS pathogenesis, these data strongly suggest that Wnts involved in non-canonical Wnt signaling and which are usually bound by Wif1 i.e. Wnt5a, Wnt7a or

Wnt11 (Surmann-Schmitt *et al.*, 2009) might restrain RMS formation, at least in mice. This part will be discussed in Chapter 7.3.

7.2 LEF1 can reduce tumor progression and can induce myodifferentiation in a subset of RMS

In order to analyze the function of LEF1 in RMS in detail, we established a stable LEF1 KD in the ARMS cell lines Rh41 and RMS-13 and in the ERMS cell line TE671. Hence, stable deletion of LEF1 resulted in a significant downregulation of the canonical WNT target *AXIN2* in RMS-13 cells but not in Rh41 LEF1 KD or TE671 LEF1 KD cells (Figure 6B). In contrast, *c-MYC* was significantly increased in both ARMS cell lines upon LEF1 KD (Figure 6B). This is similar to T-cell acute lymphoblastic leukemia, in which LEF1-inactivated cases show increased levels of MYC expression when compared with cases with intact LEF1 (Gutierrez *et al.*, 2010). Moreover, pro-B cells from Lef1-deficient mice revealed elevated levels of c-Myc (Reya *et al.*, 2000). As shown in Figure 12, the LEF1 KD in RMS-13 was also accompanied by a significant decrease of all *TCF* factors when compared to control cells, which could explain the above mentioned downregulation of *AXIN2* in this cell line upon LEF1 depletion (Figure 6B).

Most importantly, our experiments revealed that LEF1 can restrain RMS aggressiveness. Thus, depending on the used cell line, LEF1 can i) induce apoptotic signals, ii) suppress proliferation, migration and invasiveness of RMS cells *in vitro* and *in vivo* and iii) can positively influence the myogenic differentiation status of the tumor cells (Figure 13, Figure 14 and Figure 16A).

The anti-proliferative effect of LEF1 in the ARMS cell lines Rh41 and RMS-13 may be related to attenuation of *c-MYC* expression (Figure 6B). Although the role of c-MYC in ARMS has never been studied in detail, this assumption would be in line with the observation that c-MYC can foster migration, invasion and tumor-induced angiogenesis of ERMS (Bernard *et al.*, 2006; Marampon *et al.*, 2006). More precisely, growth of the ERMS cell line RD was arrested after stably over-expression of MadMyc chimera that specifically blocks c-MYC activity. Furthermore, functional inactivation of c-MYC can induce myogenic differentiation of the ERMS cell line RD (Marampon *et al.*, 2006). Thus, it could be possible that the increased *c-MYC* levels in RMS-13 LEF1 KD cells are responsible for the increase in proliferation and the more aggressive and less differentiated phenotype.

It is also possible that TCF1, TCF3 and TCF4 are associated with the LEF1-mediated RMS phenotype. Thus, while LEF1 KD in RMS-13 induces invasiveness, the opposite is the case for Rh41 cells where invasion is reduced (Figure 13). This was accompanied with a down- or upregulation of all *TCF*s, respectively (Figure 12). In TE671, neither *TCF* levels nor invasive capacity were remarkably affected (Figure 12 and Figure 13). This indicates that the dosage and/or composition of LEF1/TCF factors may regulate the invasiveness of RMS cells.

Since LEF1/TCFs play a key role in the regulation of canonical WNT signaling activity and several studies suggest that TCFs can contribute to both activation and also to repression of WNT target genes, the regulation of TCF factors by LEF1 opens a very interesting perspective in RMS. TCF3 is generally known as a repressor of WNT target genes and the full-length, β-catenin-binding form of TCF4 is also sometimes associated with target gene repression but can also act as transcriptional activator (Tang *et al.*, 2008; Cadigan *et al.*, 2012; Shah *et al.*, 2015). In contrast, full-length TCF1 and LEF1 are more often linked to WNT target gene activation (reviewed in Cadigan *et al.*, 2012). A concrete mechanism, in which LEF1 directly mediates the regulation of TCF factors, is not known. Nevertheless, there is strong evidence that LEF1 negatively regulates *IL-4* expression (independently of β-catenin), which in turn can inhibit TCF1/*TCF1* expression levels (Hebenstreit *et al.*, 2010; Maier *et al.*, 2011). Moreover, incubation of RD and Rh30 cells with IL-4 resulted in decreased MYOD protein levels (Hosoyama *et al.*, 2012). Thus, it can be speculated that RMS-13 cells possess a mechanism, in which LEF1 – e.g. *via* inhibition of IL-4 – can induce the expression of TCF factors and concomitantly myogenic differentiation.

Together the data suggest that the function of LEF1 might involve regulation of TCFs, which again occurs in dependency on the cellular context. Thus, it is possible that TCFs may play a role in myogenic differentiation (and thus aggressiveness) modulated by LEF1, at least in ARMS cell lines. Indeed, recently it has been shown that TCF4 overexpression significantly up-regulated expression of MyoD and myosin heavy chain II proteins in mesenchymal stem cells (Singh, R. *et al.*, 2009). In addition, LEF1 together with TCF1 has intrinsic HDAC activity, which is necessary for differentiation of $CD8^+$ T-cells (Xing *et al.*, 2016). In our settings, LEF1 induces the expression of *TCF1* and *TCF4* and of muscle lineage markers in RMS-13 cells (Figure 12 and Figure 16A). This is different in Rh41 cells, in which LEF1 rather suppresses *TCF1* and *TCF4* and the myogenic differentiation

marker *MYH1*. It is also different in TE671 cells where LEF1 has no effect on *TCF1*, *TCF4* or muscle differentiation. Therefore it is tempting to speculate that there are subgroups of RMS, in which differentiation (and concomitantly aggressiveness) is either epigenetically regulated by LEF1 or by LEF1-mediated modulation of TCFs. The first hypothesis would be in line with a recent study that divides RMS into four distinct subtypes based on their genetic signature and DNA methylation pattern (Seki *et al.*, 2015). However, the biological/genetic basis for a distinct epigenetic signature of RMS is currently unknown and should be addressed in the future.

To sum up, the data suggest that LEF1 can counteract the aggressiveness of RMS and is probably one of the major mediators of RMS differentiation. However, the fact that LEF1 fosters invasiveness and suppresses *MYH1* expression in Rh41 cells indicate that this tumor suppressive function may be restrained to specific RMS subgroups.

7.3 Interaction of LEF1 and WNT5A in RMS-13 cells

Our analyses revealed that all primary human RMS samples of the TMA express WNT5A (Figure 17A). On transcript level, our collection of fresh-frozen ARMS and ERMS samples also overexpressed *WNT5A* when compared to normal muscle (Figure 17B). Despite the low number of analyzed samples, *LEF1* expression apparently positively correlates with that of *WNT5A* in ARMS (Figure 17C). Since this may indicate a co-regulation of both factors, the expression of WNT5A in RMS LEF1 KD cell lines was studied. Indeed, a positive correlation of LEF1 and WNT5A was found in the ARMS cell line RMS-13. Thus, the LEF1 KD in RMS-13 resulted in downregulation of WNT5A on both mRNA and protein level (Figure 18 and Figure 19). Due to the fact that LEF1 rather has a tumor suppressive function in ARMS, we hypothesize that this also should hold true for WNT5A. In fact, WT5A can exert anti-tumorigenic functions such as inhibition of cell migration and invasiveness. As already described, WNT5A reduces the invasion of prostate cancer cells (Syed Khaja *et al.*, 2011), and inhibits the migration of multiple breast cancer cell types (Säfholm *et al.*, 2006; Hansen *et al.*, 2009). Moreover, work from our own group support a role of WNT5A in regression and differentiation of basal cell carcinoma (Nitzki *et al.*, 2010). In addition, WNT5A induces myogenic differentiation in mice and the expression of differentiation markers of colon cancer cells (Buttler *et al.*, 2013; Mehdawi *et al.*, 2016).

Hence, the data indicate that LEF1 might also regulate WNT5A, at least in a subset of ARMS. Taken together, we hypothesize that LEF1 can activate WNT5A and concomitantly inhibit the expression of c-MYC, which results in attenuation of aggressiveness of specific RMS subgroups.

We next studied whether WNT5A activates PI3K/AKT signaling in RMS-13 cells. This was based on a literature review (Zhang, S. *et al.*, 2012; Zhang *et al.*, 2014), and due to the fact that RMS frequently show phosphorylation of AKT (Cen *et al.*, 2007). Indeed, the decrease of WNT5A levels in RMS-13 LEF1 KD cells (see Figure 19) was associated with decreased levels of pAKT (Figure 20). Based on the fact that LEF1 expression itself can be induced by PI3K/AKT signaling (Huang *et al.*, 2012), we next analyzed LEF1 protein levels in the parental RMS-13 cell line (without LEF1 KD) after incubation with the dual PI3K/mTOR inhibitor PI103, the pure PI3K inhibitor GDC-0941 or the pure AKT inhibitor MK-2206. Due to a remarkable decrease in LEF1 upon PI103 and GDC-0941 but not upon MK-2206 incubation (Figure 21), we conclude that LEF1 expression in RMS-13 is positively regulated by PI3K signaling in an AKT-independent manner. Indeed, although AKT is considered to be the key downstream effector of PI3K oncogenic signaling, several studies demonstrated that PI3K and AKT can act independently of each other in cancers (reviewed in Bruhn *et al.*, 2013; Faes *et al.*, 2015). Thus, AKT-independent signaling modes of PI3K in cancer include activation of RAC, which has been shown to regulate MEK/ERK signaling in breast cancer cells (Ebi *et al.*, 2013). Besides RAC, mTORC2 represents another kinase whose activation relies on PI3K and thus might be involved in AKT-independent effects of PI3K signaling. Although strong evidence emphasizes the importance of phosphorylation and activation of AKT by mTORC2, recent studies have revealed AKT-independent functions of mTORC2 in cancer (reviewed in Faes *et al.*, 2015). In addition, emerging evidence has shown the importance of serum- and glucocorticoid-inducible protein kinase 3 (SGK3) to be involved in AKT-independent PI3K signaling. SGK3 belongs to a family of kinases, which are highly homologous to the AKT family, sharing similar upstream activators and downstream targets and has been implicated in the regulation of cell growth, proliferation, survival and migration (reviewed in Bruhn *et al.*, 2010). Thus, it is possible that PI3K also regulates LEF1 independently of AKT.

Based on the already accomplished data and the literature review, we now propose a model for a subset of ARMS, in which LEF1 and WNT5A establish a positive feedback loop that counteracts the aggressiveness by inhibition of c-MYC (Figure 22). Since WNT5A can inhibit c-MYC expression *via* increase of intracellular Ca^{2+} (Kremenevskaja *et al.*, 2005) and since *vice versa* c-MYC can repress WNT5A (Cappellen *et al.*, 2007), the regulation of c-MYC expression in this model may also involve WNT5A. Moreover, the repression of c-MYC mediated by LEF1 and/or WNT5A could be responsible for the attenuation of aggressiveness (e.g. proliferation, migration and invasion). Whether this is true or not remains to be investigated in the future.

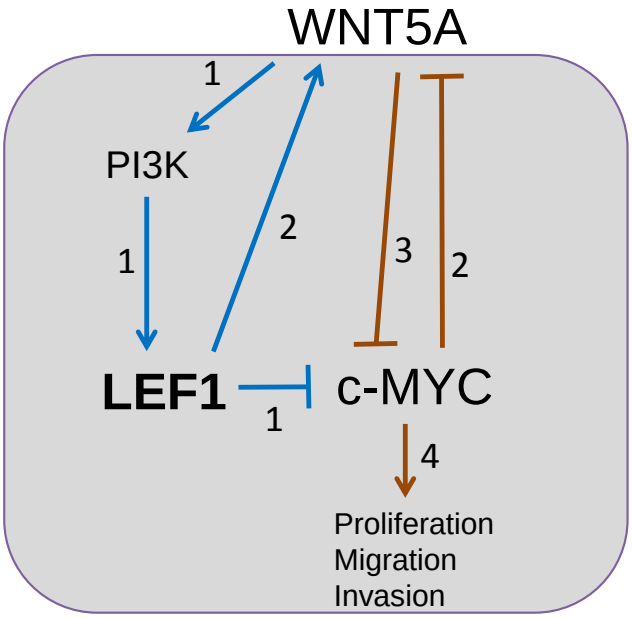

Figure 22: Current model of the interplay of LEF1, WNT5A, PI3K and c-MYC in ARMS. (1) WNT5A signaling is responsible for PI3K activation, LEF1 expression and c-MYC repression. **(2)** *Vice versa* LEF1 induces WNT5A expression either with or without the involvement of c-MYC. **(3)** WNT5A expression inhibits c-MYC expression. **(4)** WNT5A-and/or LEF1-associated c-MYC repression is responsible for attenuation of proliferation, migration and invasion of ARMS. Arrows and blocking signs in **blue** represent own data and in **brown** data provided by the literature.

7.4 Outlook

Analysis of primary RMS samples revealed a role of LEF1 but also non-canonical WNT signaling in the pathogenesis of this tumor. Based on the potential positive correlation of *LEF1* and *WNT5A* expression in ARMS, the LEF1 knockdown experiments in RMS cell lines and the treatment of RMS-13 cells with PI3K-and AKT-specific inhibitors, we

propose a positive WNT5A – PI3K – LEF1 – WNT5A signaling loop and concomitant c-MYC repression at least in a subset of ARMS (Figure 22). To verify this assumption and to strengthen our model the following experiments should be performed.

Does LEF1 induce WNT5A with or without involvement of c-MYC in RMS-13 cells?

To verify whether LEF1 induces WNT5A *via* inhibition of c-MYC, *c-MYC* should be deleted in RMS-13 LEF1 KD cells by specific shRNA followed by WNT5A expression analysis. If the c-MYC KD results in WNT5A upregulation, a c-MYC-mediated WNT5A repression is very likely. If this is not the case, LEF1 stimulates WNT5A expression in a c-MYC-independent way. Consequently, it would be useful to find possible mediator proteins, which could be identified by transcriptome analysis of RMS-13 LEF1 KD cells in comparison to control cells.

Does WNT5A activate PI3K and is this involved in regulation of LEF1 expression and attenuation of aggressiveness of RMS-13 cells?

In order to prove that WNT5A activates PI3K signaling activity, RMS-13 cells should be incubated with recombinant WNT5A. Then the PI3K activation status and AKT phosphorylation should be measured i.e. by a PI3K activation assay or Western blot, respectively. The same analyses should be done in RMS-13 cells in which WNT5A is stably deleted.

In order to show whether c-MYC is mainly inhibited by WNT5A or LEF1, RMS-13 LEF1 KD cells that do not express LEF1 or WNT5A should be incubated with recombinant WNT5A followed by c-MYC expression analysis.

Furthermore, cellular effects such as proliferation, apoptosis, migratory and invasive properties as well as the expression of muscle differentiation markers should be analyzed in RMS-13 LEF1 KD after treatment with recombinant WNT5A. This could clarify whether WNT5A influences aggressiveness of RMS-13 cells in a LEF1-independent manner.

Is LEF1 upregulated by PI3K in an AKT independent manner?

In order to analyze whether PI3K is involved in LEF1 expression, PI3K activity in RMS-13 cells should be modulated by overexpression of a constitutively active PI3K isoform or inhibition of PI3K using siRNA technology. Afterwards, LEF1 and c-MYC expression as well as PI3K activity should be examined.

Is c-MYC repression involved in proliferation, migration and invasion in ARMS?

In ERMS cells it has been demonstrated that c-MYC affects proliferation, migration, invasion and tumor-induced angiogenesis (Marampon *et al.*, 2006; Gravina *et al.*, 2016). However, in ARMS this has not yet been analyzed. Therefore, ARMS cell lines with a stable c-MYC KD should be established (i.e. in RMS-13 and Rh41 cells). Afterwards, the RMS-13 c-MYC KD and the respective control cells should be analyzed regarding apoptosis, proliferation, migration and invasion as described in this thesis. This will show whether repression of c-MYC is responsible for a less aggressive phenotype in RMS-13 cells.

Does WNT5A activate WNT/Ca^{2+} and/or WNT/JNK signaling?

WNT5A activates the WNT/Ca^{2+} signaling pathway in the presence of receptor FZD2, 3, 4, 6, and 5 that interact with the participating co-receptor ROR1/2 (He *et al.*, 1997; Slusarski *et al.*, 1997; Kühl *et al.*, 2000; Weeraratna *et al.*, 2002). Binding of WNT5A to ROR2 can also activate the WNT/JNK pathway (Oishi *et al.*, 2003). Furthermore, it has been shown that Ca^{2+}/CAMKII can activate PI3K (Joyal *et al.*, 1997). In order to see, which pathway is potentially activated by WNT5A and modulates LEF1 and c-MYC expression or PI3K activity, the RMS-13 cells could be treated with specific inhibitors of the WNT/JNK and WNT/Ca^{2+} pathways (e.g. JNK or CAMKII inhibitors; Zhang, T. *et al.*, 2012; Pellicena *et al.*, 2014). Then the expression of LEF1 and c-MYC and the PI3K activity should be analyzed. Also the activation status of WNT/JNK and WNT/Ca^{2+} signaling should be determined by analysis of the phosphorylation status of JNK and c-Jun or PKC and CaMKII, respectively.

Is *Lef1/Wnt5a* associated with a more aggressive RMS phenotype in mice?

In addition, *in vivo* studies would help to ascertain if LEF1 and/or WNT5A can induce a less aggressive RMS phenotype. For this purpose, Lef1 or Wnt5a could be conditionally inactivated in RMS of $Ptch^{del+}$ mice. To analyze whether Lef1 or Wnt5a are involved in RMS formation, the knockout of *Lef1* and *Wnt5a* can be induced in 4-weeks old mice followed by RMS monitoring. In order to analyze the role of these genes in RMS progression, the knockout could be induced in fully-developed RMS. Tumor growth could be monitored by volumetric computer tomography. Afterwards, isolated tumors should be analyzed by qRT-PCR, Western blot, histological and immunohistochemical staining e.g. regarding the expression of Lef1, Wnt5a and c-Myc and as well as of proliferative,

apoptotic and differentiation markers. This will show whether Lef1 and/or Wnt5a signaling is associated with a less aggressive phenotype in mice and whether this is accompanied by inhibition of c-Myc. Furthermore, it could give evidence if the differentiation status of the tumors is influenced by Lef1 and/or Wnt5a.

Does LEF1/WNT5A expression correlate with decreased c-MYC and Ki67 expression and better clinical prognosis in human RMS?

To prove that *LEF1* positively correlates with that of *WNT5A* expression and evaluate statistical significance, the above mentioned qRT-PCR analysis should include more fresh-frozen samples. Besides, *c-MYC* expression of the samples should also be analyzed. Additionally, the TMA could be used to perform c-MYC and also Ki67 and active Caspase-3/TUNEL staining to investigate the proliferative and apoptotic status and thus aggressiveness of the tumors. Afterwards correlation analysis of LEF1 or WNT5A expression with that of c-MYC, Ki67 and patient´s survival data could be performed. This will show whether LEF1/WNT5A expression correlate with decreased c-MYC and Ki67 expression and a better clinical prognosis in RMS.

8 References

Agarwal, M., Kumar, P. & Mathew, S. J. (2015). The Groucho/Transducin-like enhancer of split protein family in animal development. *IUBMB Life, 67*(7), 472-481.

Anastas, J. M. & Moon, R. T. (2013). WNT signalling pathways as therapeutic targets in cancer. *Nature Reviews Cancer, 13*(1), 11-26.

Annavarapu, S., Cialfi, S., Dominici, C., Kokai, G., Uccini, S., Ceccarelli, S., McDowell, H. & Helliwell, T. (2013). Characterization of Wnt/β-catenin signaling in rhabdomyosarcoma. *Lab Invest, 93*(10), 1090-1099.

Arce, L., Yokoyama, N. N. & Waterman, M. L. (2006). Diversity of LEF/TCF action in development and disease. *Oncogene, 25*(57), 7492-7504.

Archbold, H. C., Yang, Y. X., Chen, L. & Cadigan, K. M. (2012). How do they do Wnt they do?: regulation of transcription by the Wnt/β-catenin pathway. *Acta Physiol (Oxf), 204*(1), 74-109.

Asem, M. S., Buechler, S., Wates, R. B., Miller, D. L. & Stack, M. S. (2016). Wnt5a Signaling in Cancer. *Cancers, 8*(9). doi: 10.3390/cancers8090079

Belyea, B., Grondin Kephart, J., Blum, J., Kirsch, D. G. & Linardic, C. M. (2012). Embryonic signaling pathways and rhabdomyosarcoma: contributions to cancer development and opportunities for therapeutic targeting. *Sarcoma*. doi: doi:10.1155/2012/406239

Berkes, C. A. & Tapscott, S. J. (2005). MyoD and the transcriptional control of myogenesis. *Semin Cell Dev Biol, 16*(4-5), 585-595.

Bernard, S. & Eilers, M. (2006). Control of cell proliferation and growth by Myc proteins. *Results Probl Cell Differ, 42*, 329-342.

Bernardi, H., Gay, S., Fedon, Y., Vernus, B., Bonnieu, A. & Bacou, F. (2011). Wnt4 activates the canonical β-catenin pathway and regulates negatively myostatin: functional implication in myogenesis. *AM J Physiol Cell Physiol, 300*(5), 1122-1138.

Bouron-Dal Soglio, D., Rougemont, A. L., Absi, R., Giroux, L. M., Sanchez, R., Barrette, S. & Fournet, J. C. (2009). Beta-catenin mutation does not seem to have an effect on the tumorigenesis of pediatric rhabdomyosarcomas. *Pediatr Dev Pathol, 12*(5), 371-373.

Breneman, J. C., Lyden, E., Pappo, A. S., Link, M. P., Anderson, J. R., Parham, D. M., Qualman, S. J., Wharam, M. D., Donaldson, S. S., Maurer, H. M., Meyer, W. H., Baker, K. S., Paidas, C. N. & Crist, W. M. (2003). Prognostic factors and clinical outcomes in children and adolescents with metastatic rhabdomyosarcoma--a report from the Intergroup Rhabdomyosarcoma Study IV. *J Clin Oncol, 21*(1), 78-84.

Bruhn, M. A., Pearson, R. B., Hannan, R. D. & Sheppard, K. E. (2010). Second AKT: the rise of SGK in cancer signalling. *Growth Factors, 28*(6), 394-408.

Bruhn, M. A., Pearson, R. B., Hannan, R. D. & Sheppard, K. E. (2013). AKT-independent PI3-K signaling in cancer – emerging role for SGK3. *Cancer Manag Res, 5*, 281-292.

Brunelli, S., Relaix, F., Baesso, S., Buckingham, M. & Cossu, G. (2007). Beta catenin-independent activation of MyoD in presomitic mesoderm requires PKC and depends on Pax3 transcriptional activity. *Dev Biol, 304*(2), 604-614.

Buttler, K., Becker, J., Pukrop, T. & Wilting, J. (2013). Maldevelopment of dermal lymphatics in Wnt5a-knockout-mice. *Dev Biol, 381*(2), 365-376.

Cadigan, K. M. & Waterman, M. L. (2012). TCF/LEFs and Wnt signaling in the nucleus. *Cold Spring Harb Perspect Biol, 4*(11). doi: 10.1101/cshperspect.a007906

Cappellen, D., Schlange, T., Bauer, M., Maurer, F. & Hynes, N. E. (2007). Novel c-MYC target genes mediate differential effects on cell proliferation and migration. *EMBO Rep, 8*(1), 70-76.

Cen, L., Hsieh, F. C., Lin, H. J., Chen, C. S., Qualman, S. J. & Lin, J. (2007). PDK-1/AKT pathway as a novel therapeutic target in rhabdomyosarcoma cells using OSU-03012 compound. *Br J Cancer, 97*(6), 785-791.

Charrasse, S., Comunale, F., Gilbert, E., Delattre, O. & Gauthier-Rouvière, C. (2004). Variation in cadherins and catenins expression is linked to both proliferation and transformation of Rhabdomyosarcoma. *Oncogene, 23*(13), 2420-2430.

Chien, A. J., Moore, E. C., Lonsdorf, A. S., Kulikauskas, R. M., Rothberg, B. G., Berger, A. J., Major, M. B., Hwang, S. T., Rimm, D. L. & Moon, R. T. (2009). Activated Wnt/beta-catenin signaling in melanoma is associated with decreased proliferation in patient tumors and a murine melanoma model. *PNAS, 106*(4), 1193-1198.

Clevers, H. & Nusse, R. (2012). Wnt/β-catenin signaling and disease. *Cell, 149*(6), 1192-1205.

Dagher, R. & Helman, L. (1999). Rhabdomyosarcoma: an overview. *Oncologist, 4*(1), 34-44.

De, A. (2011). Wnt/Ca2+ signaling pathway: a brief overview. *Acta Biochim Biophys Sin, 43*(10), 745-756.

De Giovanni, C., Landuzzi, L., Nicoletti, G., Lollini, P. L. & Nanni, P. (2009). Molecular and cellular biology of rhabdomyosarcoma. *Future Oncol, 5*(9), 1449-1475.

Ebi, H., Costa, C., Faber, A. C., Nishtala, M., Kotani, H., Juric, D., Della Pelle, P., Song, Y., Yano, S., Mino-Kenudson, M., Benes, C. H. & Engelman, J. A. (2013). PI3K regulates MEK/ERK signaling in breast cancer via the Rac-GEF, P-Rex1. *PNAS, 110*(52), 21124-21129.

Ellison, D. W., Onilude, O. E., Lindsey, J. C., Lusher, M. E., Weston, C. L., Taylor, R. E., Pearson, A. D. & Clifford, S. C. (2005). beta-Catenin status predicts a favorable outcome in childhood medulloblastoma: the United Kingdom Children's Cancer Study Group Brain Tumour Committee. *J Clin Oncol, 23*(31), 7951-7957.

Faes, S. & Dormond, O. (2015). PI3K and AKT: Unfaithful Partners in Cancer. *Int J Mol Sci, 16*(9), 21138-21152.

Fedchenko, N. & Reifenrath, J. (2014). Different approaches for interpretation and reporting of immunohistochemistry analysis results in the bone tissue - a review. *Diagn Pathol, 9*(221).

Ford, C. E., Qian Ma, S. S., Quadir, A. & Ward, R. L. (2013). The dual role of the novel Wnt receptor tyrosine kinase, ROR2, in human carcinogenesis. *Int J Cancer, 133*(4), 779-787.

Gamallo, C., Palacios, J., Moreno, G., Calvo de Mora, J., Suárez, A. & Armas, A. (1999). beta-catenin expression pattern in stage I and II ovarian carcinomas : relationship with beta-catenin gene mutations, clinicopathological features, and clinical outcome. *Am J Pathol, 155*(2), 527-536.

Gravina, G. L., Festuccia, C., Popov, V. M., Di Rocco, A., Colapietro, A., Sanità, P., Monache, S. D., Musio, D., De Felice, F., Di Cesare, E., Tombolini, V. & Marampon, F. (2016). c-Myc Sustains Transformed Phenotype and Promotes Radioresistance of Embryonal Rhabdomyosarcoma Cell Lines. *Radiat Res, 185*(4), 411-422.

Greco, T. L., Takada, S., Newhouse, M. M., McMahon, J. A., McMahon, A. P. & Camper, S. A. (1996). Analysis of the vestigial tail mutation demonstrates that Wnt-3a gene dosage regulates mouse axial development. *Genes Dev, 10*(3), 313-324.

Grumolato, L., Liu, G., Haremaki, T., Mungamuri, S. K., Mong, P., Akiri, G., Lopez-Bergami, P., Arita, A., Anouar, Y., Mlodzik, M., Ronai, Z. A., Brody, J., Weinstein, D. C. & Aaronson, S. A. (2013). β-Catenin-independent activation of TCF1/LEF1 in human hematopoietic tumor cells through interaction with ATF2 transcription factors. *PLoS Genet, 9*(8). doi: 10.1371/journal.pgen.1003603.

Gutierrez, A., Sanda, T., Ma, W., Zhang, J., Grebliunaite, R., Dahlberg, S., Neuberg, D., Protopopov, A., Winter, S. S., Larson, R. S., Borowitz, M. J., Silverman, L. B., Chin, L., Hunger, S. P., Jamieson, C., Sallan, S. E. & Look, A. T. (2010). Inactivation of LEF1 in T-cell acute lymphoblastic leukemia. *Blood, 115*(14), 2845-2851.

Hagemann, T., Robinson, S., Schulz, M., Trümper, L., Balkwill, F. & Binder, C. (2004). Enhanced invasiveness of breast cancer cell lines upon co-cultivation with macrophages is due to TNF-alpha dependent up-regulation of matrix metalloproteases. *Carcinogenesis, 25*(8), 1543-1549.

Hansen, C., Howlin, J., Tengholm, A., Dyachok, O., Vogel, W. F., Nairn, A. C., Greengard, P. & Andersson, T. (2009). Wnt-5a-induced phosphorylation of DARPP-32 inhibits breast cancer cell migration in a CREB-dependent manner. *J Biol Chem, 284*(40), 27533-27543.

He, X., Saint-Jeannet, J. P., Wang, Y., Nathans, J., Dawid, I. & Varmus, H. (1997). A member of the Frizzled protein family mediating axis induction by Wnt-5A. *Science, 275*(5306), 1652-1654.

Hebenstreit, D., Giaisi, M., Treiber, M. K., Zhang, X.-B., Mi, H.-F., Horejs-Hoeck, J., Andersen, K. G., Krammer, P. H., Duschl, A. & Li-Weber, M. (2010). LEF-1 Negatively Controls Interleukin-4 Expression through a Proximal Promoter Regulatory Element. *J Biol Chem, 283*(33), 22490-22497.

Heuberger, J. & Birchmeier, W. (2010). Interplay of cadherin-mediated cell adhesion and canonical Wnt signaling. *Cold Spring Harb Perspect Biol, 2*(2). doi: 10.1101/cshperspect.a002915

Hinson, A. R., Jones, R., Crose, L. E., Belyea, B. C., Barr, F. G. & Linardic, C. M. (2013). Human rhabdomyosarcoma cell lines for rhabdomyosarcoma research: utility and pitfalls. *Front Oncol, 3*(183). doi: 10.3389/fonc.2013.00183

Hogan, P. G., Chen, L., Nardone, J. & Rao, A. (2003). Transcriptional regulation by calcium, calcineurin, and NFAT. *Genes Dev., 17*(18), 2205-2232.

Horvath, L. G., Henshall, S. M., Lee, C. S., Kench, J. G., Golovsky, D., Brenner, P. C., O'Neill, G. F., Kooner, R., Stricker, P. D., Grygiel, J. J. & Sutherland, R. L. (2005). Lower levels of nuclear beta-catenin predict for a poorer prognosis in localized prostate cancer. *Int J Cancer, 113*(3), 415-422.

Hosoyama, T., Aslam, M. I., Abraham, J., Prajapati, S. I., Nishijo, K., Michalek, J. E., Zarzabal, L. A., Nelon, L. D., Guttridge, D. C., Rubin, B. P. & Keller, C. (2012). IL-4R Drives Dedifferentiation, Mitogenesis and Metastasis in Rhabdomyosarcoma. *Clin Cancer Res, 17*(9), 2757-2766.

Hovanes, K., Li, T. W., Munguia, J. E., Truong, T., Milovanovic, T., Lawrence Marsh, J., Holcombe, R. F. & Waterman, M. L. (2001). Beta-catenin-sensitive isoforms of lymphoid enhancer factor-1 are selectively expressed in colon cancer. *Nat Genet, 28*(1), 53-57.

Huang, F., Chen, Y., Chang, C., Yuan, R. & Jeng, Y. (2012). Hepatocyte growth factor activates Wnt pathway by transcriptional activation of LEF1 to facilitate tumor invasion. *Carcinogenesis, 33*(6), 1142-1148.

Hughes, T. A. & Brady, H. J. (2005). Cross-talk between pRb/E2F and Wnt/beta-catenin pathways: E2F1 induces axin2 leading to repression of Wnt signalling and to increased cell death. *Exp Cell Res, 303*(1), 32-46.

Iezzi, S., Cossu, G., Nervi, C., Sartorelli, V. & Puri, P. L. (2002). Stage-specific modulation of skeletal myogenesis by inhibitors of nuclear deacetylases. *PNAS, 99*(11), 7757-7762.

Ikeya, M. & Takada, S. (1998). Wnt signaling from the dorsal neural tube is required for the formation of the medial dermomyotome. *Development, 125*(24), 4969-4976.

Ishitani, T., Kishida, S., Hyodo-Miura, J., Ueno, N., Yasuda, J., Waterman, M., Shibuya, H., Moon, R. T., Ninomiya-Tsuji, J. & Matsumoto, K. (2003). The TAK1-NLK mitogen-activated protein kinase cascade functions in the Wnt-5a/Ca(2+) pathway to antagonize Wnt/beta-catenin signaling. *Mol Cell Biol, 23*(1), 131-139.

Joyal, J. L., Burks, D. J., Pons, S., Matter, W. F., Vlahos, C. J., White, M. F. & Sacks, D. B. (1997). Calmodulin activates phosphatidylinositol 3-kinase. *J Biol Chem, 272*(45), 28183-28186.

Kaucká, M., Petersen, J., Janovská, P., Radaszkiewicz, T., Smyčková, L., Daulat, A. M., Borg, J. P., Schulte, G. & Bryja, V. (2015). Asymmetry of VANGL2 in migrating lymphocytes as a tool to monitor activity of the mammalian WNT/planar cell polarity pathway. *Cell Commun Signal, 13*(2). doi: 10.1186/s12964-014-0079-1

Khan, N. I., Bradstock, K. F. & Bendall, L. J. (2007). Activation of Wnt/beta-catenin pathway mediates growth and survival in B-cell progenitor acute lymphoblastic leukaemia. *Br J Haematol, 138*(3), 338-348.

Kimelman, D. & Xu, W. (2006). beta-catenin destruction complex: insights and questions from a structural perspective. *Oncogene, 25*(57), 7482-7491.

Komiya, Y. & Habas, R. (2008). Wnt signal transduction pathways. *Organogenesis, 4*(2), 68-75.

Korinek, V., Barker, N., Morin, P. J., van Wichen, D., de Weger, R., Kinzler, K. W., Vogelstein, B. & Clevers, H. (1997). Constitutive transcriptional activation by a beta-catenin-Tcf complex in APC-/- colon carcinoma. *Science, 275*(5307), 1784-1787.

Kremenevskaja, N., von Wasielewski, R., Rao, A. S., Schöfl, C., Andersson, T. & Brabant, G. (2005). Wnt-5a has tumor suppressor activity in thyroid carcinoma. *Oncogene, 24*(13), 2144-2154.

Kühl, M., Sheldahl, L. C., Park, M., Miller, J. R. & Moon, R. T. (2000). The Wnt/Ca2+ pathway: a new vertebrate Wnt signaling pathway takes shape. *Trends Genet, 16*(7), 279-283.

Kumawat, K. & Gosens, R. (2016). WNT-5A: signaling and functions in health and disease. *Cell Mol Life Sci, 73*(3), 567-587.

Li, Z., Mericskay, M., Agbulut, O., Butler-Browne, G., Carlsson, L., Thornell, L., Babinet, C. & Paulin, D. (1997). Desmin Is Essential for the Tensile Strength and Integrity of Myofibrils but Not for Myogenic Commitment, Differentiation, and Fusion of Skeletal Muscle *J Cell Biol, 139*(1), 129-144.

Liang, H., Chen, Q., Coles, A. H., Anderson, S. J., Pihan, G., Bradley, A., Gerstein, R., Jurecic, R. & Jones, S. N. (2003). Wnt5a inhibits B cell proliferation and functions as a tumor suppressor in hematopoietic tissue. *Cancer Cell, 4*(5), 349-360.

MacDonald, B. T., Tamai, K. & He, X. (2009). Wnt/β-catenin signaling: components, mechanisms, and diseases. *Dev Cell, 17*(1), 9-26.

Maier, E., Hebenstreit, D., Posselt, G., Hammerl, P., Duschl, A. & Horejs-Hoeck, J. (2011). Inhibition of suppressive T cell factor 1 (TCF-1) isoforms in naive CD4+ T cells is mediated by IL-4/STAT6 signaling. *J Biol Chem, 286*(2), 919-928.

Marampon, F., Ciccarelli, C. & Zani, B. M. (2006). Down-regulation of c-Myc following MEK/ERK inhibition halts the expression of malignant phenotype in rhabdomyosarcoma and in non muscle-derived human tumors. *Mol Cancer, 5*(31). doi: 10.1186/1476-4598-5-31

McCrea, P. D., Maher, M. T. & Gottardi, C. G. (2015). Nuclear Signaling from Cadherin Adhesion Complexes. *Curr Top Dev Biol, 112*, 129-196.

McEwen, A. E., Escobar, D. E. & Gottardi, C. G. (2012). Signaling from the Adherens Junction. *Subcell Biochem, 60*, 171-196.

Mehdawi, L. M., Prasad, C. P., Ehrnström, R., Andersson, T. & Sjölander, A. (2016). Non-canonical WNT5A signaling up-regulates the expression of the tumor suppressor 15-PGDH and induces differentiation of colon cancer cells. *Mol Oncol, 10*(9), 1415-1429.

Merlino, G. & Helman, L. J. (1999). Rhabdomyosarcoma--working out the pathways. *Oncogene, 18*(38), 5340-5348.

Mikels, A. J. & Nusse, R. (2006). Purified Wnt5a protein activates or inhibits beta-catenin-TCF signaling depending on receptor context. *PLoS Biol, 4*(4), 570-582.

Morin, P. J., Sparks, A. B., Korinek, V., Barker, N., Clevers, H., Vogelstein, B. & Kinzler, K. W. (1997). Activation of beta-catenin-Tcf signaling in colon cancer by mutations in beta-catenin or APC. *Science, 275*(5307), 1787-1790.

Nitzki, F., Becker, M., Frommhold, A., Schulz-Schaeffer, W. & Hahn, H. (2012). Patched knockout mouse models of basal cell carcinoma. *Skin Cancer*, 907543.

Nitzki, F., Cuvelier, N., Dräger, J., Schneider, A., Braun, T. & Hahn, H. (2016). Hedgehog/Patched-associated rhabdomyosarcoma formation from delta1-expressing mesodermal cells. *Oncogene, 35*(22), 2923-2931.

Nitzki, F., Zibat, A., König, S., Wijgerde, M., Rosenberger, A., Brembeck, F. H., Carstens, P. O., Frommhold, A., Uhmann, A., Klingler, S., Reifenberger, J., Pukrop, T., Aberger, F., Schulz-Schaeffer, W. & Hahn, H. (2010). Tumor stroma-derived Wnt5a induces differentiation of basal cell carcinoma of Ptch-mutant mice via CaMKII. *Cancer Res, 70*(7), 2739-2748.

Novitch, B. G., Mulligan, G. J., Jacks, T. & Lassar, A. B. (1996). Skeletal muscle cells lacking the retinoblastoma protein display defects in muscle gene expression and accumulate in S and G2 phases of the cell cycle. *J Cell Biol, 135*(2), 441-456.

Ognjanovic, S., Linabery, A. M., Charbonneau, B. & Ross, J. A. (2009). Trends in childhood rhabdomyosarcoma incidence and survival in the United States, 1975-2005. *Cancer, 115*(18), 4218-4226.

Oishi, I., Suzuki, H., Onishi, N., Takada, R., Kani, S., Ohkawara, B., Koshida, I., Suzuki, K., Yamada, G., Schwabe, G. C., Mundlos, S., Shibuya, H., Takada, S. & Minami, Y. (2003). The receptor tyrosine kinase Ror2 is involved in non-canonical Wnt5a/JNK signalling pathway. *Genes Cells, 8*(7), 645-654.

Olsen, A. K., Coskun, M., Bzorek, M., Kristensen, M. H., Danielsen, E. T., Jørgensen, S., Olsen, J., Engel, U., Holck, S. & Troelsen, J. T. (2013). Regulation of APC and AXIN2 expression by intestinal tumor suppressor CDX2 in colon cancer cells. *Carcinogenesis, 34*(6), 1361-1369.

Owens, G. K. (1995). Regulation of differentiation of vascular smooth muscle cells. *Physiol Rev, 75*(3), 487-517.

Pedersen, E. A., Menon, R., Thomas, D., Fearon, E. & Lawlor, E. (2015). Distinct and heterogeneous response of Ewing sarcoma cells to canonical Wnt signaling. *AACR 106th Annual Meeting, 75*(15). doi: 10.1158/1538-7445.AM2015-3270

Pellicena, P. & Schulman, H. (2014). CaMKII inhibitors: from research tools to therapeutic agents. *Front Pharmacol, 5*(21). doi: 10.3389/fphar.2014.00021

Petropoulos, K., Arseni, N., Schessl, C., Stadler, C. R., Rawat, V. P., Deshpande, A. J., Heilmeier, B., Hiddemann, W., Quintanilla-Martinez, L., Bohlander, S. K., Feuring-Buske, M. & Buske, C. (2008). A novel role for Lef-1, a central transcription mediator of Wnt signaling, in leukemogenesis. *J Exp Med, 205*(3), 515-522.

Poppy Roworth, A., Ghari, F. & La Thangue, N. B. (2015). To live or let die - complexity within the E2F1 pathway. *Mol Cell Oncol, 2*(1). doi: 10.4161/23723548.2014.970480

Reya, T., O'Riordan, M., Okamura, R., Devaney, E., Willert, K., Nusse, R. & Grosschedl, R. (2000). Wnt Signaling Regulates B Lymphocyte Proliferation through a LEF-1 Dependent Mechanism. *Immunity, 13*(1), 15-24.

Roma, J., Almazan-Moga, A., Sanchez de Toledo, J. & Gallego, S. (2012). Notch, wnt, and hedgehog pathways in rhabdomyosarcoma: from single pathways to an integrated network. *Sarcoma, 2012*, 695603. doi: 10.1155/2012/695603

Ross, D. A. & Kadesch, T. (2001). The Notch Intracellular Domain Can Function as a Coactivator for LEF-1. *Mol Cell Biol, 21*(22), 7537-7544.

Säfholm, A., Leandersson, K., Dejmek, J., Nielsen, C. K., Villoutreix, B. O. & Andersson, T. (2006). A formylated hexapeptide ligand mimics the ability of Wnt-5a to impair migration of human breast epithelial cells. *J Biol Chem, 281*(5), 40-49.

Sato, A., Yamamoto, H., Sakane, H., Koyama, H. & Kikuchi, A. (2010). Wnt5a regulates distinct signalling pathways by binding to Frizzled2. *EMBO J, 29*(1), 41-54.

Schiaffino, S., Rossi, A. C., Smerdu, V., Leinwand, L. A. & Reggiani, C. (2015). Developmental myosins: expression patterns and functional significance. *Skeletal Muscle, 5*(22).

Sebire, N. J. & Malone, M. (2003). Myogenin and MyoD1 expression in paediatric rhabdomyosarcomas. *J Clin Pathol, 56*(6), 412-416.

Seki, M., Nishimura, R., Yoshida, K., Shimamura, T., Shiraishi, Y., Sato, Y., Kato, M., Chiba, K., Tanaka, H., Hoshino, N., Nagae, G., Shiozawa, Y., Okuno, Y., Hosoi,

H., Tanaka, Y., Okita, H., Miyachi, M., Souzaki, R., Taguchi, T., Koh, K., Hanada, R., Kato, K., Nomura, Y., Akiyama, M., Oka, A., Igarashi, T., Miyano, S., Aburatani, H., Hayashi, Y., Ogawa, S. & Takita, J. (2015). Integrated genetic and epigenetic analysis defines novel molecular subgroups in rhabdomyosarcoma. *Nat Commun, 6*(7557). doi: 10.1038/ncomms8557

Seth, C. & Ruiz i Altaba, A. (2016). Metastases and Colon Cancer Tumor Growth Display Divergent Responses to Modulation of Canonical WNT Signaling. *PLoS One, 11*(3). doi: 10.1371/journal.pone.0150697

Shah, M., Rennoll, S. A., Raup-Konsavage, W. M. & Yochum, G. S. (2015). A dynamic exchange of TCF3 and TCF4 transcription factors controls MYC expression in colorectal cancer cells. *Cell Cycle, 14*(3), 323-332.

Sherwood, R. I., Maehr, R., Mazzoni, E. O. & Melton, D. A. (2012). Wnt Signaling Specifies and Patterns Intestinal Endoderm. *Mech Dev, 128*(7-10), 387-400.

Shukla, N., Ameur, N., Yilmaz, I., Nafa, K., Lau, C. Y., Marchetti, A., Borsu, L., Barr, F. G. & Ladanyi, M. (2012). Oncogene mutation profiling of pediatric solid tumors reveals significant subsets of embryonal rhabdomyosarcoma and neuroblastoma with mutated genes in growth signaling pathways. *Clin Cancer Res, 18*(3), 748-757.

Singh, R., Bhasin, S., Braga, M., Artaza, J. N., Pervin, S., Taylor, W. E., Krishnan, V., Sinha, S. K., Rajavashisth, T. B. & Jasuja, R. (2009). Regulation of Myogenic Differentiation by Androgens: Cross Talk between Androgen Receptor/ β-Catenin and Follistatin/Transforming Growth Factor-β Signaling Pathways. *Endocrinology, 150*(3), 1259-1268.

Singh, S., Vinson, C., Gurley, C. M., Nolen, G. T., Beggs, M. L., Nagarajan, R., Wagner, E. F., Parham, D. M. & Peterson, C. A. (2010). Impaired Wnt signaling in embryonal rhabdomyosarcoma cells from p53/c-fos double mutant mice. *Am J Pathol, 177*(4), 2055-2066.

Slusarski, D. C., Corces, V. G. & Moon, R. T. (1997). Interaction of Wnt and a Frizzled homologue triggers G-protein-linked phosphatidylinositol signalling. *Nature, 390*(6658), 410-413.

Surmann-Schmitt, C., Widmann, N., Dietz, U., Saeger, B., Eitzinger, N., Nakamura, Y., Rattel, M., Latham, R., Hartmann, C., von der Mark, H., Schett, G., von der Mark, K. & Stock, M. (2009). Wif-1 is expressed at cartilage-mesenchyme interfaces and impedes Wnt3a-mediated inhibition of chondrogenesis. *J Cell Sci, 122*(20), 3627-3637.

Syed Khaja, A. S., Helczynski, L., Edsjö, A., Ehrnström, R., Lindgren, A., D., U., T., A. & Bjartell, A. (2011). Elevated level of Wnt5a protein in localized prostate cancer tissue is associated with better outcome. *PLoS One, 6*(10). doi: 10.1371/journal.pone.0026539

Tang, W., Dodge, M., Gundapaneni, D., Michnoff, C., Roth, M. & Lum, L. (2008). A genome-wide RNAi screen for Wnt/beta-catenin pathway components identifies

unexpected roles for TCF transcription factors in cancer. *PNAS, 105*(28), 9697-9702.

Thiele, S., Rachner, T. D., Rauner, M. & Hofbauer, L. C. (2016). WNT5A and its receptors in the bone-cancer dialogue. *J Bone Miner Res., 31*(8), 1488-1496.

Turki-Judeh, W. & Courey, A. J. (2012). Groucho: a corepressor with instructive roles in development. *Curr Top Dev Biol, 98*, 65-96.

Uhmann, A., Dittmann, K., Nitzki, F., Dressel, R., Koleva, M., Frommhold, A., Zibat, A., Binder, C., Adham, I., Nitsche, M., Heller, T., Armstrong, V., Schulz-Schaeffer, W., Wienands, J. & Hahn, H. (2007). The Hedgehog receptor Patched controls lymphoid lineage commitment. *Blood, 110*(6), 1814-1823.

Valenta, T., Hausmann, G. & Basler, K. (2012). The many faces and functions of β-catenin. *EMBO J, 31*(12), 2714-2736.

Van de Wetering, M., Castrop, J., Korinek, V. & Clevers, H. (1996). Extensive alternative splicing and dual promoter usage generate Tcf-1 protein isoforms with differential transcription control properties. *Mol Cell Biol, 16*(3), 745-752.

Vladar, E. K., Antic, D. & Axelrod, J. D. (2009). Planar cell polarity signaling: the developing cell's compass. *Cold Spring Harb Perspect Biol, 1*(a002964).

von Maltzahn, J., Chang, C. N., Bentzinger, C. F. & Rudnicki, A. M. (2012). Wnt Signaling in Myogenesis. *Trends Cell Biol, 22*(11), 602-609.

Weeraratna, A. T., Jiang, Y., Hostetter, G., Rosenblatt, K., Duray, P., Bittner, M. & Trent, J. M. (2002). Wnt5a signaling directly affects cell motility and invasion of metastatic melanoma. *Cancer Cell, 1*(3), 279-288.

Willert, K., Brown, J., Danenberg., Duncan, A., Weissman, I., Reya, T., 3rd., Y. J. & Nusse, R. (2003). Wnt proteins are lipid-modified and can act as stem cell growth factors. *Nature, 423*(6938), 448-452.

Xing, S., Li, F., Zeng, Z., Zhao, Y., Yu, S., Shan, Q., Li, Y., Phillips, F. C., Maina, P. K., Qi, H. H., Liu, C., Zhu, J., Pope, R. M., Musselman, C. A., Zeng, C., Peng, W. & Xue, H. H. (2016). Tcf1 and Lef1 transcription factors establish CD8(+) T cell identity through intrinsic HDAC activity. *Nat Immunol, 17*(6), 695-703.

Yamamoto, H., Oue, N., Sato, A., Hasegawa, Y., Yamamoto, H., Matsubara, A., Yasui, W. & Kikuchi, A. (2010). Wnt5a signaling is involved in the aggressiveness of prostate cancer and expression of metalloproteinase. *Oncogene, 29*(14), 2036-2046.

Yuan, Y., Niu, C. C., Deng, G., Li, Z. Q., Pan, J., Zhao, C., Yang, Z. L. & Si, W. K. (2011). The Wnt5a/Ror2 noncanonical signaling pathway inhibits canonical Wnt signaling in K562 cells. *Int J Mol Med, 27*(1), 63-69.

Zeitler, P., Pahnke, J. & Marx, A. (2004). Expression of stromelysin-1 (MMP-3), gelatinase B (MMP-9), and plasminogen activator system during fetal calvarial development. *Histopathology, 44*(4), 360-366.

Zhang, A., Shuanghua, H., Xiaoliang, S., Lianghua, D., Xinnan, B. & Neng, W. (2014). Wnt5a promotes migration of human osteosarcoma cells by triggering a phosphatidylinositol-3 kinase/Akt signals. *Cancer Cell Int., 14:15*. doi: 10.1186/1475-2867-14-15

Zhang, S., Chen, L., Cui, B., Chuang, H.-Y., Yu, J., Wang-Rodriguez, J., Tang, L., Chen, G., Basak, G. B. & Kipps, T. J. (2012). ROR1 is expressed in human breast cancer and associated with enhanced tumor-cell growth. *PloS One, 7*(3). doi: 10.1371/journal.pone.0031127

Zhang, T., Inesta-Vaquera, F., Niepel, M., Zhang, J., Ficarro, S. B., Machleidt, T., Xie, T., Marto, J. A., Kim, N., Sim, T., Laughlin, J. D., Park, H., LoGrasso, P. V., Patricelli, M., Nomanbhoy, T. K., Sorger, P. K., Alessi, D. R. & Gray, N. S. (2012). Discovery of potent and selective covalent inhibitors of JNK. *Chem Biol, 19*(1), 140-154.

Zhao, Y., Zhang, C., Huang, Y., Yu, Y., Li, R., Li, M., Liu, N., Liu, P. & Qiao, J. (2015). Up-regulated expression of WNT5a increases inflammation and oxidative stress via PI3K/AKT/NF-κB signaling in the granulosa cells of PCOS patients. *J Clin Endocrinol Metab, 100*(1), 201-211.

Zibat, A., Uhmann, A., Nitzki, F., Wijgerde, M., Frommhold, A., Heller, T., Armstrong, V., Wojnowski, L., Quintanilla-Martinez, L., Reifenberger, J., Schulz-Schaeffer, W. & Hahn, H. (2009). Time-point and dosage of gene inactivation determine the tumor spectrum in conditional Ptch knockouts. *Carcinogenesis, 30*(6), 918-926.

9 Abbreviations

AKT	v-akt murine thymoma viral oncogene homolog
ALL	acute lymphoblastic leukemia
APC	adenomatosis polyposis coli
ARMS	alveolar rhabdomyosarcoma
ATF2	activating transcription factor 2
BCA	bicinchoninic acid
β-catS33Y	*pCl-neo-β-cateninS33Y*
β-Trcp	β-transducin repeat containing protein
BMP	bone morphogenetic protein
bp	base pairs
BrdU	5-bromo-2-deoxyuridine
BSA	bovine serum albumin
CAM	chorio-allantoic membrane
CAMKII	calcium/calmodulin-dependent kinase II
CBP	CREB-binding protein
cDNA	complementary deoxyribonucleic acid
CK1	casein kinase 1
CKM	creatine kinase, muscle
CM	conditioned medium
CMV	cytomegalovirus
control	control transduced
CREB	cAMP-response element-binding protein
DAAM1	dishevelled-associated activator of morphogenesis 1
DAB	3,3'-diaminobenzidine
DAPI	4',6-diamidin-2-phenylindol
Dkk	dickkopf

Dvl	dishevelled
ddH_2O	double distilled water
DMEM	Dulbecco's Modified Eagle Medium
DMSO	dimethyl sulfoxide
DNA	deoxyribonucleic acid
dNTP	deoxyribonucleotide triphosphate
DTT	dithiothreitol
E. coli	*Escherichia coli*
EDTA	ethylenediaminetetraacetic acid
ER	endoplasmatic reticulum
ERK	extracellular-signal regulated kinase
ERMS	embryonal rhabdomyosarcoma
EtOH	ethanol
FCS	fetal calf serum
FOP	*SuperFOPFlash*
FZD	frizzled
GAPDH	glyceraldehyde 3-phosphate dehydrogenase
GFP	green fluorescent protein
GSK3	glycogen synthase kinase 3
GTPase	guanosine triphosphate hydrolase
gDNA	genomic deoxyribonucleic acid
HDAC	histone deacetylase
HE	haematoxylin eosin
HLA	human leukocyte antigen
HMG	high-mobility group
HRP	horseradish peroxidase
HSC-70	heat shock protein 70
IP_3	inositol 1,4,5-trisphosphate

JNK	c-Jun-N-terminal kinase
KD	knockdown
LAR II	Luciferase Assay Reagent II
LB	lysogeny broth
LEF1	lymphoid enhancer factor 1
LRP	low-density lipoprotein receptor-related protein
MAPK	Mitogen-activated protein kinase
MEK	MAPK/ERK kinase
MHC	major histocompatibility complex
mRNA	messenger ribonucleic acid
mTOR	mammalian target of rapamycin
Myc	myelocytomatosis oncogene
Myf5	myogenic factor 5
MYH1	myosin heavy chain 1
NLS	nuclear localization signal
ON	over night
PBS	phosphate buffered saline
PCP	planar cell polarity
PCR	polymerase chain reaction
PFA	paraformaldehyde
PI3K	phosphatidylinositol-3-kinase
PKC	protein kinase C
PLC	phospholipase C
PMSF	phenylmethanesulfonylfluoride
Ptch	*Patched*
Ptk7	protein tyrosine kinase 7
Pygo	Pygopus
qRT-PCR	quantitative real-time polymerase chain reaction

Rac	Ras-related C3 botulinum toxin substrate
Ras	rat sarcoma
Rho	Ras homologue
RMS	rhabdomyosarcoma
RNA	ribonucleic acid
ROCK	Rho-associated kinase
ROR	tyrosine kinase-like orphan receptor
RT	room temperature
RYK	receptor tyrosine kinase-like
scr	scrambled
SEM	standard error of the mean
SDS	sodiumdodecylsulfate
SMAD	Sma and Mad-related protein
TBE	tris-boric acid-EDTA
TBS	tris-buffered saline
TBST	tris-buffered saline-Triton X-100
TCF	T-cell factor
TGF	transforming growth factor
TLE	transducin-like enhancer of split
TMA	tissue micro array
TOP	*SuperTOPFlash*
Wif1	Wnt inhibitory factor 1
WNT	wingless-type MMTV integration site family member
WRE	WNT responsive element
v/v	volume/volume
vt	*vestigial tail*
w/v	weight/volume

10 Acknowledgement

I would like to thank the following people which supported me throughout my doctoral study and contributed to this thesis, which would not have been possible without their help.

Firstly, I would like to express my sincere gratitude to my advisor Prof. Dr. Heidi Hahn for the continuous support of my Ph.D. study and related research, for her patience, motivation, and immense knowledge. Her guidance helped me in all the time of research and writing of this thesis. I could not have imagined having a better advisor and mentor for my Ph.D. study.

Besides my advisor, I would like to thank the rest of my thesis committee members: Prof. Dr. Holger Bastians and Prof. Dr. Tobias Pukrop for their insightful comments and encouragement, but also for the hard questions which incented me to widen my research from various perspectives.

My sincere thanks also go to Prof. Dr. Wilting, Prof. Dr. Pukrop and Dr. Florian Klemm, Dr. Katja Simon-Keller and Prof. Dr. Alexander Marx, who provided me an opportunity to join their team, and who gave access to the laboratory and research facilities. Without their precious support it would not have been possible to conduct this research. In particular, I would like to thank Berti Mannshausen, Sonja Schwoch, Lena Ries and Matthias Schulz for working together and for their support. Very special thanks go again to my collaboration partner Dr. Katja Simon-Keller for her outstanding encouragement and personal guidance.

Special thanks go to Dr. Kai Dittmann for all your support and advice in all the experiment requiring flow cytometry.

Big thanks go also to the animal care takers, especially Susann Peter and Jennifer Flemming for the excellent animal care.

Many thanks go to all my colleagues in the laboratory. In particular, I would like to thank Dr. Anja Uhmann for your competent knowledge, huge helpfulness and for sharing everything in one office with you. Many thanks go to Julia Heise who took care of my mice during my thesis writing and for her reliability in all aspects.

Similarly, my gratitude goes to Anke Frommhold and Ina Heß for technical support an. Many thanks also go to all the other past and present lab members: Dr. Rosalie Ridzewski, Dr. Frauke Nitzki, Dr. Marco Becker, Dr. Benedikt Linder, Dr. Nicole Cuvelier, Joanna Pyczek and Natalie Hönig.

Most importantly, I would like to thank my family, my partner and my friends. Liebe Muttni, lieber Papi, liebe Anni-Maus thanks for all your help and support in any life situation. Liebe Oma Inge und Opa Gerhard, thanks for always being there for me and your endless trust, also in heaven. Liebe Oma Elli thanks for all your support. Dear Rosi, thanks for the nice time in the lab together and all the moments we had and still will have together. Caro Loni, grazie mille per tutto e che tu eri sempre lì per me.